THESIS

DAMMED PONDS! A STUDY OF POST-FIRE SEDIMENT AND CARBON DYNAMICS IN BEAVER PONDS AND THEIR CONTRIBUTIONS TO WATERSHED RESILIENCE

Submitted by

Sarah B. Dunn

Department of Geosciences

In partial fulfillment of the requirements

For the Degree of Master of Science

Colorado State University

Fort Collins, Colorado

Summer 2023

Master's Committee:

Advisor: Sara Rathburn

Ellen Wohl
Ryan Morrison

ABSTRACT

DAMMED PONDS! A STUDY OF POST-FIRE SEDIMENT AND CARBON DYNAMICS IN BEAVER PONDS AND THEIR CONTRIBUTIONS TO WATERSHED RESILIENCE

Excess sediment generated by wildfires threatens stream water quality, riparian habitat, and infrastructure. Beavers construct dams that pool water and capture sediment. Beaver ponds may bolster watershed resilience by providing sediment and carbon storage following wildfire. I tested the hypotheses that (1) burned ponds store greater relative volumes of sediment compared to unburned ponds, (2) post-fire sedimentation rates exceed pre-fire and unburned rates, and (3) post-fire sediment stored in beaver ponds is coarser and has a higher abundance of organic carbon relative to pre-fire sediment. I surveyed 48 beaver ponds in the Colorado Rocky Mountains. Approximately half of the ponds are in areas that burned in 2020 wildfires, whereas the other half remain unburned. Sites also spanned a range of geomorphic, vegetation, and individual pond characteristics. I conducted sediment probe surveys and collected sediment cores to quantify pond sediment storage and characterize sediment composition. Stratigraphic units present in sediment cores were analyzed for grain size and total organic carbon (TOC). Results indicate that beaver ponds in the Rocky Mountains store high volumes of sediment (mean = 796 m^3). Burned ponds contain statistically significantly more relative sediment storage and have higher sedimentation rates than unburned ponds. Beaver ponds recorded high post-fire sedimentation rates (median = 19.8 cm/yr). Moreover, post-fire sedimentation rates are an order of magnitude higher than pre-fire rates in ponds with both pre- and post-fire sediments. Total sediment volume, sedimentation rates, grain size, and TOC content did not vary significantly between burned and unburned ponds. Geomorphology, vegetation, and pond characteristics exert additional influences on pond sediment dynamics. Pond characteristics determine the sediment trapping efficiency of ponds. Larger ponds store greater volumes of sediment, as do off-channel and older ponds. Ponds abandoned by beaver store greater volumes of sediment than actively maintained or human-constructed dams. Beaver activity and dam maintenance is critical for maintaining storage availability in ponds. Additionally, sedimentation rates are higher in ponds that are on-channel and recently constructed compared to off-channel and older ponds. These findings indicate that beaver-based restoration can be implemented prior to fire to provide critical post-fire sediment storage, thus enhancing watershed resilience and recovery.

ACKNOWLEDGEMEMTS

I would like to acknowledge the many people and organizations who made this research possible. First and foremost, I extend my thanks to my advisor, Dr. Sara Rathburn who offered invaluable support, thoughtful guidance, and compassionate advice throughout the course of this project. From her I have learned how to adeptly handle the ups and downs of field work with a sense of humor and plenty of snacks, and Sara's unbounded enthusiasm and support ensured a successful research experience. I remain deeply grateful to Dr. Ellen Wohl and Dr. Ryan Morrison for sharing their time, advice, and feedback as members of my thesis committee. Additional thanks to Ellen for helping formulate this project after reservoirs proved windier than expected. I thank Dr. Christy Briles for sharing her expertise, lab space, and equipment for collecting and processing sediment cores. I'd also like to thank the coring crew: Hillary Hillam, Rose Grenan, Amanda Vanmeter, and Micah Rogers; and give a huge thanks to those that helped me process the reservoir sediment cores: Trent Erickson, Cody Clemens, and Casey Caduff. Thank you to all those who were willing to spend a day squelching through pond sediments and navigating willow thickets while carrying unwieldly equipment. My thanks goes out to John Kemper, Mickey Means-Brous, Shayla Triantafillou, Theo Kuhn, Danny White, and Lisa Baron for generously helping in the field, and to Adam Mack for lending use of his truck to get to a remote field site. A special thanks to Jana Stich, my outstanding field assistant, for her unwavering curiosity and level-headed problem-solving. Thank you to Dr. Ann Hess and the Colorado State University Statistics Consulting Lab for statistical consultations, and to Celeste Wieting and Collin Barry for assistance wrangling watershed data. I thank the fluvial geomorphology research group at CSU for sharing so much advice, support, and laughter. Thank you to all my friends and family who have shared hikes, long phone calls, chocolate, and words of encouragement. I cannot thank you enough for your unending support. I am ever grateful to the private landowners, Arapahoe and Roosevelt National Forest, and Rocky Mountain National Park staff for granting me access to the lands they manage. I also acknowledge, with respect, the Arapahoe, Cheyenne, and Ute Nations and peoples as the original inhabitants and stewards of this land and all the relatives within it. Additionally, I acknowledge the traditional ecological knowledge and leadership shared by indigenous communities in partnering with other than human kin including beaver. Finally, I extend my thanks to the Colorado Water Center, American Water Resources Association, Geological Society of America Continental Scientific Drilling Division, City of Fort Collins, National Science Foundation (NSF-EAR 2101068), Colorado State University and Warner College of Natural Resources for funding this project.

TABLE OF CONTENTS

LIST OF TABLES

LIST OF FIGURES

1. INTRODUCTION

Large scale wildfires are becoming increasingly common and intense (Dennison et al., 2014). Wildfires increase the amount of sediment shed from hillslopes into fluvial systems (Kunze and Stednick, 2006) through reduced ground cover that alters hillslope roughness, evapotranspiration, and runoff generation (Blount et al., 2020). Intense heat also decreases infiltration rates by altering soil properties (DeBano, 2000; Ebel and Moody, 2017). High severity fires combust vegetation more completely, which decreases canopy interception of precipitation (Stoof et al., 2012). Exposed sediment paired with increased infiltration excess overland flow contributes to greater hillslope erosion rates after fire (Moody and Martin, 2001). The highest rates of sediment loading occur immediately following fire, declining rapidly in the years following as soil repellency declines and vegetation regrows (Benavides-Solorio and MacDonald, 2005; Rathburn et al., 2018; Ebel, 2020). Influxes of sediment and carbon to rivers impact drinking water quantity and quality, water supply infrastructure, and aquatic habitat (Rust et al., 2018). The years immediately following fire constitute a "window of disturbance" when sediment and carbon flux is highest (Figure 1), and water supply is most vulnerable. Short-term sediment and carbon attenuation may dampen downstream fluxes during this critical period (Robichaud et al., 2000). Fluvial systems modulate sediment movement and contribute to watershed resilience to disturbance, especially when there is a high degree of physical complexity such as multithread channels or logjams (Rathburn et al., 2018).

Beavers (*Castor canadensis, Castor fiber*) are geomorphic agents and ecosystem engineers whose dam building and excavation activities alter landscape processes (Brazier et al., 2021). Beaver dams increase river corridor spatial heterogeneity and contribute to feedback loops that increase sediment and carbon attenuation (Polvi and Wohl, 2012, 2013; Wohl et al., 2022). Beaver ponds actively store sediment and carbon (Butler and Malanson, 1995; Puttock et al., 2018) and create the conditions for attenuation of post-fire sediment and nutrient fluxes. Beaver mimicry structures such as beaver dam analogues (BDA), entice beaver to streams as well as promote aggradation (Pollock et al., 2007). There is growing consideration toward using these structures on fire-prone landscapes where sedimentation poses a challenge. Although previous studies have characterized the composition, thickness and distribution of beaver pond sediments, little research exists on pond retention of excess sediment and carbon after disturbances such as wildfire and the potential for beaver-based restoration to enhance resilience to fires (Bigler et al., 2001).

1.1 Research objectives and hypotheses

Several large wildfires burned in Colorado in 2020, providing an opportunity to study the immediate post-fire sediment response and transient storage in beaver ponds. This study evaluates the conditions under which beaver ponds most effectively attenuate post-disturbance sediments. To this end, I quantify sediment volume and sedimentation rates through an inventory of beaver ponds in burned areas and examine the role of additional controls on sediment dynamics including geomorphic context, vegetation, and pond characteristics, all to improve understanding of the sedimentary structure of beaver ponds. Additionally, I quantify the grain size and total organic carbon (TOC) content of sediments found in beaver ponds to provide insight on sediment transport and carbon cycling. Understanding how natural features like beaver ponds modulate sediment and carbon in river systems may help managers implement strategies to enhance watershed resilience to fire and dampen the impacts of excess sedimentation after fire. I present three hypotheses and rationale below.

1.1.1 Hypothesis 1

Burned ponds will contain greater relative sediment volumes compared to unburned ponds and burn severity and degree of vegetation regrowth will correspond to sediment storage. Additionally, pond position in relation to the channel and to other ponds, beaver activity, pond age, and drainage area will correspond with sediment storage.

1.1.2 Hypothesis 2

Post-fire sedimentation rates will exceed pre-fire rates, and sedimentation rates in burned ponds will exceed rates in unburned ponds. Sedimentation also will correspond to geomorphic, vegetation, and pond characteristics.

1.1.3 Rationale for hypotheses 1 & 2

Previous research has documented how hillslope erosion processes increase sediment supply after fire (Benavides-Solorio and MacDonald, 2005). Fire may alter the timing, magnitude, duration, and volume of stream flow, such that the hydrograph is peakier, increasing the sediment transport capacity of the stream (Shakesby and Doerr, 2006). Increasing the sediment supply and sediment transport capacity of streams leads to a greater volume of sediment passing through the fluvial system after fire (Moody and Martin, 2001). Burn severity and vegetation regrowth likely influence the magnitude of response (Figure 1) (Wagenbrenner et al., 2006). Beaver ponds alter the hydrology of streams by slowing velocities, reducing the amount of discharge passed downstream and increasing overbank flooding (Meentemeyer and Butler, 1999; Nyssen et al., 2011). Thus, the ponds promote sediment deposition, which will increase in response to the increased volume of sediment available.

Geomorphology of a basin, such as drainage area, relief ratio, and valley geometry, influences sediment production and transport as well (Wohl, 2018). Large watersheds, with high relief ratios and steep and narrow valleys are expected to have higher sediment loads and thus are expected to contain beaver ponds with lower remaining storage. However, the increased stream power and sediment transport capacity may mean that ponds scour or fail more readily in these systems, so the trapping effects of dams might be countered. Wide, unconfined valleys often correlate with shallow stream slopes and a multithreading planform, which beaver may prefer and enhance (Polvi and Wohl, 2013). These areas, sometimes referred to as ‘river beads’, are disproportionately important for sediment and carbon storage (Wohl et al., 2018).

Additionally, I expect that upstream ponds will attenuate greater volumes of sediment compared to downstream ponds because the sediment supply will be depleted lower in the sequence (Figure 1) (Puttock et al., 2018). Off-channel ponds are predicted to store less sediment because they are disconnected from the channel and only receive wash or overbank flows. Beavers actively maintain dams and use mud to reinforce their structures. In addition to reworking sediments, they may build dams higher as ponds fill with sediment to create more accommodation space. When ponds are abandoned, the dams may deteriorate or partially breach allowing for more sediment to pass through (Butler and Malanson, 2005). However, ponds are more likely to be disconnected from the channel via avulsion after they are abandoned, so I expect that active ponds will have more remaining storage capacity than inactive ponds. BDAs constructed by humans use different techniques than beavers and are typically not actively maintained by either humans or beavers. As such, I expect that BDAs will retain sediment differently than beaver constructed ponds. I expect that sedimentation rates and residual volumes will remain closely related as the same processes govern these metrics, though only sedimentation rate captures the temporal dimension.

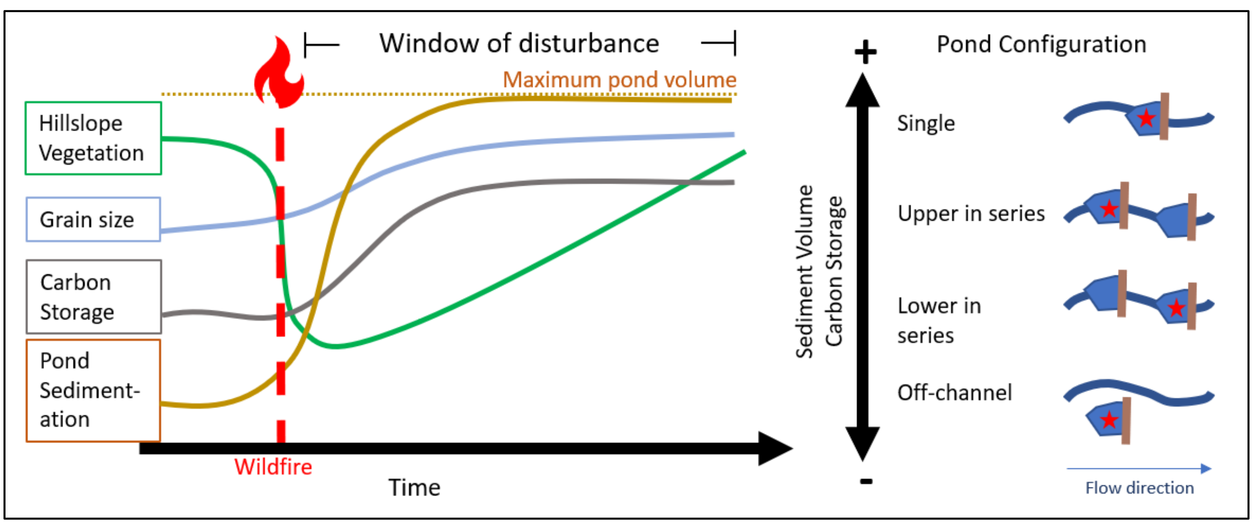

Figure 1: Conceptual diagram illustrating beaver pond sedimentation (volume and rate), grain size, and carbon storage in relation to hillslope vegetation as a function of time since wildfire. Volumes and rates of sedimentation are expected to increase after fire, corresponding with more carbon storage and larger grain sizes. Ponds may fill to a maximum sediment volume governed by pond geometry, after which dams may breach and lose sediment, though vegetation regrowth is expected to stabilize much of the

ponded sediment. Sedimentation and carbon storage are also expected to vary as a function of pond position in relation to other ponds and the stream channel. Red stars indicate the pond under consideration.

1.1.4 Hypothesis 3

Post-fire sediment will be coarser and have a higher abundance of TOC relative to pre-fire sediment and sediment in unburned ponds.

1.1.5 Rationale for hypothesis 3

I expect that the composition of post-fire sediment will differ from pre-fire sediment due to alterations of the sediment supply and hydrology of the watershed by fire (Figure 1). Coarse, charcoal-bearing sediment has been interpreted as post-fire debris flow deposits potentially responsible for breaching beaver dams in the Greater Yellowstone region (Persico and Meyer, 2009), indicating that fire, flooding, and sedimentation may be linked in these systems. Beaver ponds are distinguished from other ponds as they have a current running through, so they contain a mix of fluvial and lacustrine processes and deposits (John and Klein, 2004; Puttock et al., 2018). Some studies have documented distinct stratigraphic layering within pond sediments (e.g., John and Klein, 2004) whereas others have found little stratigraphy (Butler and Malanson, 1995). The magnitude and timing of high flows varies between pond systems and may explain the different observations of stratification. Changes in dam effectiveness may alter flow velocities and the trapping efficiency of the pond, such that organic-rich layers might reflect high effectiveness and coarse mineral sediments may reflect dam failures or high discharge (John and Klein, 2004). I predict that pre-fire sediments will vary in composition depending on the pond characteristics but will be generally fine and nutrient rich. Increased discharges after wildfire will increase the stream power, allowing for the transport of larger sediment sizes into ponds. Therefore, I expect that post-fire deposits will be coarser than pre-fire deposits and sediments in unburned ponds.

Wildfire alters carbon cycling pathways, which I expect will be reflected in beaver pond sediments. Water quality monitoring has recorded elevated pyrogenic carbon (PyC), dissolved organic carbon (DOC), nutrient, and turbidity levels in streams following fire (Rhoades et al., 2011, 2019; Oropeza and Heath, 2013; Cotrufo et al., 2016; Chow et al., 2019; McDaniel, 2021). DOC levels relate to the extent of burning and burn severity within a watershed, where incompletely burned watersheds have the highest DOC levels (Rhoades et al., 2019). High severity fires combust organic material more completely, releasing carbon to the atmosphere, so less is delivered to streams (Chow et al., 2019). Therefore, I expect that ponds in partially burned watersheds with moderate severity will contain the highest post-fire carbon content from PyC delivered from hillslopes to streams. I expect that the TOC concentration will exceed pre-fire levels, but older, disconnected ponds have high levels of in-pond biotic production and may have reduced carbon content post-fire. Geomorphology influences post-fire sediment dynamics in river systems, so I expect that the geomorphic context of beaver ponds also contributes to their efficacy of carbon sequestration and storage (Wohl et al., 2020).

1.2 Background

1.2.1 Beaver as geomorphic agents

Beavers (*Castor canadensis, Castor fiber*) are recognized as ecosystem engineers and geomorphic agents due to their ability to alter river corridors through dam-building (Rosell et al., 2005; Larsen et al., 2021). Ponds provide beavers refuge from predators while promoting the growth of riparian species that serve as a food source and building material. Beavers thrive in a wide range of environments, although they prefer to construct dams on small to medium sized streams in wide valleys with low slopes (Persico and Meyer, 2009; Scamardo et al., 2022). Historically, beavers were widespread across North America and Europe, and their near-extinction due to excessive trapping has resounding implications for sediment storage and carbon cycling (Naiman et al., 1986; Butler and Malanson, 2005; Wohl, 2013). Habitat loss limits the recovery of river corridor function mediated by beaver, but unutilized habitat remains available across the American West (Macfarlane et al., 2014, 2017, 2019, 2020; Scamardo et al., 2022).

Beaver dams impact how fluxes of water, sediment, and nutrients move throughout a river corridor. Dams increase lateral connectivity while reducing longitudinal connectivity in the channel, thus decreasing the rate at which sediment pulses are propagated through the system (Burchsted et al., 2010, Westbrook et al., 2011). Even inactive beaver structures influence the geomorphic landscape, modulating downstream fluxes of sediment (Laurel and Wohl, 2019). The retained sediment and TOC may constitute a large portion of valley sediment storage (Polvi and Wohl, 2012), although long-term aggradation rates are low (Persico and Meyer, 2009).

1.2.2 Beaver pond sediment characteristics

Previous research has investigated predictors of the sediment volume within beaver ponds. A positive relationship between beaver pond surface area and sediment storage is well established (Naiman et al., 1986; Butler and Malanson, 1995; Puttock et al., 2018). Additionally, pond age logarithmically relates to sediment volume (Butler and Malanson, 1995; Meentemeyer and Butler, 1999; Bigler et al., 2001). Beavers frequently build ponds in sequences along a channel, and the location of a pond in a sequence may correlate with the volume of sediment stored (Butler and Malanson, 1995; Puttock et al., 2018). However, the thickness of pond sediments is highly heterogeneous both within a pond and between ponds along stream reaches (Butler and Malanson, 1995; Meentemeyer and Butler, 1999; Bigler et al., 2001; John and Klein, 2004). Although authors have theorized that beaver dam and valley geometry exert a control on sediment storage, empirical evidence has yet to indicate a relationship (Naiman et al., 1986; Meentemeyer and Butler, 1999; Pollock et al., 2003). These early studies indicate potential controls on beaver pond sedimentation but are limited in geographic scope and in number of ponds studied.

Sedimentation rates in beaver ponds are higher than surrounding channels and other wetland types, but they may vary greatly between ponds and through time (John and Klein, 2004). Larsen and co-authors (2021) reviewed 12 studies documenting beaver pond sedimentation in North American and

Europe and found that sedimentation estimates ranged between 0.2 cm/yr and 45 cm/yr. Studies of relict beaver pond sediments indicate that although damming may contribute to valley bottom aggradation, average rates are quite slow over millennia and may reach an upper plateau (Persico and Meyer, 2009; Polvi and Wohl, 2012). Factors documented as influencing pond sedimentation rates include the overall energy of the system, discharge, and pond age (Butler and Malanson, 1995).

The composition of beaver pond sediments appears highly heterogenous and relatively few studies have investigated compositional changes within a pond or between ponds, especially after disturbances. Beaver ponds generally consist of finer-grained and more nutrient-rich sediments compared to the surrounding channel (Puttock et al., 2018; McCreesh et al., 2019). The difference is attributed to the lowered flow velocity and increased roughness from the dam, vegetation and complex channel forms, and reworking and biotic production within the pond (Butler and Malanson, 1995; Meentemeyer and Butler, 1999). The rates of sediment influx and biotic production change over the life span of a pond (Naiman et al., 1986; Puttock et al., 2018). If the pond becomes disconnected from the channel, less flushing will occur and biotic processes will dominate, resulting in a eutrophic environment that is rich with nutrients (Butler and Malanson, 1995).

1.2.3 Post-fire pyrogenic carbon dynamics

Incomplete combustion of biomass produces pyrogenic carbon (PyC), commonly referred to as black carbon, which describes a continuum of combustion products including charred biomass, ash, and soot (Masiello, 2004). PyC is recalcitrant and although it is nearly biologically inert, PyC degrades water quality and hinders municipal treatment (Chow et al., 2019). The burn severity of a fire contributes to the abundance and distribution of PyC; moderate severity burns contain the highest abundances by area of PyC on the forest floor compared to unburned and high severity burned patches (Boot et al., 2015). Burn severity describes the degree of fire-induced loss or decomposition of organic matter above and below ground (Keeley, 2009). The low density of PyC allows it to be preferentially transported by surface runoff, although some is incorporated into soils (Cotrufo et al., 2016). Erosion from hillslopes introduces sediments, including PyC, to river systems, increasing the sediment supply (Shakesby and Doerr, 2006).

Wildfire disturbance may also compound secondary disturbances such as flooding and debris flows, which at least temporarily increase the sediment transport capacity of a river system (McGuire et al., 2019; Brogan et al., 2019b, 2019a). Fire impacts on stream hydrology are variable, but fire-affected streams commonly exhibit greater and more variable discharge, changing the timing and energy available to do geomorphic work (Schmeer et al., 2018; Brogan et al., 2019a; Blount et al., 2020). Sediment may be transported as bedload or suspended sediment, or stored in fluvial deposits, which may persist for millennia (Moody and Martin, 2001; Wilkinson et al., 2009; Cotrufo et al., 2016). The geomorphic context matters for sediment and carbon accumulation: confined reaches may see a loss of carbon following fire whereas unconfined reaches may see an increase (Wohl et al., 2020). Atmospheric deposition is another pathway by which fine sediments, nutrients, and PyC may enter streams and waterbodies (Hauer and Spencer, 1998). Wind direction controls PyC deposition as recorded in lake sediments, and elevated PyC may be found in waterbodies proximal to fire-affected watersheds (Gardner and Whitlock, 2001).

Post-fire carbon dynamics also contribute to global carbon cycling. Atmospheric carbon dioxide and methane are of great concern due to the widespread and cascading impacts of human caused climate change (IPCC, 2022). Wetland ecosystems have the highest terrestrial carbon density of any ecosystem type, and they may function as both significant carbon sources and sinks, so understanding the processes responsible for carbon delivery and attenuation in wetlands is critical for carbon budgeting (Kayranli et al., 2010). Beaver-constructed wetlands may produce anerobic conditions that result in increased sediment carbon storage (Naiman et al., 1986; Wohl, 2013). They may also increase the net aquatic ecosystem productivity, although flooding and harvesting activities might decrease the woody biomass of an area, depending on preceding conditions (Larsen et al., 2021).

1.2.4 Management challenges and significance

Increasing fire activity leads to heightened risk from fire and fire-related processes. Larger and more severe fires can be attributed to anthropogenic climate change and fire suppression activities. Additionally, climate change limits vegetation recovery from wildfire (Nolan et al., 2021). The trend in fire activity intersects with development along the urban wild interface and increasing recreational use of forest lands, leading to heightened risk to communities (Higuera et al., 2023). Direct threats from fire are compounded by risk to water supply and ecosystem function.

Excess sediment and PyC pose a risk to critical water supplies and aquatic ecosystems (Emelko et al., 2011; Bladon et al., 2014). Water quality may be degraded by increased nutrients, major ions, and metals in the years following fire, although regional and site factors contribute to a high degree of variability in water quality response (Rust et al., 2018). In particular, drinking water treatment may be hindered by elevated suspended sediment that reduces the rate of water processing (Smith et al., 2011). Water supply infrastructure such as treatment intake pipes and reservoirs may be filled more rapidly with fire-derived sediment (Bladon et al., 2014; Gannon et al., 2021). Additionally, increased nutrient loads can cause eutrophication and toxic algal blooms, disrupting water supply and aquatic ecosystems (Bladon et al., 2014). Treatment of fire-elevated constituents introduces further challenges (Emelko et al., 2011). Chlorination can transform PyC into carcinogenic disinfection by-products (Chow et al., 2019). Estimates of the economic consequence of sedimentation ranged from 1.6 to 37.5 USD Mg^{-1} with a mean of 18.1 USD Mg^{-1} on top of standard treatment and maintenance costs for structures impacted by the 2012 High Park Fire in Colorado (Gannon, 2020).

Fire functions as a disturbance to aquatic and riparian ecosystems. In many cases, species' life histories have adapted to, are shaped by, and depend on disturbances including fire (Dunham et al., 2003). However, the excess sediments delivered to streams following fire may cause detrimental short-term impacts to aquatic populations. Sediment-laden water with low dissolved oxygen may trigger fish die-offs, which may occur even a couple of years after the initial fire disturbance (Bozek and Young, 1994; Lyon and O'Connor, 2008). Indeed, managers observed substantial decreases in trout populations in fire-impacted stream reaches and downstream of a fire-related debris flow that occurred in 2021 in the Cameron Peak burn area (Battige et al., 2022). Additionally, influxes of sediment may change habitat availability and stability, and alter the community structure and dynamics, which may place threatened native species at risk (Dunham et al., 2003; Arkle et al., 2010).

Common post-fire sediment management strategies range from installing individual structures to treating entire watersheds. Wattles, contour felling, and erosion barriers capture sediment and dissipate energy on hillslopes and low-order tributaries (Robichaud et al., 2008; De Girolamo et al., 2022). Aerial mulching seeks to shield exposed soils and increase surface roughness on hillslopes in order to reduce erosion (Robichaud et al., 2013). The effectiveness of mulching treatment is debated and the costs are very expensive (Schmeer et al., 2018; Maiolo-Heath, 2021). Revegetation by aerial seeding or hand planting faces similar challenges of scale and cost (Robichaud et al., 2000). Approaches targeting stream channels include replanting riparian species such as willow (*Salix* spp.), installing or promoting the formation of log jams, and constructing straw bale, rock, or log check dams (Graham, 2003; "Coalition for the Poudre River Watershed-Post-Fire Water Quality Protection"). There is growing consideration toward using beaver reintroduction and mimicry to achieve post-fire recovery goals.

Beaver populations respond both to physiographic factors, such as habitat availability, and management strategies (Morrison et al., 2015). Beaver-related restoration is growing in popularity as management adapts to acknowledge traditional ecological knowledge and the ballooning body of scientific work documenting the wide impacts of beaver (Castro et al., 2015). Managers are reintroducing beaver, protecting habitat, and mimicking their work to enhance river connectivity and bolster watershed resilience with a long list of related goals (Baker, 2003; Dittbrenner, 2019; Nash et al., 2021; Jordan and Fairfax, 2022). In 2021, Colorado Parks and Wildlife added beaver to a list of priority species with designated funding to improve habitat (Colorado Parks and Wildlife). Beaver mimicry structures such as beaver dam analogues (BDA), simulated beaver structures (SBS), and post assisted log structures (PALS), entice beaver to streams as well as promote aggradation (Pollock et al., 2007). There is growing consideration toward using these structures on fire-prone landscapes where sedimentation poses a challenge.

The term resilience may reference physical, ecological, and social systems (McWethy et al., 2019). I use the term to describe the ability of a system to maintain similar processes and configurations when faced with disturbance (Yi and Jackson, 2021). Beaver ponds enhance the ecological resilience of surrounding areas to wildfires. High water tables and large areas of surface water increase landscape resistance to burning while also speeding up vegetation regrowth after a burn (Fairfax and Whittle, 2020). Ponds may also serve as refugia for aquatic organisms impacted by the high temperatures generated by fire (Fairfax and Whittle, 2020). Beaver ponds and related wetlands have the potential to store high volumes of fire-generated carbon, offsetting some of the impacts of fire on the carbon cycle, but this has yet to be well quantified across a variety of sites (Wohl, 2013). There remain critical gaps in knowledge of the interactions between beaver damming, sediment, and carbon dynamics in a post-fire context, and knowledge of this may lead to increased management success.

1.3 Study Area

Several large wildfires burned in Colorado in 2020, providing an opportunity to study the immediate post-fire sediment dynamics in beaver ponds. The region of study (Figure 2) in the Colorado Rocky Mountains is characterized by relatively uniform geology as well as a glacial history and climate shaping dynamic ecologies.

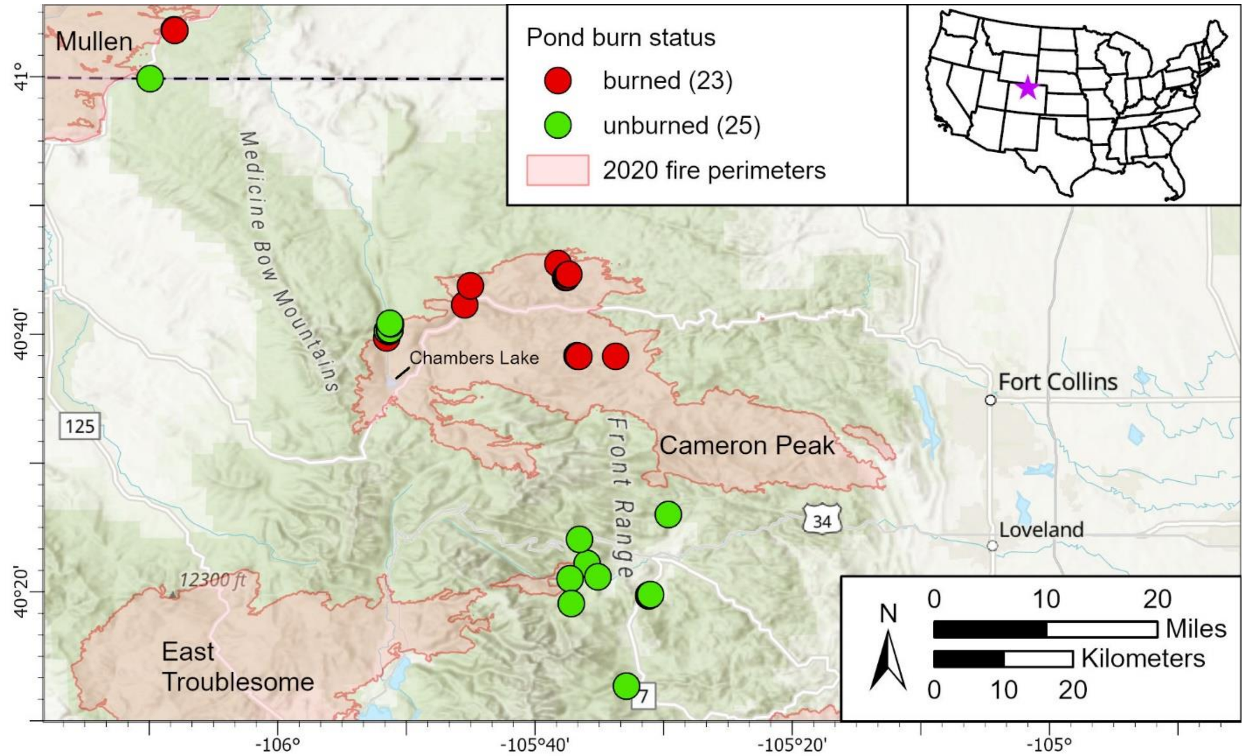

Figure 2: Locations of beaver ponds included in this study, categorized by their burn status. Red outlines indicate the perimeter of the large wildfires that burned in 2020.

1.3.1 Geology

The study area is predominantly underlain by crystalline rocks, providing a relatively consistent geologic template. Precambrian- and Proterozoic-aged granitoids and gneisses comprise the majority of the high Colorado Rocky Mountains (Horton, 2017). Clastic sedimentary units comprise a small portion of the study region; these lithologies are more prevalent in the northern portion of the study area near the Wyoming border (Horton, 2017). The crystalline bedrock weathers into gravelly to sandy surficial deposits of grus that consist of feldspar, quartz, mica, and amphiboles (Birkeland et al., 2003). On hillslopes, grus forms thin, coarse, and permeable soils, although aeolian deposition may introduce fine silts and clays. Valleys contain Quaternary deposits of glacial drift, colluvium, and alluvium.

1.3.2 Glacial history

Glaciers occupied pre-existing mountain valleys in multiple episodes during the Pleistocene (Madole et al., 1998). Most glaciers in the region did not extend below 2,450 m (8,000 ft), but the maximum down-valley extent of glaciation in the Cache la Poudre valley is 2,325 m (Madole et al., 1998). The glaciers left till deposits comprised of poorly sorted crystalline clasts with low permeability, as well as moderately sorted glaciofluvial deposits. Glacial deposits form thick sediment packages in high alpine valleys, typically with weakly developed soils (Madole et al., 1998; Kramer, 2011). Glacial landforms including moraines, outwash terraces, and overfit valleys form the physical template for beaver occupation.

1.3.3 Climate and hydrology

Elevation controls several aspects of climate in the Colorado Rocky Mountains including temperature, precipitation, humidity, and wind (Doesken et al., 2003). Beaver ponds in the study area range in elevation from 2,366 to 2,734 m (7,762 – 8,969 ft). Persistent wintertime snow accumulation may occur at these elevations, but factors such as aspect, shading, and wind shelter exert local controls (Harrison et al., 2021). Winter snowmelt and summer thunderstorms are the dominant sources of stream runoff in the mountains. Convective summer thunderstorms locally generate high intensity, short duration rainfall (Doesken et al., 2003). Although these storms may not comprise a major part of the hydrograph, they can produce flooding, initiate mass movements, and transport large volumes of sediment from hillslopes and in channels (Anderson et al., 2015; Rathburn et al., 2018). Most study sites are on ungaged tributaries, but a U.S. Geological Survey streamgage on the Big Thompson River directly below a beaver pond in Moraine Park demonstrates that peak discharge typically occurs during late spring snowmelt (Figure 3). Headwater regions contribute the majority of drinking water to major population centers: the Cache la Poudre watershed provides drinking water to more than 350,000 Colorado Front Range residents (Smith et al., 2011).

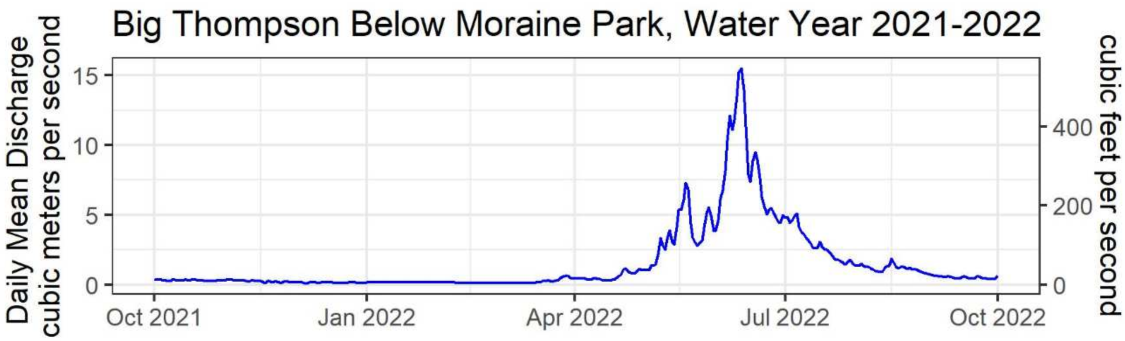

Figure 3: Daily mean discharge from USGS 402114105350101 BIG THOMPSON BL MORAINE PARK NR ESTES PARK, CO. Data from the National Water Information System (NWIS) accessed 1/13/2023.

1.3.4 Ecology

The study area spans the boundary between the mid-elevation forests and subalpine forests Level IV Ecoregions (Chapman et al., 2006). The mid-elevation forest commonly includes aspen (*Populus tremuloides*), ponderosa pine (*Pinus ponderosa*), Douglas-fir (*Pseudotsuga menziesii*), as well as areas of lodgepole pine (*Pinus contorta*) and limber pine (*Pinus contorta*). Subalpine forests contain Engelmann spruce (*Picea engelmannii*), subalpine fir (*Abies lasiocarpa*), aspen and lodgepole pine. The riparian corridors support herbaceous and woody-shrub flora with an abundance of willows (*Salix* spp.*)* which are browsed by ungulates and harvested by beaver (Malone et al., 2019). Disturbances, including wildfire, occurring over millennia have structured ecosystems in the Rocky Mountains such that they are resilient to perturbation (Minckley et al., 2012), but high severity fires may result in an alternative state (Nolan et al., 2021).

1.3.5 Fire history

Fires of varying severity have burned in the Rocky Mountain region for millennia, forming part of the disturbance regime that shapes ecology and biogeochemical cycles (Dunnette et al., 2014). Modern fires in the Rocky Mountains differ from the historical record in their size, intensity, frequency, and the elevations at which they burn (Higuera et al., 2021). In 2020, warm temperatures and dry and windy conditions allowed hundreds of blazes to rapidly spread, defying containment. The three largest fires recorded in Colorado State history burned that year ("WFIGS Wildland Fire Perimeters Full History"). My study area encompasses areas burned in the Cameron Peak (845.44 km^2), Mullen (715.80 km^2), and East Troublesome (784.33 km^2) fires (Figure 2). All three fires are thought to be human-caused, although the incidents are still under investigation. The blazes occurred unusually late in the season and at higher elevations than the usual fire-prone areas with fire-adapted ecology.

2. METHODS

I used a combination of field, laboratory, and geospatial methods to examine post-fire sediment dynamics in beaver ponds (Table 1). Field methods included ground surveys of ponds perimeters, water and sediment depths, and the collection of pond sediment cores. Laboratory methods included stratigraphic description of the sediment cores and the identification of charcoal within stratigraphic units, as well as total organic carbon and grain size analyses of each unit. In addition, I used aerial imagery to inform the history of each beaver pond. Finally, I used GIS and statistical software for data compilation and analysis.

Table 1: Summary of methods, data products, and purpose.

Methods	**Data Product(s) and Purpose**
Topographic surveying	• Pond and dam location and dimensions
Sediment probing	• Water, sediment, and total pond volume
Sediment coring	• Stratigraphic description of pond sediments • Identification of charcoal to determine fire occurrence • Sedimentation in reservoirs
Particle grain size analysis	• Grain size distribution within stratigraphic units of pond sediments
Loss on ignition (LOI)	• Total organic carbon for stratigraphic units within pond sediments
Analysis of aerial and satellite imagery	• Pond age • Age as a constraint on sedimentation rates • Beaver activity and pond abandonment • Location relative to other ponds

Geospatial analyses	• Watershed delineation
	• Burn characteristics
	    ○ Burn extent
	    ○ Burn severity
	• Vegetation characteristics
	    ○ NDVI values
	• Geomorphic characteristics
	    ○ Drainage area (current and historical)
	    ○ Watershed slope
	    ○ Relief ratio
	    ○ Valley gradient
	    ○ Valley width

Statistical analyses	• Hypothesis testing • Relative importance of explanatory variables
Sensitivity analyses	• Uncertainty in pond age estimates • Uncertainty in cored sediment depths • Impact on sedimentation rate results

2.1 Site selection

I selected beaver ponds representing a range of site characteristics while considering the accessibility of the ponds. First, I gathered a spatial database of beaver pond locations in the northern Colorado Rocky Mountain region by soliciting local knowledge and visually searching Google Earth imagery to identify possible ponds. I also compiled a list of BDAs in the region with known installation dates. I then overlaid land management and road layers to select sites located on public lands and within a reasonable hiking distance from roads and trails. I preliminarily classified each pond as burned or unburned based on published 2020 fire perimeter data. Additionally, I used aerial imagery and local knowledge to determine whether ponds were actively maintained by beaver. When selecting sites, I attempted to maintain a balance between burned and unburned sites. Some proposed sites were not included due to access difficulties or time constraints. In a few cases, ponds located from imagery were not actually beaver ponds, so these were omitted. Some sites had ponds not visible in satellite imagery that were still included.

2.2 Sediment survey and sediment collection

I validated my initial classification of ponds' burn status and beaver activity in the field and recorded additional information about each site. For the purposes of this study, I classified ponds as either on- or off-channel. I used this binary classification to describe the likelihood of sediment delivery from the channel to the pond, recognizing that a pond's connectivity to the channel may change over time. I classified pond position at the time of the field survey, generally reflecting low-flow conditions.

Additionally, I described each pond's position in relation to other ponds along a reach. Reaches are defined as distinct units separated by distance or major tributary input (thus altering hydrology and sediment supply). Ponds were classified by whether they were the only pond on a reach, "single"; if they were the upstream-most pond along the reach, "upstream"; or if they were downstream of any ponds on the reach, "downstream". Breached dams with no ponded water were not included. Dense vegetation made it difficult to detect all ponds from the ground, so I used recent satellite imagery to verify my field observations of pond sequencing. In some cases, not all ponds in a sequence were surveyed, but the sequencing order includes all ponds on a reach.

2.2.1 RTK-GPS survey

At each site, I surveyed pond coordinates and elevations with a Topcon GR-5 Real Time Kinematic (RTK) GPS (0.01 m horizontal accuracy and 0.015 m vertical accuracy). I surveyed points along the perimeter of the pond, which I defined by the presence of open standing water or standing water among wetland vegetation that appeared inundated for much of the year. I also surveyed the beaver dam crest and upstream and downstream base at several locations along the dam in order to map dam geometry. Additionally, I surveyed the location of inflow and outflow channels from the pond, along with the water surface elevation. Finally, I marked the starting and ending points of each sediment survey transect to constrain instrument drift.

The RTK base station was left running for at least two hours to collect enough data for a full correction. The correction was performed by uploading the base station files and vertical height to the NOAA Online Positioning User Service (OPUS). Surveyed points were corrected by the horizontal and vertical distance between the RTK base station and corrected base station coordinate. Due to minor equipment malfunctions, alternate GPS units were used to survey some ponds, noted in Appendix I.

2.2.2 Sediment transects

I measured the pond width with a laser range finder along each pond's longest axis, either perpendicular or parallel to the dam. I divided the distance by 3 to 8 (aiming for 5) to establish transect start points. At each start point, I strung a meter tape across the pond to the opposite shore. Sediment measurements were taken along intervals field-scaled to the pond ranging from 0.1 to 3 m. At each point along the transect, I measured water depth by gently extending a tape measure until the metal tang hit sediment. I then pushed a 2.43-m (8-foot) tile probe marked with 5 cm intervals through the unconsolidated pond sediments until refusal indicated a compacted layer. When the sediment depth exceeded the probe length, I recorded the depth as a minimum value (>2.4 m). I calculated the sediment thickness as the water depth subtracted from the total probed depth. I also noted the general texture of the sediment as determined by vibrations in the probe, the relative resistance to pushing, and audible cues.

2.2.3 Sediment cores

I used the sediment transect data to select two sites within each pond to collect sediment cores (in some cases only 1 core was collected, and at some sites 3-4 cores were collected). I targeted locations with the thickest sediments to obtain the longest record of sedimentation. I avoided areas with water depths greater than ~0.5 meters to allow for greater sediment recovery. Additionally, I attempted to select the two locations from different parts of the pond, either on different transects or at far ends, to capture the spatial variability in sediment deposition.

Cores were collected with a 1.83 m (6 ft) long, 1.9 cm (1¾ in) inner diameter polycarbonate tube. The tube was pounded into the sediment until refusal, then capped on top and pulled upward until the base was above the sediment but still submerged so a rubber stopper could be inserted. I recorded the water level at total inserted depth, the sediment thickness, and the water depth. Cores were transported and stored vertically in the tubing until they could be extruded in the laboratory.

2.2.4 Reservoir sedimentation

In August 2021, I collected four sediment cores from Chambers Lake, a high-elevation water-supply reservoir near Cameron Pass (Figure 2). Cores were collected with a 7.62 cm (3 in) diameter short corer by boat in the southwest quadrant of the reservoir (Figure 4). Coring targeted the shallow delta deposits at the mouths of Joe Wright Creek (drainage area = 48 km^2) and Fall Creek (drainage area = 13 km^2). The watersheds feeding Chambers Lake burned severely in the 2020 Cameron Peak Fire, and sedimentation rates obtained from the reservoir cores are used to compare post-fire beaver pond sedimentation with other sediment storage locations.

Figure 4: Chambers Lake sediment coring locations, August 2021.

2.2.5 Little Beaver Creek monitoring

Little Beaver Creek is a tributary to the South Fork of the Poudre with on-going post-fire research. I compiled a series of measurements at this site. First, I conducted an initial survey of pond sediment depths and collected a single short sediment core from each pond in Fall 2021 using a 7.62 cm (3 in) tube. A second, more complete survey was conducted summer 2022 using the methods described above. The pond perimeters were surveyed twice in 2022, a month apart. Game cameras captured images of two of the ponds on a 15-minute interval from May to September 2022. The images provide qualitative data on precipitation, water levels in the ponds, and sediment redistribution. I installed two pressure transducers in the main channel above and below the beaver pond reach, but a large flood washed out the sensors.

2.3 Sediment core analysis

2.3.1 Stratigraphy

The Initial Core Description methodology guided my processing of the sediment cores ("Core Processing"). Water at the top of the core column was carefully decanted from the collection tube. A rubber stopper was inserted into the top of the tube and used to push the core from the top out into a plastic-wrap-lined cradle. I sliced the extruded core in half with a knife to view stratigraphy. I then visually examined the core to identify stratigraphic units and describe them by color, texture, grain size and presence of charcoal. I collected a sample from each unit and examined it under a dissecting microscope to identify charcoal and estimate the relative abundance of sediment constituents including minerals by grain size, charcoal, colloidal material, wood, and root fibers. Cores were refrigerated to slow decomposition of organic material and alteration of minerals during storage.

2.3.2 Core selection and fire identification

The relative abundances of core constituents were used to construct visual representations of each sediment core's stratigraphy (Figure 5). Cores from each pond were visually compared. If the cores were similar, the longest one was selected for carbon and grain size analysis. If they were dissimilar, both were analyzed. The depth at which a spike in charcoal was detected was recorded. Some cores contained multiple spikes or a gradual increase in charcoal towards the surface; in these cases, a conservative upper depth and liberal lower depth was recorded to bracket possible interpretations of the fire history. These layers could represent variable transport of charcoal to the pond, multiple fire events, or mixing of pond sediments after deposition. Ultimately, the conservative (upper) interpretation was used to classify stratigraphic units as burned or unburned, and for calculating sedimentation rates. Cores from ponds located in unburned watersheds were uniformly assigned the unburned classification, even if small levels of charcoal were detected (these could be from proximal watersheds or sources other than wildfire).

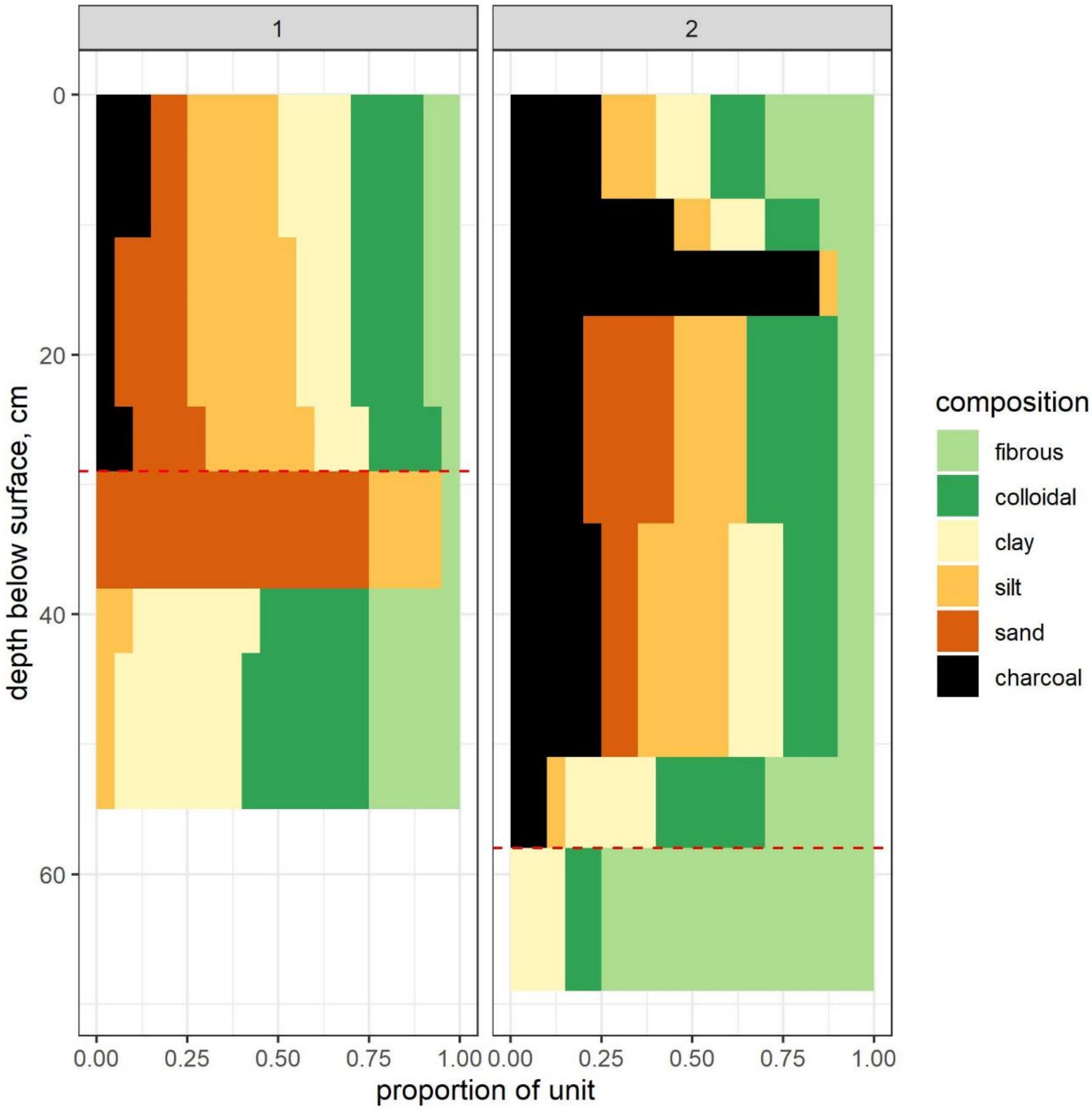

Figure 5: Example of visual plot used to identify charcoal spikes and classify stratigraphic units as pre- or post-fire. The stratigraphic units are shown by increasing depth below the mud surface and the proportion of the unit composed of each sediment class is denoted by the color blocks. The appearance of charcoal is denoted by the dashed red line on each core. The two cores visualized are from the OF-2 pond. The amount of sediment recovered from each core varied, as did the depth of charcoal accumulation.

2.3.3 Sedimentation rates

Three types of sedimentation rates were calculated. The first, lifetime sedimentation, describes the average rate of sediment accumulation over the entire lifespan of a pond. It was calculated for each sediment core by dividing the total core thickness by the age of the pond, and the mean rate was computed for ponds with more than one core. Post-fire sedimentation rate describes the rate of sediment accumulation in the years after wildfire and was calculated by dividing the thickness of sediments identified as post-fire by the number of years following wildfire. Pre-fire sedimentation rates were calculated in a similar manner to lifetime sedimentation rates, only including the pre-fire sediment thickness, and calculating the pond age at the time of fire.

2.3.4 Total Organic Carbon by Loss on Ignition (LOI)

Homogenized samples from each stratigraphic unit weighing greater than 50 grams were stored in a freezer and shipped to a professional laboratory for analysis for total organic matter by loss on ignition (Ward, 2022). Samples were dried at 105° C for two hours, cooled and weighed to obtain the dry weight. The samples were then placed in a muffle furnace at 360° C for two hours and 15 minutes, cooled and weighed to obtain the ash weight. The percent loss on ignition (LOI), or percent organic matter (OM), is calculated as:

$$\%\,OM = \%\,LOI = \left(dry\ weight - \frac{ash\ weight}{dry\ weight}\right) * 100$$

The percent organic matter may be used to estimate the percent carbon (C) using the following equations:

$$\%\,OM = \%\,C * 2$$

$$\%\,TOC \approx \%\,C = \%\,OM * 0.5$$

The 0.5 conversion factor comes from empirical studies of peat soils and the median factor across several soil types (Pribyl, 2010). This conversion factor is used rather than the Van Bemelen factor because of the organic-rich nature of beaver pond sediments. The percent carbon is assumed to be closely equivalent to the percent total organic carbon (TOC) because of the low occurrence of carbonate rocks within the region.

2.3.5 Grain size

The same stratigraphic units analyzed for TOC were resampled for grain size from the other half of the sediment core. The samples were heated in a muffle furnace at 550° C for 6 hours to remove organic material, following the method outlined by Heiri and others (2001). Cooled samples were bagged and then weighed. The samples were then gently disaggregated with a mortar and pestle and brushed through a 1 mm sieve. They were returned to the bag and weighed, and the difference in pre- and post-sieving weight was used to calculate the greater than 1 mm grain size fraction. The finer than 1 mm fraction was measured in a Malvern particle size analyzer at Utah State University with a detection range between 0.1 – 1000 microns. Each sample aliquot was run three times and data output as percent of total sample within each size class. The percentages were adjusted to account for the >1 mm size fraction and assigned a grain size class following the Wentworth grade scale. The median grain size (d_{50}) as well as the 10th (d_{10}) and 90th (d_{90}) percentiles were computed from the binned data by finding the two closest binned percentages and calculating the equation for the line between these points. Ultimately, the percent fines were used in analysis in line with previous research (e.g., Lininger et al., 2018). The median grain size, d_{50}, showed relationships with explanatory variables that were similar to percent fines, so this metric was not included in the formal analysis.

2.4 Geospatial data compilation

2.4.1 Burn

Burn characteristics capture watershed-scale fire impacts and were calculated from published spatial datasets. The recent history of fire occurrence was checked by intersecting the watershed layer with the WFIGS – Wildland Fire Perimeters Full History dataset ("WFIGS Wildland Fire Perimeters Full History"). One pond's watershed burned in 2021 in a small fire adjacent to the 2020 Mullen fire perimeter. This pond (site ID = BOS-1; Appendix I) was excluded from analysis because of the confounding burn history. The burn severity within each watershed was summarized from the Soil Burn

Severity dataset for each major fire (USDA Forest Service, Geospatial Technology and Applications Center, BAER Imagery Support Program, 2020a, 2020b, 2021). Burn severity was incorporated into two metrics: the total percent of each area burned at any severity (% burned), and the percent of each area burned at moderate and high severities (% burned (severity)). These two burn severity metrics were analyzed for entire watersheds and locally within 200 m buffered polygons around each pond.

2.4.2 Vegetation

Vegetation characteristics were derived using the Normalized Difference Vegetation Index (NDVI), which is a measure of greenness. NDVI values were calculated from Landsat 8 satellite imagery with a 30 m resolution. A Google Earth Engine script compiled images collected between July and September for the years 2017-2022 (Appendix II). A cloud mask filter was applied, and median values used to form a composite image for each year. The NDVI raster files were exported to ArcPro, where summary spatial statistics for each year and watershed were calculated then exported as a table for statistical analysis in R. Median 2019 NDVI values are considered as representative of pre-fire condition whereas 2022 is used for the post-fire condition. Additionally, the difference in median NDVI values between 2021 and 2022 was used to quantify the magnitude of post-fire vegetation recovery. The three vegetation metrics were analyzed at the same two scales as burn severity (watershed and a "local" 200 m buffered pond polygon).

2.4.3 Geomorphic

Watersheds were delineated with the ArcPro watershed (ready to use) tool. The tool used the 30 m resolution National Elevation Dataset (NED) to delineate watersheds with the beaver ponds' exact locations as pour points. The pour point locations were manually adjusted to reflect field conditions (connected vs disconnected to the channel) where necessary (current watershed area). A second watershed delineation ran with a 250 m snap tolerance for the pour points to simulate the historical condition of ponds that were once connected to the channel but are no longer (historical drainage area).

The current watershed area was used in calculating burn and vegetation characteristics. The pond perimeters measured by RTK-GPS were buffered with a 200 m surrounding polygon, which was used to calculate local burn and vegetation characteristics.

Relief ratio captures the difference between the highest and lowest elevations in a watershed divided by the straight-line distance between those points; it was calculated from 10 m DEMs provided by the USGS ("USGS," 2023a; "USGS," 2023b; "USGS," 2023c). Slope was generated in ArcPro and the mean slope calculated for each pond's watershed. The valley gradient was also compiled from these DEMs by manually digitizing 100 m lines along the valley axis upstream of each beaver pond. Valleys were identified using both the DEM shaded relief and vegetation changes visible in satellite imagery. The change in elevation between the start and end points of this line, divided by the distance, yielded the gradient. One negative slope value occurred in a reach heavily impacted by beaver. Because this value is attributed to beaver modification rather than underlying geomorphology, the value was corrected to 0 for analysis. The resolution of the DEM did not permit accurate calculations of stream gradient, especially on small multithread channels impacted by beaver. The valley width was calculated at each beaver pond by manually drawing a line perpendicular to the valley axis. In incised reaches, the width of the historical floodplain was measured.

2.5 Analytical methods

2.5.1 Pond volume interpolation

RTK-GPS point measurements were used to construct polygons of ponds and plot sediment measurements along the transect lines (Appendix II). The ArcPro Spline with Barriers tool interpolated water depth, sediment depth, and sediment thickness between probe measurement points, bounded by the pond perimeter. The sediment volume was calculated by summing the sediment thickness of all grid cells in the pond area. The residual pool volume (V^*) was calculated as the proportion of the total pool volume free of sediment (Lisle and Hilton, 1992; Scamardo et al., 2022). V^* is independent of discharge and pond size, allowing for comparison between sites. Notably, total sediment volume differs from residual volume in that sediment volume is an absolute measured amount rather than a percentage.

2.5.2 Pond age

Pond ages were determined by examining Google Earth imagery and identifying when ponds became visible. Imagery was available at most sites from the years 1985, 1999, 2005, 2011, 2013, 2016, and 2019, providing decadal comparison. Dates of pond establishment were bracketed into a minimum and maximum, describing the time frames between no pond and pond. If the pond was visible in the oldest available, the age of this imagery was used as a minimum age. Similarly, pond abandonment was bracketed by full pond/growth, and pond shrinkage/infilling. Dates of pond abandonment are less certain because of the seasonal variability in pond size and vegetation growth, and because of variations in beaver habitation. Thus, the abandonment age is meant as a general indication of pond persistence rather than an absolute date. If there appeared to be multiple periods of pond occupation, the oldest establishment year was used along with the most recent abandonment year.

The pond age was calculated by subtracting the mean of the bracketed establishment years from 2022 (the year of field surveying). Because of the inconsistent interval between imagery, pond ages were summarized into three age classes. In this classification, ponds older than 2000 are considered old, those dating between 2000 and 2015 are moderate, and those established after 2015 are recent. A sensitivity analysis used the minimum and maximum establishment years to determine whether statistical response variables were impacted by this method of age selection.

2.5.3 Sedimentation rate sensitivity analysis

Lifetime sedimentation rates were calculated by dividing measured sediment thicknesses from sediment cores by pond age. Pond ages were estimated from aerial imagery, which introduces uncertainty because imagery was not available at uniform time-steps. Additionally, sediment thickness was measured by probing and from sediment cores. I conducted a sensitivity analysis to determine how much of an influence my interpretation of pond ages and choice of pond depth measurement have on calculations of lifetime sedimentation rates and the subsequent analysis of explanatory variables that influence those rates. It is important to emphasize that post-fire sedimentation rates were not impacted by the age uncertainty because the year of fire was known and post-fire sediment thicknesses were visually measured from sediment cores.

I evaluated my certainty about pond establishment dates by dividing ponds into certainty classes. The first consists of ponds with known establishment dates. This class consisted of seven ponds including BDAs with known construction details, and ponds recently constructed by beaver where local knowledge confidently identifies establishment time. A second class of 13 ponds encompassed those constrained between two years of nonconsecutive imagery, so the pond was known to have been established between the first date and the last. A third class included 19 ponds that were established before the first year of imagery with sufficiently high resolution to detect valley features, so pond establishment is unconstrained. To compare the implications of choosing different establishment dates, I calculated sedimentation rates using the minimum and maximum dates of the constrained ponds. For the unconstrained ponds, I calculated rates arbitrarily, assuming that ponds were 50 and 100 years old.

I also calculated lifespan sedimentation rate using three sediment thicknesses. The total thickness of cored pond sediments constitutes the first group. This is the rate I used in my full analysis because it is consistent with my method for calculating post-fire sedimentation rates, and because I visually inspected the sediments present in the core, so I can confidently interpret the sediments as ponded in origin. I compare the core rate to two rates derived from probed thicknesses: mean and maximum thicknesses of probed points within each pond.

I tested differences between the pond lifetime sedimentation rates used in my full analysis and each of the other age and depth-varied rates using the Kruskal Wallis and Dunn tests. I evaluated whether substituting the constrained minimum and maximum or the unconstrained 50 and 100-year-old rates into the complete lifetime sedimentation rate dataset changed the outcome of hypothesis testing between three arbitrarily selected categorical explanatory variables. These variables were: pond burn status, position in relation to the channel, and age classification (based on the mean pond age used in the full analysis). I repeated this outcome comparison with full substitution of the rates calculated by different depth method.

2.5.4 Statistical analysis

I focused my statistical analyses on the residual pool volume, sedimentation rates, grain size distribution, and TOC content of beaver ponds. My analytical goals and methods were descriptive and explanatory rather than predictive. I use the terminology of explanatory and response variables to distinguish between the independent controls and outcomes of empirical data. A full list of explanatory and response variables is presented in Figure 6**.** Statistical analyses were conducted using R 4.2.2 software and packages (Cribari-Neto and Zeileis, 2010; Wickham et al., 2019; Kassambara, 2022; R Core Team, 2022; Lenth, 2023). The distribution of data was examined with histograms, QQ-plots, and the Shapiro-Wilk test. All computed p-values were evaluated for significance using a threshold of $\alpha<0.05$.

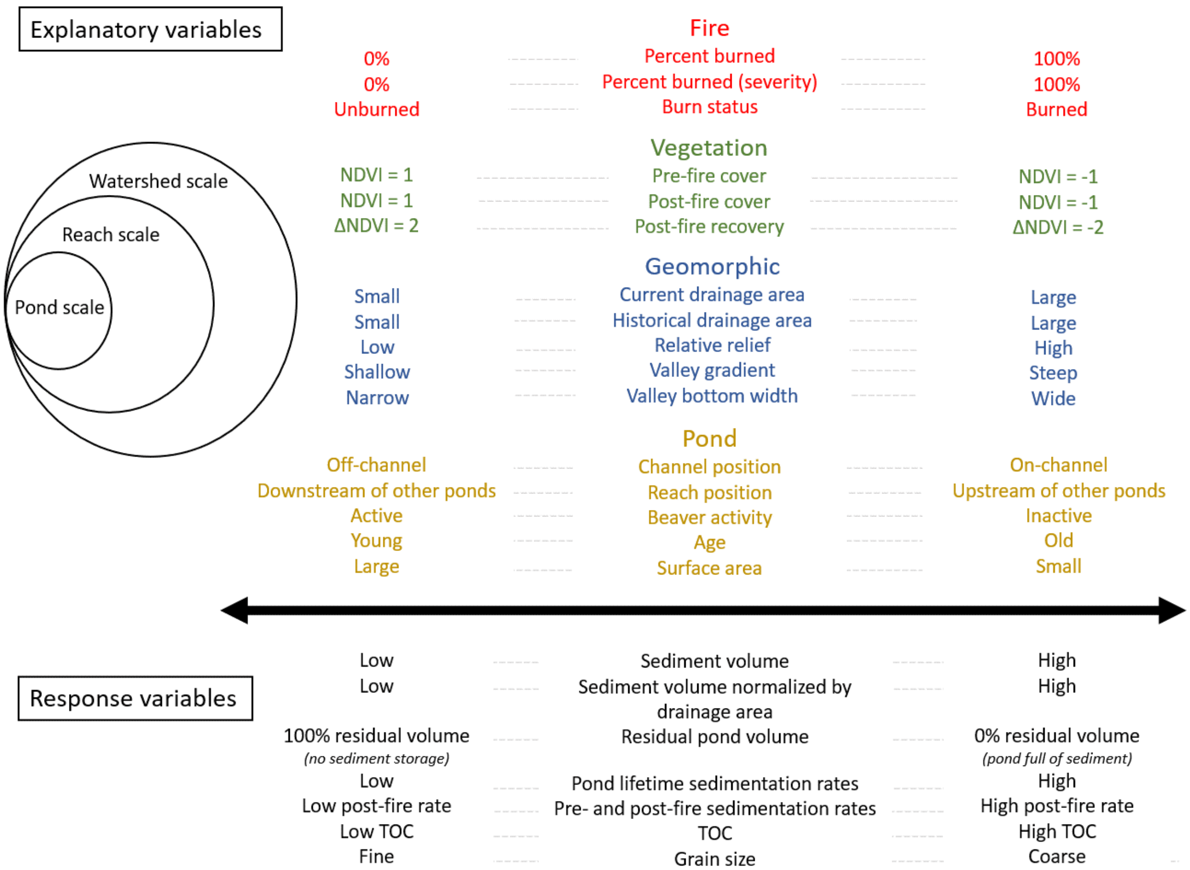

Figure 6: Conceptual diagram showing how burn, vegetation, geomorphic, and pond characteristics are expected to influence pond sediment characteristics. The explanatory variables tested in this study are grouped and colored by characteristic. The response variables used to test the three hypotheses are shown in black below. The theoretical end-member responses are shown on either side of the arrow. Correspondingly, the direction of expected impact and end-member responses are shown for the explanatory variables. For example, higher percentages of watershed burned are expected to correspond to lower residual pool volumes, higher sedimentation rates, and coarser and more carbon-rich sediment. Explanatory variables may also be considered in terms of their spatial scale and are organized in decreasing extent.

Most of the explanatory and response variables were non-normally distributed, even after standard transformations, so non-parametric statistical tests were used to evaluate differences and relationships. Two-sample Wilcoxon signed rank tests were used for categorical explanatory variables with two groups (Wilcoxon, 1945). Where three or more groups were present, the Kruskal-Wallis rank sum test evaluated whether the group medians were significantly different (Kruskal and Wallis, 1952). If the Kruskal-Wallis test indicated a difference, Dunn's test was used to determine which groups were different (Dunn, 1961). A paired samples Wilcoxon test was used to compare pre- and post-fire sedimentation rates and compositions (Wilcoxon, 1945).

Linear models and beta regressions were used to evaluate the strength of relationship between continuous explanatory and response variables. Because the response variables residual pond volume and TOC take the form of a percentage, beta regressions were used to model the distribution and response (Kieschnick and McCullough, 2003; Ferrari and Cribari-Neto, 2004). For both beta and linear regression models, the modeled residuals were used to evaluate model assumptions. The p-value was used to determine the significance of the model and the adjusted, or in the case of beta regression, pseudo R^2 value indicated the goodness of fit.

Multiple linear regression allowed for assessment of the relative importance of each explanatory variable. For each response variable, a full model was constructed and compared with selective models. The selective models were constructed by first removing covariates that were strongly and intuitively correlated (for example, current and historical watershed area), with preference given to the more process-oriented variable. Explanatory terms were then added one by one to the model in order of significance until any additional variables were not significant or there were three terms, whichever came first. The three-term cutoff was implemented to avoid overfitting of the models. Like the pairwise analysis, model assumptions were evaluated and the adjusted R^2 values were used to compare between models. The same transformations of response variables were used as in the pairwise analysis, except for TOC, which was transformed solely for multiple linear regression.

3. RESULTS

A total of 48 ponds were visited during the 2022 field season, but three ponds were excluded from analysis. At one location, the two ponds were muddy topographic depressions with minimal standing water and thus did not meet the pond criteria (site ID = ELK-1 & ELK-2, Appendix I). A small fire had burned another pond in 2021 (site ID = BOS-1, Appendix I), creating compounding signals from the 2020 fire also in the watershed. Table 2, Table 3, and Table 5 present summaries of explanatory and response variables across all 45 sites. The full dataset is included in Appendix I. Several of the explanatory variables quantify similar attributes and processes and may be correlated as a result. Indeed, I found that burn metrics and vegetation recovery are strongly correlated (Figure 7). Many vegetation metrics are correlated across time periods and between the local and watershed scales. Geomorphic characteristics also exhibit strong correlations; for instance, the relief ratio of a watershed strongly correlates to its mean slope (corr = 0.5). In contrast, the mean watershed slope negatively correlates to the 2019 pre-fire median NDVI of the watershed (corr = -0.5). These correlations informed choice of variables for inclusion in multiple linear regression analyses, a summary of which is presented in Table 4. The results of hypothesis testing, as described in the following sections and linear regression plots, are provided in Appendix IV.

Table 2: Summary of mean burn and vegetation metrics by pond category.

		Burn			Vegetation					
		number of ponds	**percent burned**	**percent burned (severity)**	**pre-fire watershed vegetation cover (NDVI)**	**pre-fire local vegetation cover (NDVI)**	**post-fire watershed vegetation cover (NDVI)**	**post-fire local vegetation cover (NDVI)**	**post-fire watershed vegetation recovery (ΔNDVI)**	**post-fire local vegetation recovery (ΔNDVI)**
Burn status	**burned**	21	57	27	0.21	0.25	0.16	0.19	0.02	0.01
	unburned	24	14	5	0.19	0.27	0.17	0.25	0.00	-0.02
Channel position	**on-channel**	30	37	17	0.19	0.26	0.17	0.23	0.02	0.00
	off-channel	15	28	11	0.21	0.25	0.16	0.21	0.00	-0.02
Reach position	**single**	6	35	21	0.17	0.30	0.13	0.27	0.00	-0.01
	upstream	9	34	13	0.20	0.25	0.17	0.22	0.01	-0.01
	downstream	30	35	17	0.22	0.26	0.18	0.22	0.02	0.00
Beaver activity	**active**	7	20	12	0.21	0.29	0.18	0.27	0.02	-0.01
	inactive	28	49	21	0.21	0.25	0.16	0.21	0.01	0.00
	BDA	10	2	0	0.17	0.26	0.17	0.23	0.00	-0.03
Age	**recent**	19	19	12	0.18	0.27	0.17	0.23	0.01	-0.01
	moderate	9	50	11	0.21	0.28	0.19	0.27	0.02	0.00
	old	17	43	20	0.21	0.24	0.15	0.19	0.01	-0.01

Table 3: Summary of mean geomorphology and pond metrics by pond category.

		Geomorphology						Pond	
		current drainage area, km^2	historical drainage area, km^2	watershed slope	relief ratio	valley gradient	valley width, m	pond surface area, m^2	pond age, years
Burn status	**burned**	7	11	3522	0.12	0.026	143	950	18
	unburned	15	29	10944	0.23	0.030	184	886	12
Channel position	**on-channel**	16	19	2810	0.17	0.034	151	760	10
	off-channel	2	24	14652	0.19	0.016	192	1227	25
Reach position	**single**	42	55	9435	0.21	0.010	236	1721	10
	upstream	7	15	5744	0.21	0.028	159	767	17
	downstream	7	18	7047	0.16	0.040	136	873	12
Beaver activity	**active**	35	38	402	0.18	0.022	243	2049	6
	inactive	5	20	10014	0.17	0.021	163	936	21
	BDA	12	12	1	0.21	0.050	114	64	4
Age	**recent**	21	22	16	0.18	0.042	123	478	4
	moderate	4	28	12634	0.21	0.016	237	1130	20
	old	4	16	9939	0.16	0.018	173	1291	25
All ponds		*11*	*21*	*7142*	*0.18*	0.18	*165*	*916*	*15*

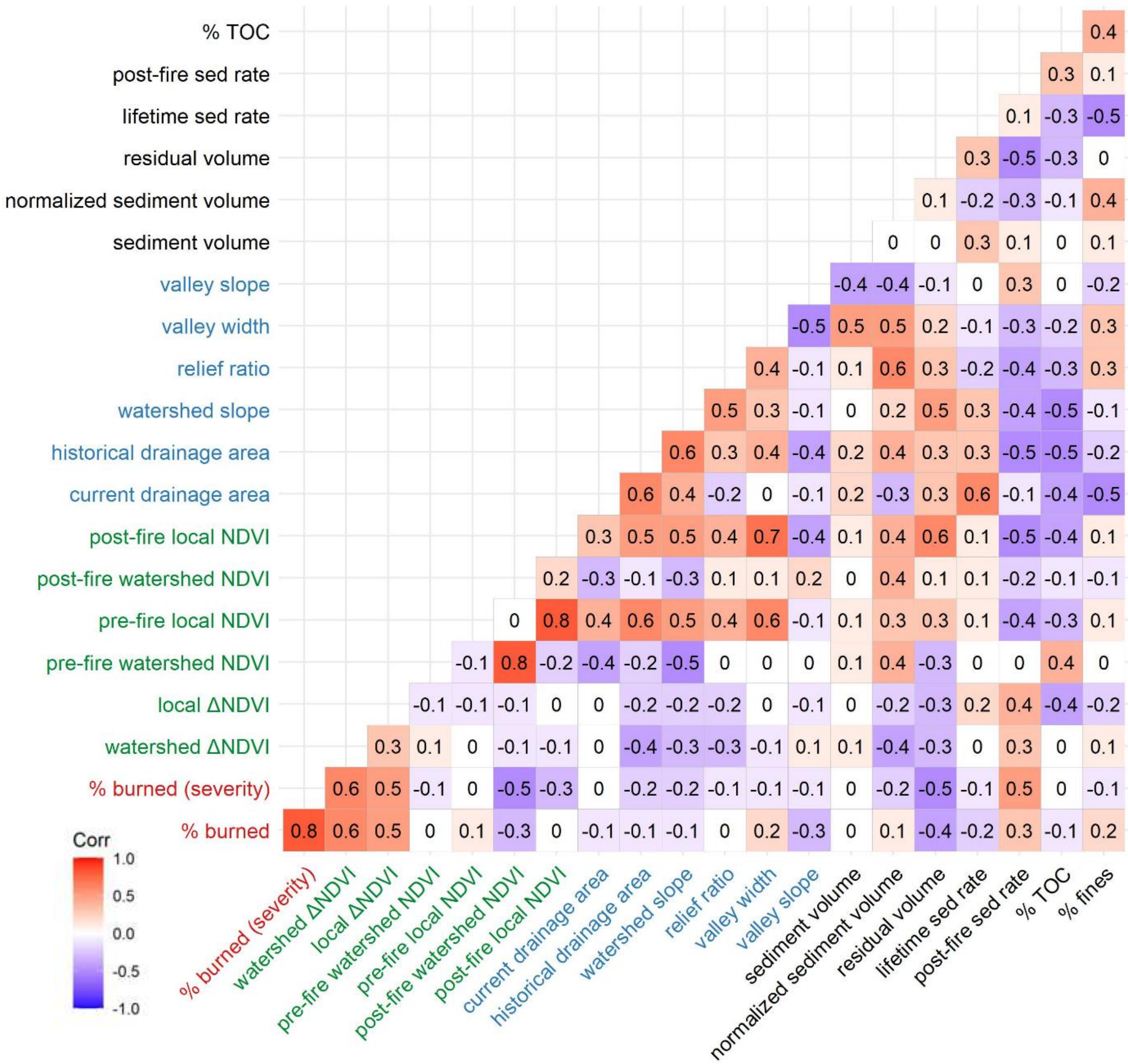

Figure 7: Correlogram showing the correlation between all variables included in hypothesis testing and regression modelling. Explanatory variables grouped and colored by type such that burn characteristics are red, vegetation characteristics are green, and geomorphic characteristics are blue. Response variables are shown in black. The correlation coefficients for each pair of variables are presented within the grid, and grid cells are colored by the strength of the correlation. Strong positive correlation is indicated by red, strong negative correlation is indicated by blue, and weaker correlation in whites.

Table 4: Summary of multiple linear regression models. The best fit model for each response variable is summarized by the multiple R^2 value, explanatory variables included, and the category of those variables.

Response Variable	Multiple R^2	Explanatory Variables	Type
Sediment volume	0.85	pond surface area	pond
		beaver activity	pond
		age class	pond
Sediment volume normalized by drainage area	0.78	age class	pond
		relief ratio	geomorphology
		beaver activity	pond
Residual volume	0.47	watershed slope	geomorphology
		total percent burned	burn
		channel position	pond
Lifetime sedimentation rate	0.66	age class	pond
		relief ratio	geomorphology
Post-fire sedimentation rate	0.19	valley slope	geomorphology
Grain size	0.32	current drainage area	geomorphology
		pre-fire NDVI local	vegetation
TOC	0.63	reach position	pond
		channel position	pond
		watershed slope	geomorphology

3.1 Sediment storage

3.1.1 Pond sediment volume pairwise comparisons

The median volume of sediment stored in 40 individual ponds was 465 m^3 with a mean of 796 m^3 and a range from 4 m^3 to 4888 m^3. A cube root transformation corrected the strong right skew of the sediment volume data and was used in regressions with continuous explanatory variables. Burn and vegetation characteristics did not significantly relate to pond sediment volume, and only one geomorphic characteristic significantly related. The percent of burning within a watershed (adjusted R^2 = -0.01, p = 0.39) and percent that burned at moderate and high severities (adjusted R^2 = -0.02, p = 0.61) showed weak positive relationships with sediment volume. Burned ponds stored greater volumes of sediment (n = 21, median = 563 m^3) than unburned ponds (n = 19, median = 361 m^3) but the difference is not significant (p = 0.07).

Table 5: Summary of mean sediment response metrics by pond category. V indicates residual pond volume.*

		Sediment						
		sediment volume, m^3	**normalized sediment volume, m^3/km^2**	**% *V****	**lifetime sedimentation rate, cm/yr**	**post-fire sedimentation rate, cm/yr**	**% TOC**	**% fines**
Burn status	**burned**	958	3522	17.7	4.6	15.7	9.3	48.0
	unburned	601	10944	45.4	8.5	3.7	5.0	44.3
Channel position	**on-channel**	670	2810	34.8	9.0	11.3	4.8	40.5
	off-channel	981	14652	24.3	2.3	9.3	10.9	54.2
Reach position	**single**	903	9435	44.1	13.8	2.1	1.9	26.5
	upstream	821	5744	30.7	4.4	10.9	9.0	50.4
	downstream	746	7047	21.7	7.5	15.3	6.3	49.7
Beaver activity	**active**	1574	402	50.3	18.9	8.9	3.7	35.0
	inactive	780	10014	22.0	3.7	12.3	8.6	50.2
	BDA	13	1	52.9	8.3	0.5	3.0	30.8
Age class	**recent**	391	16	39.0	15.3	11.4	4.1	32.1
	moderate	744	12634	34.7	2.0	5.1	6.5	55.1
	old	1109	9939	22.1	2.7	12.8	9.8	52.2
All ponds		*784*	*7142*	*30.9*	*6.3*	*10.5*	*7.4*	*46.5*

Vegetation characteristics showed no indication of any relationship with sediment volume except for watershed post-fire vegetation recovery which showed a weak and non-significant positive correlation to sediment volume (adjusted R^2 = -0.01, p = 0.40). Watershed pre- (adjusted R^2 = 0.00, p = 0.32) and post-fire (adjusted R^2 = -0.01, p = 0.48) vegetation cover were not correlated to sediment volume, nor were local pre- (adjusted R^2 = -0.02, p = 0.72) and post-fire (adjusted R^2 = -0.03, p = 0.93) vegetation cover and local post-fire vegetation recovery (adjusted R^2 = -0.03, p = 0.97).

Of the geomorphic characteristics, only valley gradient significantly related to sediment volume such that ponds in steeper valleys stored lower volumes of sediment (adjusted R^2 = 0.25). In contrast, valley width (adjusted R^2 = 0.14) positively correlated with sediment volume. The current (adjusted R^2 = -0.03, p = 0.93) and historical drainage area (adjusted R^2 = 0.02, p = 0.17), and relief ratio (adjusted R^2 = -0.01, p = 0.50), also positively correlated with sediment volume, although not significantly. The mean watershed slope showed no relationship to sediment volume (adjusted R^2 = -0.02, p = 0.54).

The pond surface area strongly correlated with sediment volume such that larger ponds contained more sediment (adjusted R^2 = 0.59). Off-channel ponds (n = 15, median = 763 m^3), store significantly more sediment than on-channel ponds (n = 25, median = 241 m^3), and inactive ponds (n = 28, median = 628 m^3) store significantly more sediment than either active ponds (n = 6, median = 306 m^3) or BDAs (n = 6, median = 12 m^3) (Figure 8). Additionally, older ponds (n = 17, median = 756 m^3) store more sediment than recently constructed ponds (n = 14, median = 79 m^3), although not significantly more than moderately aged ponds (n = 9, median = 416 m^3, p = 0.22). The position of the pond on a reach did not significantly correspond with sediment storage (p = 0.96), but upstream ponds contained more sediment (n = 8, median = 504 m^3) than downstream ponds (n = 26, median = 491 m^3), followed by ponds that were solitary on a reach (n = 6, median = 343 m^3).

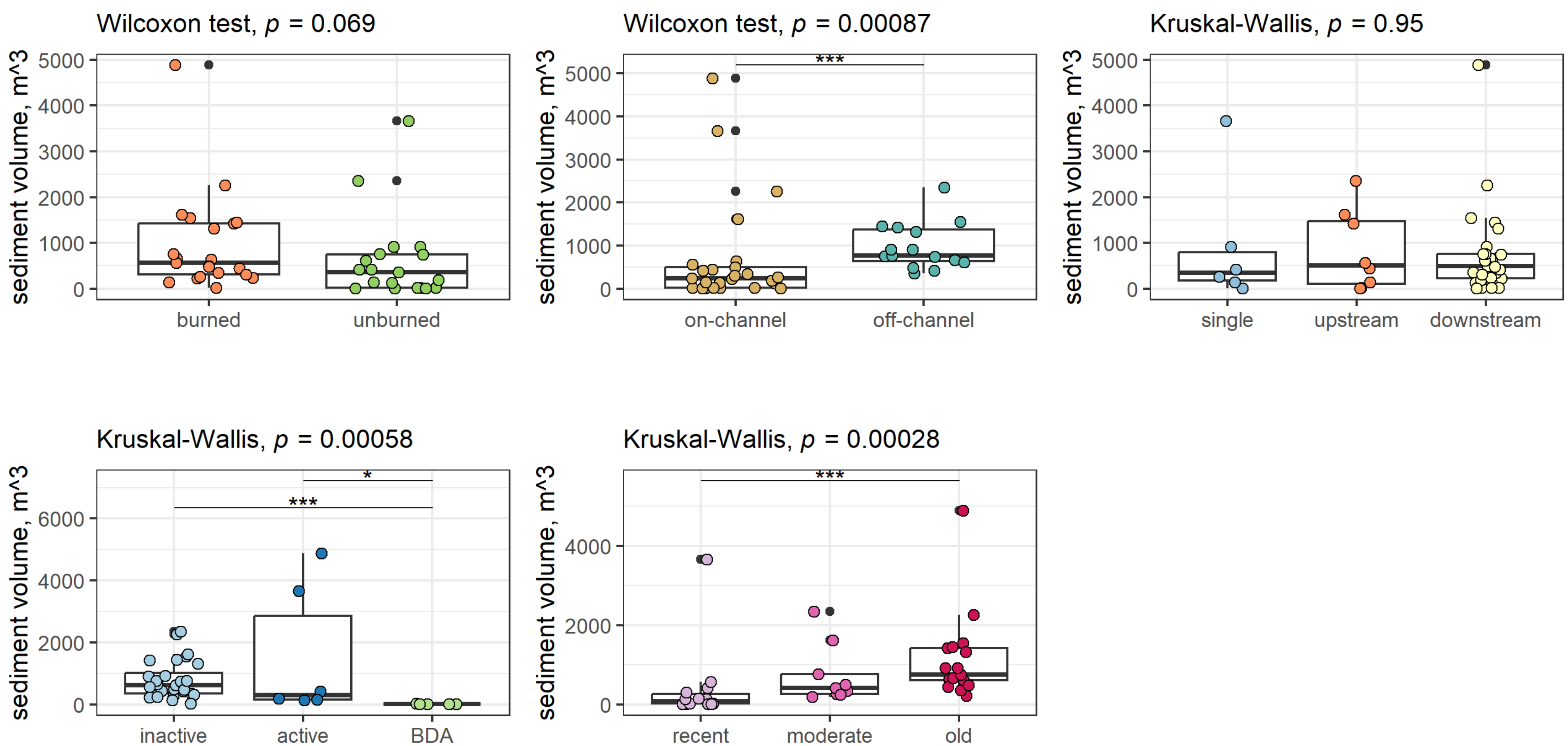

Figure 8: Results of pairwise analyses of explanatory variables and pond sediment volume (m^3). Differences in sediment volume by categorical explanatory variables are shown with box plots. The results of hypothesis testing via the Wilcoxon rank signed test or Kruskal-Wallis test are displayed above each plot. Additionally, connecting lines and asterisks show significant differences in medians between groups and the number of asterisks designate the level of significance.

3.1.2 Pond sediment volume multiple linear regression

Because of the right-skewedness of the sediment volume data, a cube root transformation was used to achieve a normal distribution for multiple linear regression analysis. The multiple linear regression analysis yields three explanatory variables that best describe the variation in pond sediment volume. The ponds' surface area, beaver activity, and the pond age class collectively describe much of the variation ($R^2 = 0.85$). The regression equation is:

$$cbrt(sediment\ volume) = 5.73 + 0.002 * (surface\ area) - 0.96 * (activity_{active}) - 3.57 * (activity_{BDA}) + 0.71 * (age_{moderate}) + 1.88 * (age_{old})$$

3.1.3 Normalized pond sediment volume pairwise comparisons

Pond sediment volume normalized by the current drainage area had a median value of 150 m^3/km^2 and a range from 0.4 m^3/km^2 to 56,546 m^3/km^2. A log transformation corrected the strong right-skewedness of the normalized pond sediment volume data. The transformed response was used as the response variable in linear regressions with continuous explanatory variables.

Burn characteristics did not significantly relate to normalized sediment volumes. The extent of burning (adjusted $R^2 = 0.03$, $p = 0.16$) and the severity of burning (adjusted $R^2 = -0.02$, $p = 0.55$) in a watershed showed no relationship to normalized sediment volume. Burned ponds store greater normalized sediment volumes ($n = 21$, median = 164 m^3/km^2) than unburned ponds ($n = 19$, median = 45 m^3/km^2) ($p = 0.57$).

Pre-fire watershed vegetation cover significantly correlated with the normalized sediment volume in a positive direction (adjusted $R^2 = 0.21$). Post-fire watershed (adjusted $R^2 = 0.03$, $p = 0.14$), and pre- (adjusted $R^2 = -0.02$, $p = 0.57$) and post-fire (adjusted $R^2 = 0.00$, $p = 0.30$) local vegetation cover all corresponded positively with normalized sediment volume but not significantly. Local post-fire vegetation recovery showed a weak negative correlation (adjusted $R^2 = 0.00$, $p = 0.36$) whereas watershed post-fire vegetation recovery did not relate to normalized sediment volume (adjusted R^2 = -0.03, p = 0.89).

Of the geomorphic characteristics, relief ratio, valley gradient, and valley width significantly related to normalized sediment volumes. The valley gradient (adjusted R^2 = 0.32) negatively corresponded to normalized sediment volume whereas relief ratio (adjusted R^2 = 0.18) and valley width (adjusted R^2 = 0.20) showed positive relationships. The mean watershed slope also showed a non-significant weak negative correlation with normalized sediment volume (adjusted R^2 = -0.02, p = 0.68).

Off-channel ponds (n = 15, median = 796 m^3/km^2) have significantly higher normalized sediment volumes than on-channel ponds (n = 21, median = 41 m^3/km^2) (Figure 9). Inactive ponds (n = 28, median = 406 m^3/km^2) have significantly higher normalized sediment volumes than BDAs (n = 6, median = 0.7 m^3/km^2). Normalized volumes in active ponds (n = 6, median = 25 m^3/km^2) are higher than BDAs and lower than inactive ponds although neither difference is significant. Recently constructed ponds (n = 14, median = 3 m^3/km^2) have significantly lower normalized sediment volumes than either moderately aged ponds (n = 9, median = 1890 m^3/km^2) or older ponds (n = 17, median = 462 m^3/km^2). Ponds downstream of others on a reach (n = 6 median = 8 m^3/km^2) had the lowest normalized sediment volume followed by upstream ponds (n = 8, median = 162 m^3/km^2) and single ponds (n = 26, median = 324 m^3/km^2) but the difference is not significant (p = 0.26). Pond surface area showed a significant positive correlation with normalized sediment volume (adjusted R^2 = 0.12).

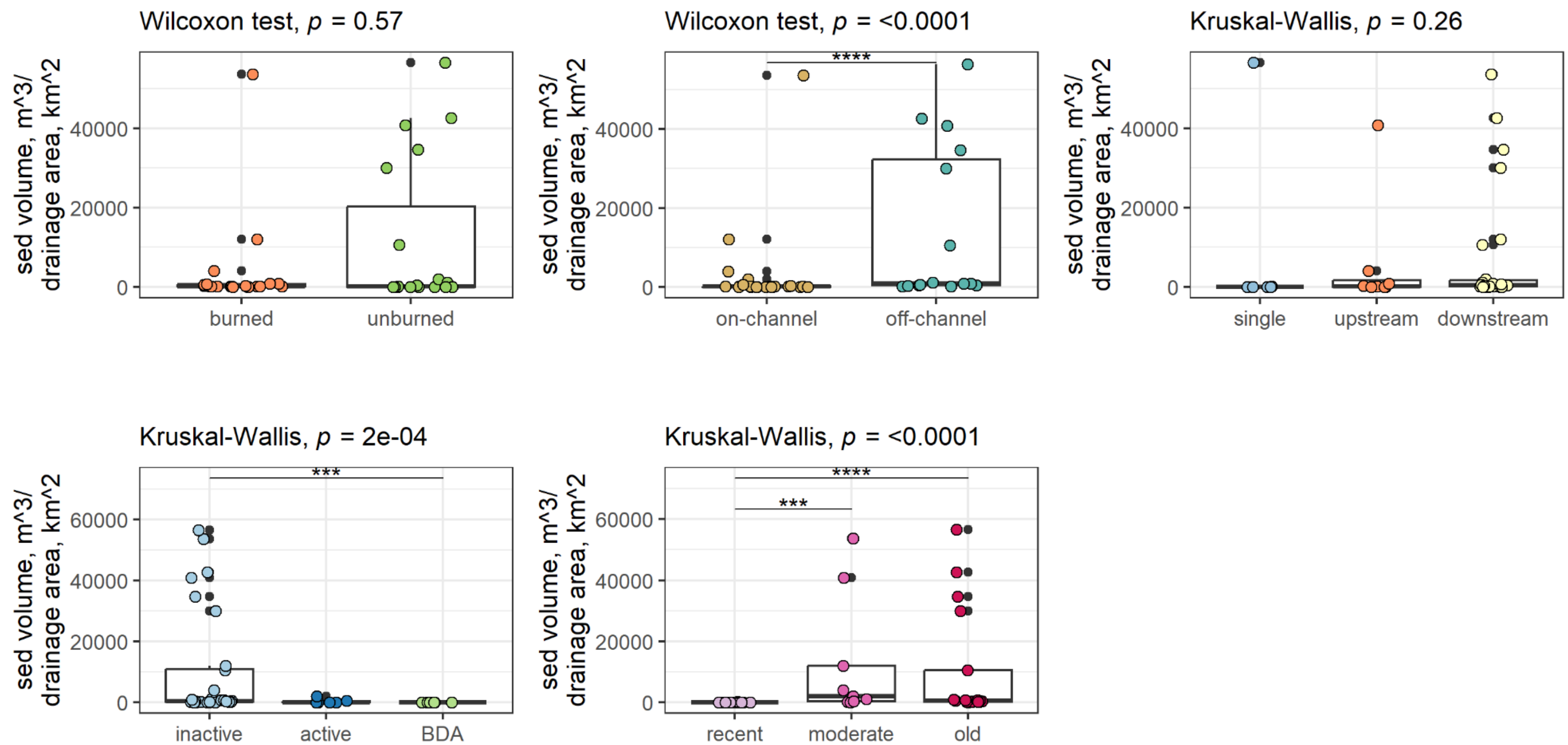

Figure 9: Results of pairwise analyses of explanatory variables and pond sediment volume (m^3) normalized by drainage area (km^2). Differences in normalized sediment volume by categorical explanatory variables are shown with box plots. The results of hypothesis testing via the Wilcoxon rank signed test or Kruskal-Wallis test are displayed above each plot. Additionally, connecting lines and asterisks show significant differences in medians between groups and the number of asterisks designate the level of significance.

3.1.4 Normalized pond sediment volume multiple linear regression

Multiple linear regression indicated that over three fourths of the variation in normalized sediment volume could be explained by three variables: pond age, beaver activity, and the watershed relief ratio (multiple $R^2 = 0.78$). The equation is given as:

$$\log\left(\frac{sediment\ volume}{drainage\ area}\right) = 0.44 + 1.61\ (age_{moderate}) + 1.55 * (age_{old}) + 5.65 *\ (relief\ ratio) - 0.29 * (activity_{active}) -\ 1.53 * (activity_{BDA})$$

3.1.5 Residual volume pairwise comparisons

Residual pond volume was calculated for 40 ponds, resulting in a median of 29.5% remaining storage and a range from 0.1% to 70.2% (Table 5, Appendix I). Burn characteristics generally related to the residual volume. The percentage of the watershed burned was significantly related to the residual volume (pseudo $R^2 = 0.21$) such that higher percentages of burned area corresponded to lower residual volumes, meaning greater volumes of sediment in storage. The percentage of the watershed burned at moderate and high severities was also significant and had higher explanatory strength (pseudo $R^2 = 0.37$). Local observations of each pond's burn status indicate that burned ponds contain less remaining storage space (n = 21, median = 15.3 *V**) than unburned ponds (n = 19, median = 41.9 *V**) (Figure 10).

Vegetation recovery, measured as post-fire ΔNDVI, also significantly related to residual volume at both watershed and local scales, although in opposing directions. Local post-fire ΔNDVI, within the 200 m area surrounding ponds, has a positive relationship with residual volume and higher explanatory strength (pseudo $R^2 = 0.43$) than watershed post-fire ΔNDVI, which has a negative relationship and lower explanatory strength (pseudo $R^2 = 0.17$). Both pre- and post-fire vegetation cover, measured as median NDVI, relate positively to residual volume at the local scale, although pre-fire has less strength (pseudo $R^2 = 0.0.07$) than post-fire (pseudo $R^2 = 0.43$). These vegetation metrics do not relate at the watershed scale, although their p-values are low (pre-fire p = 0.11, post-fire p = 0.08) (they have a negative relationship that is not significant).

Geomorphic characteristics do not consistently relate to residual volume. Larger historical watershed area (pseudo $R^2 = 0.09$) and steeper mean watershed slope (pseudo $R^2 = 0.14$) significantly correspond to higher residual volume, meaning less sediment storage. The current watershed area (pseudo $R^2 = 0.03$, p = 0.17) and relief ratio (pseudo $R^2 = 0.04$, p = 0.10) shows similar positive trends, although the relationship is not significant. Valley width has a significant positive relationship with residual volume, such that ponds in wider valleys store less sediment (pseudo $R^2 = 0.09$). Valley gradient exhibits a non-significant negative relationship such that higher gradients correspond to lower residual volumes (pseudo $R^2 = 0.09$).

Of the pond characteristics, only beaver activity significantly related to residual volume (Figure 10). Inactive ponds had lower residual volumes (n = 28, median = 22.3 V^*), meaning more sediment storage than active ponds (n = 6, median = 49.4 V^*), closely followed by human constructed BDAs (n = 6, median = 52.5 V^*). Although not significant, on-channel ponds had higher residual volumes (n = 25, median = 34.2 V^*), or less storage, than off-channel ponds (n = 15, median = 27.5 V^*; p = 0.16). Solitary ponds on a reach had higher residual volumes (n = 6, median = 43.1 V^*) than ponds downstream of others (n = 8, median = 19.2 V^*), followed by the upstream-most pond on a reach (n = 26, median = 29.5 V^*, p = 0.10). Pond age also did not significantly relate to residual volume. However, recently constructed ponds had the highest residual volumes (n = 14 median = 44.7 V^*), followed by moderate aged ponds (n = 9, median = 27.5 V^*), and older ponds (n = 17, median = 44.7 V^*). Pond surface area exhibited a non-significant positive relationship to residual volume; larger ponds stored less sediment (pseudo $R^2 = 0.04$, p = 0.09).

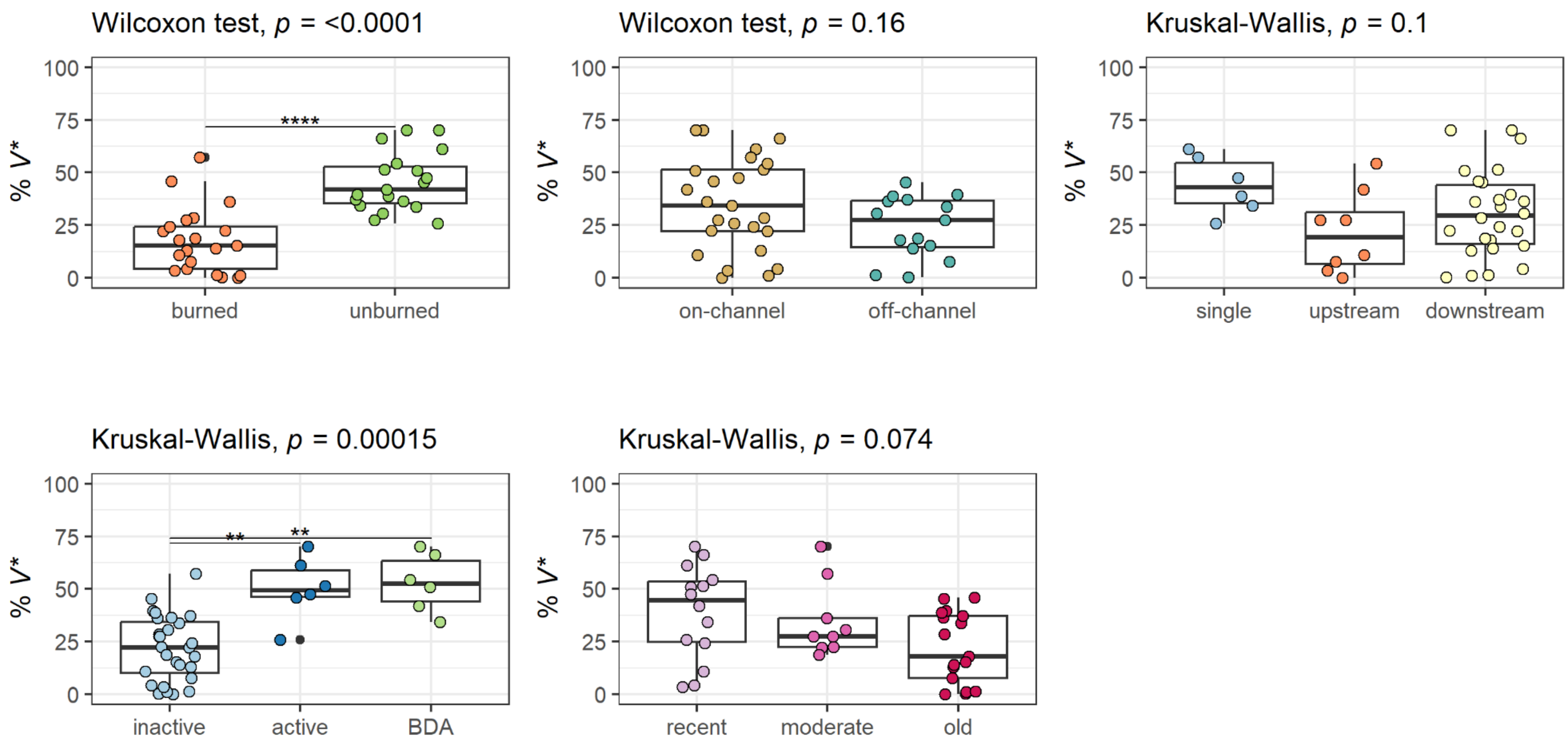

Figure 10: Results of pairwise analyses of explanatory variables and residual volume (% V). Differences in residual volume by categorical explanatory variables are shown with box plots. The results of hypothesis testing via the Wilcoxon rank signed test or Kruskal-Wallis test are displayed above each plot. Additionally, connecting lines and asterisks show significant differences in medians between groups and the number of asterisks designate the level of significance.*

3.1.6 Residual volume multiple linear regression

A multiple linear regression analysis yielded three explanatory variables that in combination best describe residual volume. The mean watershed slope, total percent of the watershed burned, and the pond's channel position combine into a model with the equation:

$$residual\ volume =$$
$$23.46 + 0.78 * (watershed\ slope) - 0.2 * (total\ percent\ burned) - 13.63 * (off\ channel)$$

Collectively, the model accounts for about a third of the variation present in the residual volume data (multiple $R^2 = 0.47$).

3.2 Sedimentation rates

3.2.1 Lifetime sedimentation pairwise comparisons

The lifetime sedimentation rate of a pond refers to the average rate of sediment accumulation since the pond was established. The median lifetime sedimentation rate was 2.96 cm/yr, but rates varied widely (min = 0.425 cm/yr, max = 52.2 cm/yr, sd = 9.76). The strong right skewedness of the total sedimentation rate was partially corrected with a base-10 logarithmic transformation. Although the transformation did not result in fully normally distributed data, it resulted in more acceptable residual distribution and thus was used in linear modeling.

There is no evidence of any relationship between burn characteristics and lifetime sedimentation rates. The percent of watersheds burned (adjusted $R^2 = -0.03$, $p = 0.97$) and percent burned at moderate and high severities (adjusted $R^2 = -0.03$, $p = 0.97$) had similarly low explanatory strength and were not significant. Field observations of burn status had a much lower p-value ($p = 0.08$) but were still not significant (Figure 11).

Vegetation characteristics including pre- and post-fire NDVI and post-fire ΔNDVI are significantly related to lifetime sedimentation at the local scale. Local pre-fire NDVI is negatively related to lifetime sedimentation such that ponds with higher greenness values accumulated sediment more slowly, although this relationship was not significant (adjusted $R^2 = 0.06$, $p = 0.09$). Both local post-fire NDVI (adjusted $R^2 = 0.10$) and post-fire ΔNDVI (adjusted $R^2 = 0.10$) exhibited significant negative relationships with lifetime sedimentation.

Of the continuous explanatory variables, geomorphic characteristics corresponded most strongly to lifetime sedimentation rates. The current drainage area of each watershed was positively related to lifetime sedimentation (adjusted $R^2 = 0.23$), whereas the historical drainage area (adjusted $R^2 = -0.03$, $p = 0.84$) and mean watershed slope showed no indication of any relationship. Elevation-based metrics showed negative relationships such that steeper relief corresponded to lower rates of sediment accumulation. The relative relief (adjusted $R^2 = 0.11$) and mean slope (adjusted $R^2 = -0.00$, $p = 0.76$) of the current watershed demonstrate this negative relationship. In contrast, the valley gradient (adjusted $R^2 = 0.18$) and valley width (adjusted $R^2 = 0.11$) expressed significant positive relationships to lifetime sedimentation.

At the pond level, the position in relation to the channel and pond age emerged as the two significant predictors of lifespan sedimentation (Figure 11). On-channel ponds exhibited higher sedimentation rates (n = 20, median = 3.99 cm/yr) than off-channel ponds (n = 15, median = 2.25 cm/yr). Young ponds had significantly higher rates (n = 9, median = 12.4 cm/yr) than both moderately aged (n = 9, median = 1.9 cm/yr) and old ponds (n =17, median = 2.78 cm/yr), which did not vary significantly from each other. Sedimentation was also higher in BDAs (n = 4, median = 8.2 cm/yr) and actively maintained beaver ponds (n = 3, median = 4.98 cm/yr) compared to abandoned ponds (n = 28, median = 2.80 cm/yr), although this difference is not statistically significant, likely due to small group sizes. Solitary ponds likewise exhibited high sedimentation rates (n = 4, median = 4.5 cm/yr) compared to the upstream-most ponds (n = 4, median = 3.28 cm/yr) and downstream ponds (n =24, median = 2.87 cm/yr) although this difference is also not significant, again likely due to small group sizes. The surface area of the pond showed a negative relationship with lifetime sedimentation rates such that larger ponds accumulated sediment more slowly, although this relationship is not significant (adjusted $R^2 = 0.01$, $p = 0.24$).

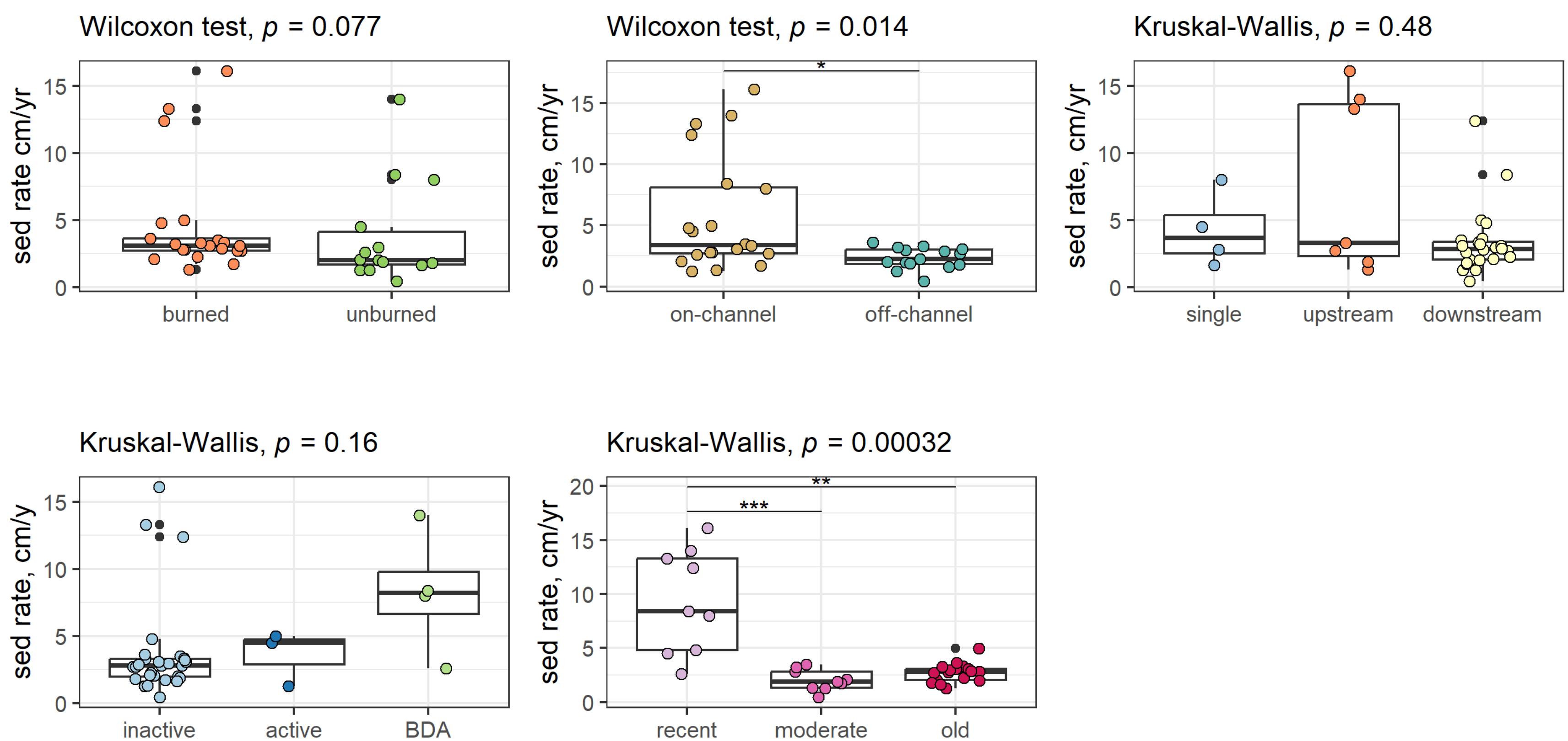

Figure 11: Results of pairwise analyses of explanatory variables and lifetime sedimentation rate (sed rate, cm/yr). Differences in lifetime sedimentation rate by categorical explanatory variables are shown with box plots. The results of hypothesis testing via the Wilcoxon rank signed test or Kruskal-Wallis test are displayed above each plot. Additionally, connecting lines and asterisks show significant differences in medians between groups and the number of asterisks designate the level of significance.

3.2.2 Lifetime sedimentation multiple linear regression

A multiple linear regression analysis indicated that the pond age category combined with the relief ratio accounted for nearly two-thirds of the variation in lifetime sedimentation rate (multiple R^2 = 0.66). The regression equation is expressed as:

$$lifetime\ sedimentation =$$
$$0.58 - 0.15 * (age_{moderate}) + 0.59\,(age_{recent}) - 0.9 * (relief\ ratio)$$

3.2.3 Post-fire sedimentation rates pairwise comparisons

Post-fire sedimentation rates were computed for 23 ponds with cores containing charcoal that could be confidently attributed to 2020 wildfires. The sedimentation rates were normally distributed, so no transformation was applied. The median post-fire sedimentation rate was 19.8 cm/yr, ranging from 2.0 to 40.3 cm/yr with standard deviation of 8.8 cm/yr. Post-fire sedimentation rates were normally distributed. None of the explanatory variables tested showed evidence of a significant relationship with post-fire sedimentation rates. Although not significant, the direction of relationships and differences mirrored the results of total sedimentation rates.

For instance, there is a slight positive relationship between percent of the watershed burned at moderate and high severities and post-fire sedimentation rate such that higher percentages burned correspond with more rapid sedimentation (adjusted R^2 = 0.01, p = 0.29). Likewise, ponds with local observations of burning exhibited higher sedimentation rates (n = 19, median = 19.8 cm/yr) than ponds that had not burned but still recorded charcoal deposition (n = 4, median = 16.1 cm/yr) (Figure 12).

Vegetation metrics did not show consistent relationships to post-fire sedimentation rates. Watershed and local post-fire vegetation recovery ΔNDVI showed weak positive relationships with post-fire sedimentation (adjusted R^2 = 0.01, p = 0.29, adjusted R^2 = 0.01, p = 0.29). Pre- and post-fire NDVI values negatively related to sedimentation at both scales.

Geomorphic explanatory variables had the lowest explanatory strength, exemplified by mixed direction signals. The current drainage area exhibited a weak positive relationship (adjusted R^2 = -0.06, p = 0.62) with post-fire sedimentation rates whereas the historical drainage area exhibited a negative relationship (adjusted R^2 = 0.0, p = 0.33). The valley gradient showed a weak positive relationship (adjusted R^2 = -0.03, p = 0.58) whereas the valley bottom width (adjusted R^2 = 0.0, p = 0.36), relief ratio (adjusted R^2 = 0.08, p = 0.19), and mean watershed slope (adjusted R^2 = 0.01, p = 0.69) showed a weak negative relationship.

Differences between ponds showed no significant results, likely in part due to small and uneven group sizes (Figure 12). On-channel ponds had higher post-fire sedimentation rates (n = 9, median = 20.8 cm/yr) than off-channel ponds (n = 14, median = 17.5 cm/yr). Recently constructed beaver ponds had higher post-fire sedimentation rates (n = 6, median = 23.2 cm/yr) than the oldest ponds (n = 12, median = 19.8 cm/yr) or moderately aged ponds (n = 5, median = 6.0 cm/yr), which had the lowest rates. Pond surface area held no relationship with post-fire sedimentation rate (adjusted R^2 = -0.05, p = 0.82). There were not enough solitary ponds or upstream-most and BDAs or active ponds with charcoal identified to be able to meaningfully compare these explanatory variables.

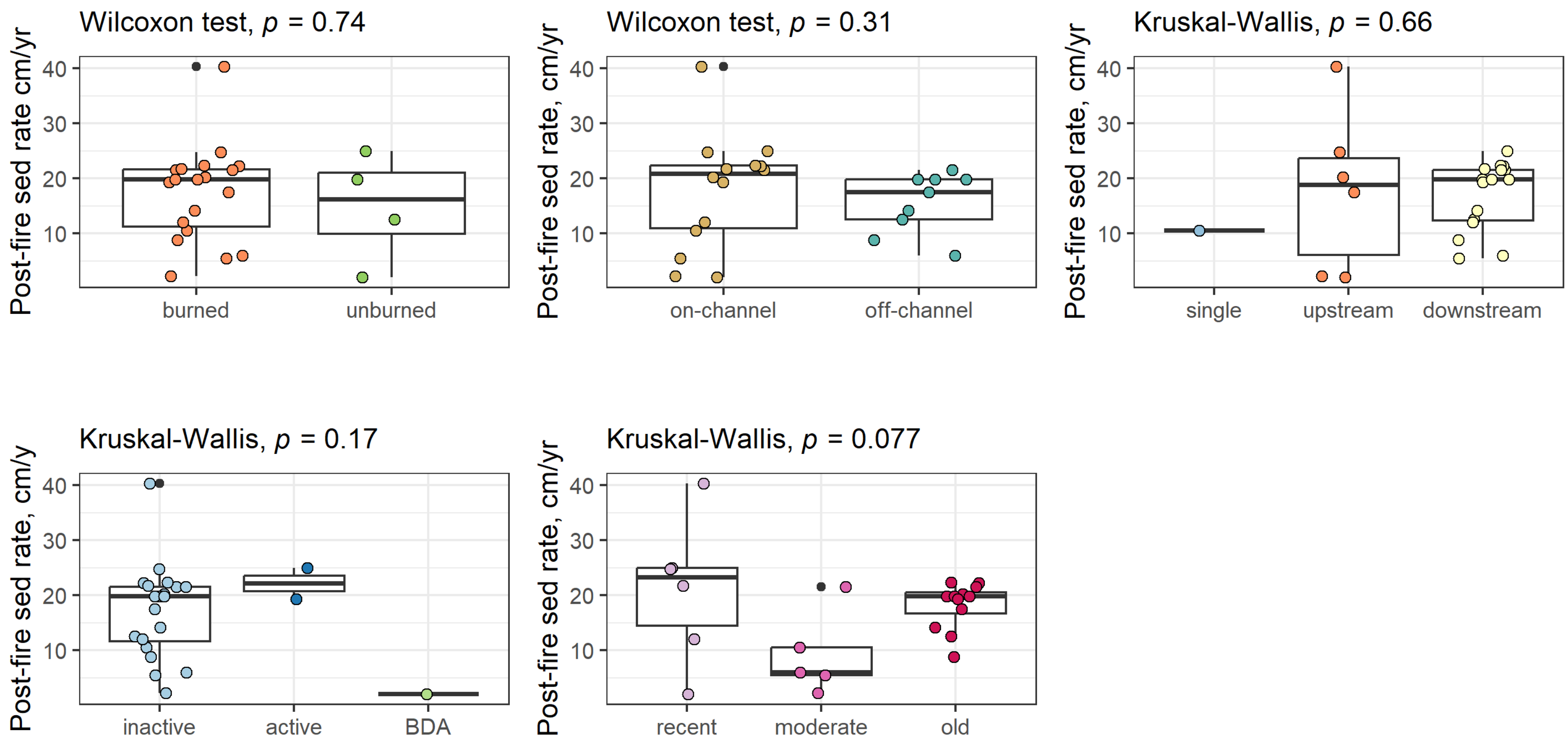

Figure 12: Results of pairwise analyses of explanatory variables and post-fire sedimentation rates (post-fire sed rate, cm/yr). Differences in post-fire sedimentation rates by categorical explanatory variables are shown with box plots. The results of hypothesis testing via the Wilcoxon rank signed test or Kruskal-Wallis test are displayed above each plot. Additionally, connecting lines and asterisks show significant differences in medians between groups and the number of asterisks designate the level of significance.

3.2.4 Post-fire sedimentation multiple linear regression

The multiple linear regression analysis indicates that only valley gradient significantly contributes to a model of post-fire sedimentation rates. The model only accounts for one-fifth of the variation ($R^2 = 0.19$) but it is significant, unlike the pairwise comparison. The regression equation is:

$$post - fire\ sedimentation\ rate = 11.28 + 227.54 * valley\ gradient$$

3.2.5 Pre- vs post-fire sedimentation

I sampled 21 ponds where both pre- and post-fire sedimentation rates could be estimated from sediment cores. Only one pond recorded a lower post-fire sedimentation rate compared to the pond's pre-fire rate. This pond was impounded behind a BDA constructed in 2020, and although the upper parts of the watershed burned, the area around the pond did not. Because of the short time frame for calculating both pre- and post-fire sedimentation rates and complicated watershed burn history, this pond was considered an outlier and excluded from analysis. In the remaining 20 ponds, post-fire sedimentation rates are higher and more variable (median = 20.4 cm/yr, min = 4.5 cm/yr, max = 25.5 cm/yr, standard deviation = 7.4 cm/yr) than pre-fire rates (median = 1.8 cm/yr, min = 0.6 cm/yr, max = 13.5 cm/yr, standard deviation = 2.9 cm/yr) (Figure 13). The difference in sedimentation rates spans over an order of magnitude and is significant.

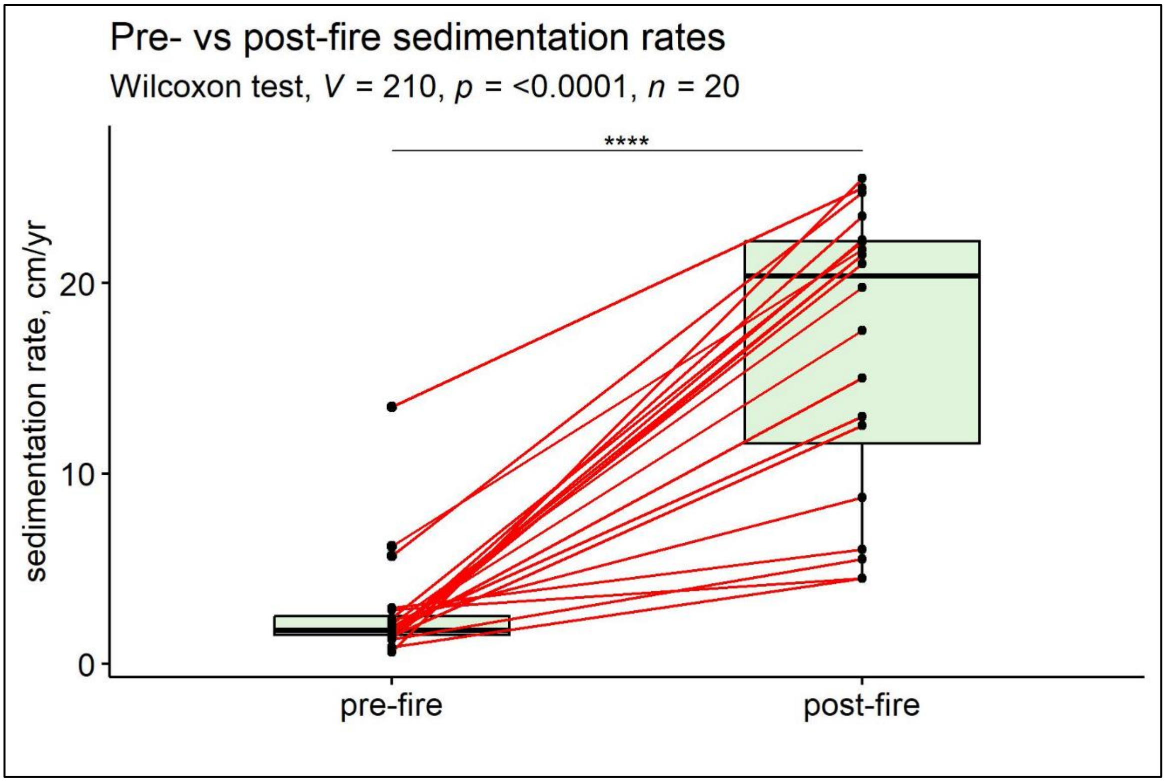

Figure 13: Paired comparison of pre- and post-fire sedimentation rates (cm/yr) from ponds where pre- and post-fire sediments were present and easily distinguished. Paired observations are connected by red lines showing that post-fire sedimentation is unilaterally higher than pre-fire sedimentation rates. Boxplots show that the median post-fire rate is higher than the pre-fire rate, supported by the results of the Wilcoxon paired test displayed above. Post-fire sedimentation rates are also more spread than pre-fire rates, indicating greater variation.

3.2.6 Reservoir sedimentation

Charcoal was present in three of the four sediment cores collected from Chambers Lake one year after the 2020 Cameron Peak Fire. Post-fire sedimentation rates for these cores are calculated as 12.5, 18.5, and 20.5 cm/yr. The final core was 32 cm long with no visible charcoal, indicating no detectable post-fire sedimentation.

3.3 Grain size

Grain size was analyzed for 32 ponds and is reported as percent fines, which includes the silt and clay size fractions (< 0.0625 mm). The median texture is 46.7% fines with a range from 5.9 to 77.4% fines. In addition to displaying the percent fines, grain size is visualized with ternary diagrams showing the gravel, sand, and fines (clay & silt) fractions (Figure 14). Although the d_{50} was analyzed, it showed fewer significant relationships to explanatory variables, so the results are not reported here. Percent fines were not normally distributed, but standard base-10 logarithmic, square root, and cube root transformations did not result in more a normal distribution, so no transformation was used.

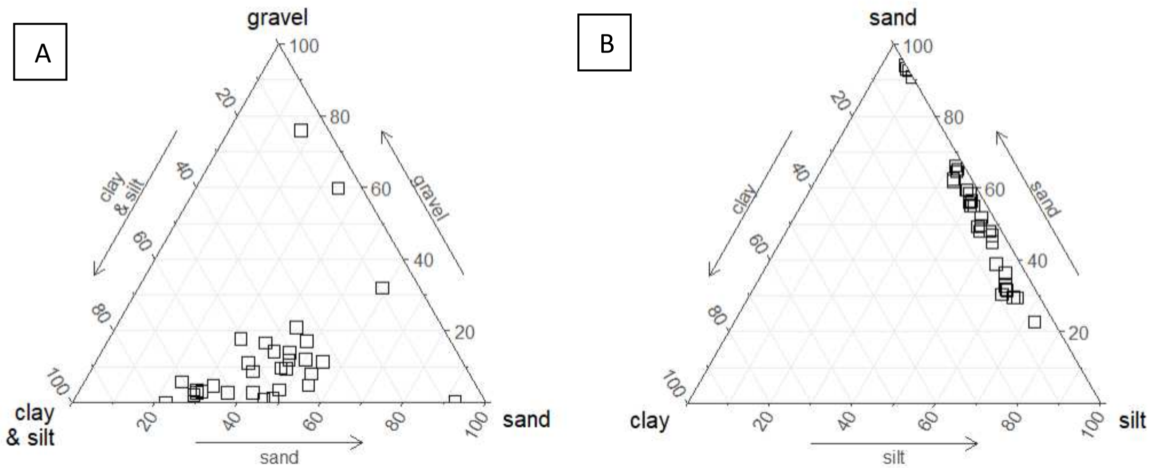

Figure 14: Ternary diagrams plotting the relative percentages of the mean grain sizes within each pond. (A) Mean pond grain size plotted by percent gravel, sand, and fines which are comprised of clay and silt. Most ponds plot along the sand and clay & silt axis, meaning that they have low abundances of gravel, although four ponds are much coarser than the rest and plot along the sand-gravel axis. (B) Mean pond grain size plotted by percent sand, silt, and clay. The sand end member consists of all sediment greater than 62 microns, including gravel. Samples plot primarily along the sand-silt axis, indicating overall low fractions of clay. The majority of the ponds are texturally similar, and no grouping is immediately apparent.

3.3.1 Pairwise comparisons

Burn characteristics did not significantly relate to grain size. The percent of watershed burned expressed a positive relationship with grain size (adjusted $R^2 = 0.01$, $p = 0.24$) such that pond sediments were finer in ponds located in more burned watersheds. However, the percent burned at moderate and high severities showed a very weak negative relationship (adjusted $R^2 = -0.03$, $p = 0.76$). Burned ponds contained finer sediments ($n = 19$, median = 50.4 % fines) than unburned ponds ($n = 13$, median = 41.7%), although this relationship was not significant ($p = 0.85$). Additionally, I calculated the percent fines for each stratigraphic unit then compared the variation in data, reported as the standard deviation, between burned and unburned ponds. I found that burned ponds had more variation in grain size (sd =

17.7%) compared to unburned ponds (sd = 13.1%), but this difference is not significant ($p = 0.09$) (Figure 15).

Vegetation characteristics also did not significantly relate to grain size, with mixed signals across scales. Watershed post-fire vegetation recovery ΔNDVI showed a slight positive relationship with grain size (adjusted $R^2 = -0.03$, $p = 0.69$), whereas the direction was negative for local post-fire vegetation recovery ΔNDVI (adjusted $R^2 = 0.03$, $p = 0.18$). The pre-fire 2019 median NDVI values were slightly positively related to grain size in the watershed area (adjusted $R^2 = -0.03$, $p = 0.83$), whereas the local values were slightly negatively related (adjusted $R^2 = -0.03$, $p = 0.77$). Conversely, the post-fire 2022 median NDVI watershed values positively related to grain size (adjusted $R^2 = -0.01$, $p = 0.43$), whereas the local values positively related (adjusted $R^2 = -0.02$, $p = 0.52$).

The geomorphic characteristics of current drainage area significantly relate to grain size (adjusted $R^2 = 0.19$). It has a negative relationship to percent fines such that ponds with larger watersheds and higher relief stored coarser sediment. The historical drainage area (adjusted $R^2 = -0.01$, $p = 0.40$), valley gradient (adjusted $R^2 = 0.01$, $p = 0.29$), and mean watershed slope (adjusted $R^2 = 0.01$, $p = 0.65$) also displayed negative relationships with grain size, but these were not statistically significant. The valley bottom width (adjusted $R^2 = 0.05$, $p = 0.11$) and relief ratio (adjusted $R^2 = 0.09$, $p = 0.10$) positively related to grain size but not significantly.

Of the pond characteristics, only the position along the reach significantly related to grain size. Ponds that were upstream of others contained the finest sediment (n = 7, median = 52.0 % fines), closely followed by downstream ponds (n = 20, median = 50.6 % fines), whereas single ponds were significantly coarser (n = 5, median = 33.8 % fines). Off-channel ponds contained finer sediment (n = 14, median = 53.6 % fines) than on-channel ponds (n = 18, median = 42.9 % fines). BDAs contained much coarser sediment (n = 3, median = 7.5 % fines) than either active (n = 4, median = 41.1 % fines) or inactive ponds (n = 23, median = 50.8 % fines) constructed by beaver. Moderate aged ponds were finer (n = 6, median =

57.7 % fines) than old (n = 16, median = 52.1 % fines) and recent (n = 10, median = 39.1 % fines) ponds. Finally, the pond surface area did not exhibit any relationship with sediment texture (adjusted R^2 = -0.03, p = 0.94).

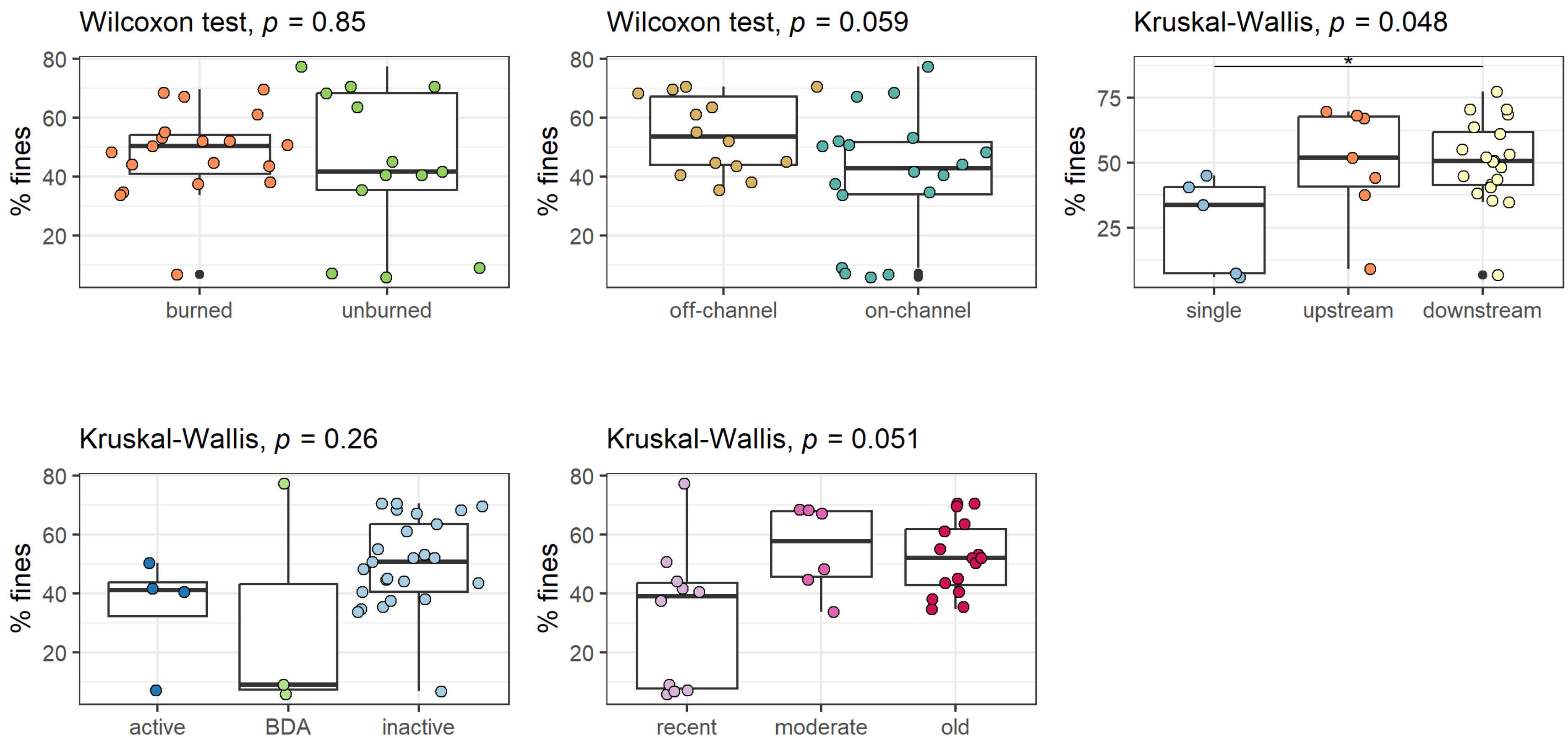

Figure 15: Results of pairwise analyses of explanatory variables and the percent fines (silt & clay). Differences in percent fines by categorical explanatory variables are shown with box plots. The results of hypothesis testing via the Wilcoxon rank signed test or Kruskal-Wallis test are displayed above each plot. Additionally, connecting lines and asterisks show significant differences in medians between groups and the number of asterisks designate the level of significance.

3.3.2 Multiple linear regression

Multiple linear regression indicates that the combination of current drainage area and local pre-fire (2019) vegetation cover best describe variation between ponds in the percent fines. These two explanatory variables account for one third of the overall variation ($R^2 = 0.32$). The equation for the regression is:

$$grain\ size = \sim 7.16\ -\ 0.56\ *\ current\ area\ +\ 182.92\ *\ local\ pre\ fire\ NDVI$$

3.3.3 Pre- vs post-fire comparison

I analyzed grain size from sediment cores in 17 ponds where pre- and post-fire stratigraphic units were easily distinguished. Post-fire units contained finer sediments (median = 52.5 % fines) than pre-fire units (median = 41.2 % fines), but this difference is not significant ($p = 0.24$) (Figure 16). Post-fire sediments display a wider spread of grain sizes (IQR = 23.1) compared to pre-fire sediments (IQR = 12.3). Individual ponds showed mixed responses. Grain size decreased in some ponds after fire, but increased in others.

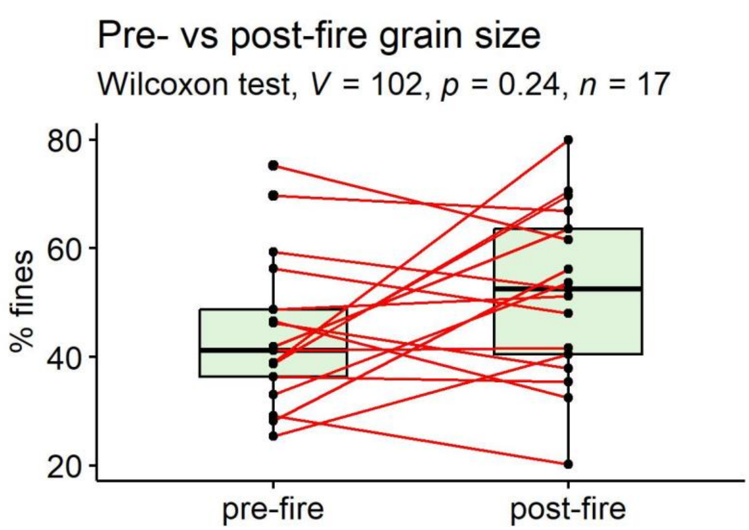

Figure 16: Comparison of grain size pre- and post-fire grain size, measured as the percent of fines (clay and silt), for ponds with both pre- and post-fire sediments.

3.4 Total organic carbon (TOC)

Cores from 35 ponds were analyzed for total organic carbon (TOC) by each stratigraphic unit and used to calculate the weighted mean for each pond. The median TOC across the 35 ponds was 6.4% with a range from 0.2% to 23.2% and standard deviation of 5.7%. The TOC data were right-skewed, so beta regression was used to analyze relationships between continuous variables.

3.4.1 Pairwise comparisons

Burn characteristics did not relate to pond TOC. Both the percent of the watershed burned and the percent burned at moderate and high severity exhibited weak positive relationships with TOC such that more burned watersheds had higher TOC, but this relationship was not significant in either case (pseudo R^2 = 0.02, p = 0.36; pseudo R^2 = 0.02, p = 0.39). Field observations show a similar trend where burned ponds had insignificantly (p = 0.09) higher TOC (n = 20, median = 6.6%) compared to unburned ponds (n = 15, median = 5.1%) (Figure 17). Burned ponds had a significantly higher standard deviation (sd = 4.2 %) in the TOC content of individual stratigraphic units compared to unburned ponds (sd = 2.5 %).

Vegetation characteristics also did not significantly relate to pond TOC, except post-fire NDVI at the local scale. At the watershed scale, pre-fire NDVI showed a weak positive relationship with TOC (pseudo R^2 = 0.06, p = 0.14) as did post-fire ΔNDVI (pseudo R^2 = 0.003, p = 0.69), although the explanatory strength of both is low and insignificant. At the local scale, in contrast, pre-fire NDVI and post-fire ΔNDVI showed negative relationships with TOC (pseudo R^2 = 0.09, p = 0.12; pseudo R^2 = 0.08, p = 0.07). Post-fire NDVI negatively related to TOC at the watershed scale (pseudo R^2 = 0.003, p = 0.33) and at the local scale, this relationship was significant although with low explanatory strength (pseudo R^2 = 0.15).

Drainage area and mean watershed slopes emerged as the significant geomorphic variables for explaining variation in TOC. The current drainage area (pseudo R^2 = 0.35) and mean watershed slope (pseudo R^2 = 0.01) exhibited a negative relationship with TOC: ponds with larger drainage areas and steeper slopes had lower mean TOC. The historical drainage area followed the same trend (pseudo R^2 = 0.25). The valley gradient gave no indication of correlation to TOC (pseudo R^2 = 0.00, p = 0.84) whereas the valley width was weakly negatively correlated such that wider valleys had lower TOC (pseudo R^2 = 0.01, p = 0.65). Ponds with higher relative reliefs also contained less TOC (pseudo R^2 = 0.01, p = 0.42).

Pond position in relation to the channel and other ponds, as well as pond age, significantly related to TOC. Off-channel ponds (n = 15, median = 8.0 %) were richer in TOC than on-channel ponds (n = 20, median = 4.3 %). Downstream ponds were richer in TOC (n = 25, median = 6.9 %) than upstream ponds (n = 7, median = 3.7 %) or single ponds on a reach (n = 5, median = 2.3 %). Younger ponds contained less TOC (n = 10, median = 2.7 %) than older ponds (n = 17, median = 6.9 %), although there was no significant difference for moderate aged ponds (n = 8, median = 6.3 %). Inactive ponds (n = 27, median = 6.8 %) contained nearly double the TOC as active ponds (n = 5, median = 3.7 %), both of which were an order of magnitude greater than BDAs (n = 3, median = 0.8 %), but these differences are not significant. Pond surface area presented a non-significant negative relationship to TOC such that larger ponds contained lower percentages of TOC (pseudo R^2 = 0.07, p = 0.25).

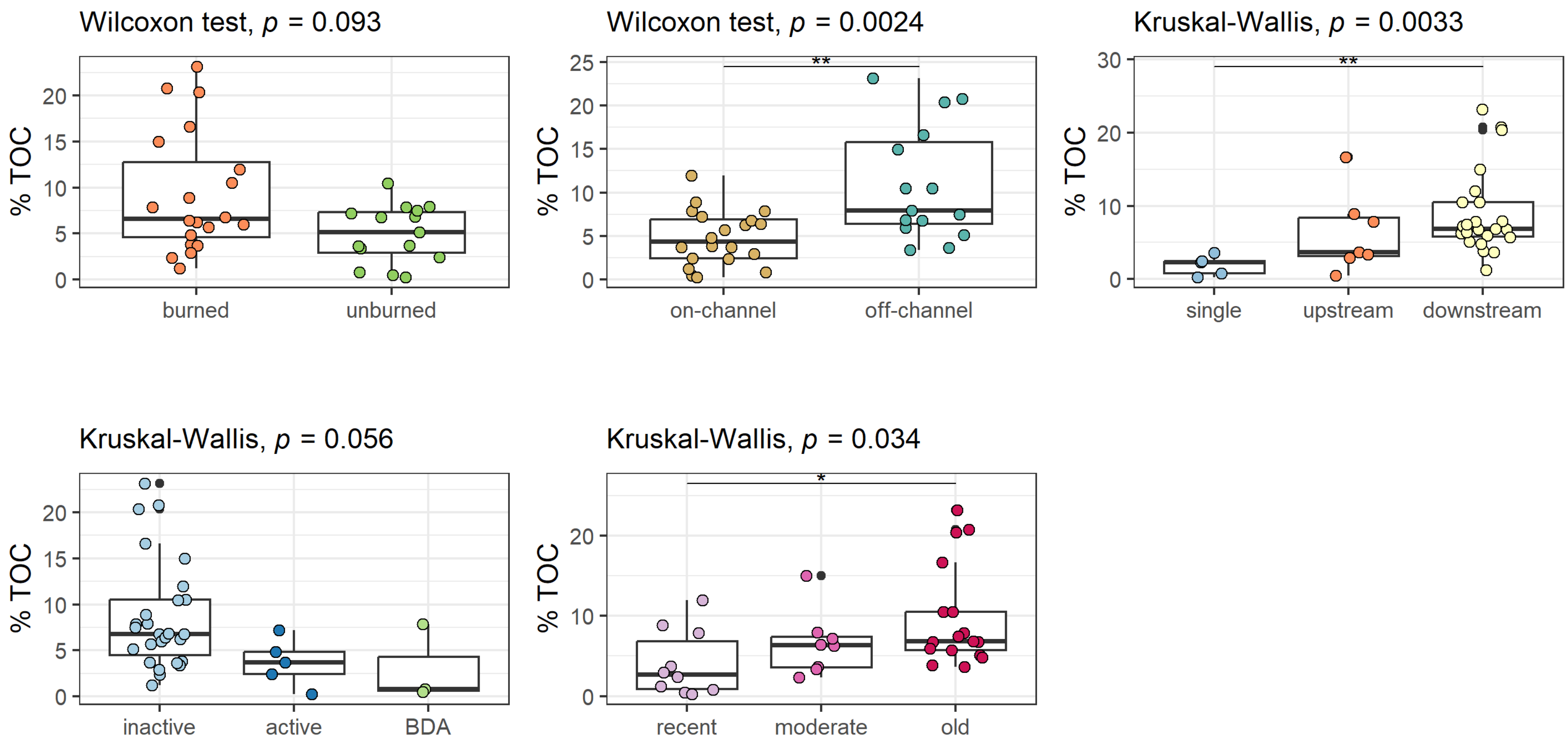

Figure 17: Results of pairwise analyses of explanatory variables and total organic carbon (% TOC). Differences in residual volume by categorical explanatory variables are shown with box plots. The results of hypothesis testing via the Wilcoxon rank signed test or Kruskal-Wallis test are displayed above each plot. Additionally, connecting lines and asterisks show significant differences in medians between groups and the number of asterisks designate the level of significance.

3.4.2 Multiple linear regression

Because of the right-skewedness of the TOC data, a cube root transformation was used to achieve a normal distribution for multiple linear regression analysis. This transformation was not applied in the pairwise analyses because normality is not a requirement for beta regression. The multiple linear regression analysis yields three explanatory variables that best describe the variation in TOC between ponds. The ponds' reach position, channel position, and watershed slope collectively describe two thirds of the variation ($R^2 = 0.63$). The regression equation is:

$$TOC = 2.2 + 0.21 * (reach\ position) - 0.48 * (on\ channel) - 0.02 * (watershed\ slope)$$

3.4.3 Pre- vs post-fire comparison

I sampled TOC from 17 ponds where pre- and post-fire stratigraphic units were readily distinguished. TOC was more abundant in pre-fire sediments (median = 9.35 % TOC) than post-fire sediments (median = 7.59 % TOC), although this difference is not significant ($p = 0.28$) (Figure 18). Pre-fire sediments also exhibited a wider spread in TOC values (IQR = 12.0) compared to post-fire sediments (IQR = 5.72). Most individual ponds show small decreases in TOC after fire, although a couple show steep increases.

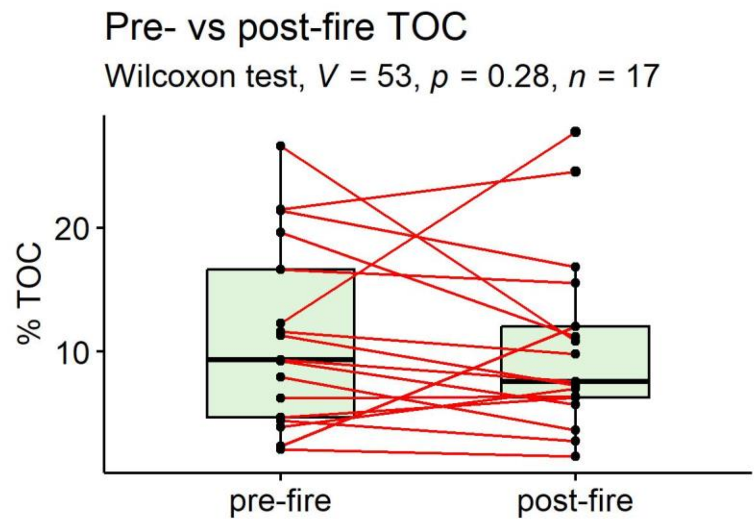

Figure 18: TOC content, reported as percent TOC, in pre- and post-fire stratigraphic units from ponds with both pre- and post-fire sediments distinguishable.

4. DISCUSSION

I interpret and evaluate the observations and analytical results of sedimentation in beaver ponds to address my three research objectives and hypotheses. I discuss my findings in light of these hypotheses and apply these interpretations to form a broad understanding of fire impacts on beaver pond sediment processes and dynamics, and the pond characteristics that most effectively attenuate excess sediment. Finally, I discuss the management implications of my results to mitigate post-fire sediment fluxes and suggest ways to enhance watershed resilience to wildfire.

4.1 Sediment volumes

I find that beaver ponds store high volumes of sediment. The total volume of sediment stored in ponds in the study area is 32,139 m^3 with a combined drainage area of 468 km^2 (n = 41). This finding is consistent with previous research documenting high volumes of sediment storage in beaver ponds across a variety of landscapes (Larsen et al., 2021). Butler and Malanson (2005) used a conservative estimated range of average pond sediment volume (200-500 m^3) to estimate continental scale sediment storage in beaver ponds. Interestingly, I found a much higher mean pond sediment volume in my study area (796 m^3). This variation could indicate regional differences in sediment storage, implying that continental-scale sediment storage could be higher than the authors estimated. Additionally, beaver ponds have higher storage capacities than hillslope retention structures such as contour-felled logs because the dams are typically taller and ponds are situated in wide low-gradient valleys (Wagenbrenner et al., 2006). Conversely, ponds have lower storage capacities than engineered water supply reservoirs, which are characterized by large surface areas and deep, typically dredged, basins (Moody and Martin, 2001; Rathburn et al., 2018). A study of small ponds in headwater catchments demonstrated that, depending on the spatial position of ponds within the river system, ponds can exert a dominant influence on nutrient and sediment retention in headwater catchments (Schmadel et al., 2019). Additionally, beaver ponds studied in Poland demonstrated very high trap efficiency in a watershed with high fluxes of silt-sized sediments, implying that beaver ponds are capable of attenuating meaningful volumes of sediment (Giriat et al., 2016).

Sediment budgets developed from other parts of the Rocky Mountains impacted by fires suggest that the storage provided by beaver ponds is substantial (Moody and Martin, 2001; Rathburn et al., 2018). The proportion of a watershed's sediment flux stored in beaver ponds may be roughly estimated by comparing sediment yields calculated from both burned and unburned areas to the volume of sediment stored in beaver ponds. If sediment accumulates steadily over the lifetime of a pond, unburned ponds accumulate an average of 29 m^3/yr (Table 6). In contrast, the mean background sediment production for the same watersheds is estimated as 235 m^3/yr using a mean ^{10}Be exhumation rate for the region from Foster and others (2015). Exhumation rates differ from watershed sediment yields depending on storage within a watershed over different time scales. I assume that Foster's exhumation rates applied across the entire watershed area are roughly equivalent to sediment yields. Compared with this background sediment yield, unburned ponds effectively trap approximately 12% of the sediment transported out of a watershed. If the sediment volume of burned ponds is also assumed to accumulate over the entire lifespan of the pond, I calculate a mean sediment storage rate of 63 m^3/yr compared to a mean watershed sediment yield of 203 m^3/yr which is 31% of background rates. However, if all the sediment stored in burned ponds was generated post-fire, then the mean storage rate increases to 479 m^3/yr which is 236% greater than background rates. Likely, sediment accumulation falls somewhere between these two endmembers, with some sediment storage prior to fire but higher rates of accumulation after. These accumulation rates are similar to post-flood sedimentation rates in a water supply reservoir in the Colorado Rocky Mountains which ranged from 92% to 132% in the six years following the 2013 Front Range Flood (Eidmann et al., 2022). These estimations add further evidence that sedimentation is episodic and beaver ponds effectively capture a significant portion of sediment moving through watersheds.

Table 6: Sediment storage compared to estimated watershed sediment yields.

Burn status	**sedimentation period**	**pond storage rate, m^3/yr**	**watershed background yield m^3/yr**	**% of watershed yield stored in ponds**
This study: beaver ponds, post 2020 fires				
Unburned	lifetime	29	235	12
Burned	lifetime	63	203	31
Burned	post-fire	479	203	236
Regional comparison: Ralph Price Reservoir, post 2013 flood				
Unburned	2015-2017	10000	7595	132
Unburned	2018-2019	7000	7595	92

Watershed sediment yields are also higher in the years following wildfire (Moody and Martin, 2001; Benavides-Solorio and MacDonald, 2005; Wagenbrenner et al., 2006). Published post-fire sediment yields vary greatly, likely reflecting both real physical variation in sedimentation rates by region, fire characteristics, and post-fire recovery, as well as methodological biases and assumptions (Kirchner, 2001). I calculated sediment yields from published equations and found estimates varied by several orders of magnitude and thus were too unreliable to include in this analysis.

It becomes apparent that, although storage within an individual pond might be negligible, the compounding effect of many ponds across a landscape can be quite large even when watershed sediment yields are increased during the post-fire period. I conducted a statistical analysis of the total sediment volume stored within all ponds on each stream reach (Appendix V). However, this analysis is restricted because I intentionally prioritized measuring ponds from different reaches over measuring all ponds present on a reach to increase the spatial diversity and capture the range of conditions inhabited by beavers in the Rocky Mountains. The calculated reach storage should be considered a minimum estimate because many reaches contained ponds that were not measured. Furthermore, summing ponds by reach substantially reduced the statistical sample size. I found no significant relationship between explanatory variables and reach-summed sediment volume or reach-summed sediment volume normalized by drainage area. A general trend emerged, however, where reaches with more ponds measured contained greater volumes of sediment. Thus, it is reasonable to assume that additional beaver ponds increase the sediment storage capacity of a reach.

To my knowledge, only one study has used residual pool volume to compare relative sediment storage between beaver ponds along a single stream reach in the United Kingdom (Puttock et al., 2018). The authors documented about twice as much (55.7% V^*) remaining storage across the pond complex as I found at my sites (29.5% V^*). The difference may be due to pond-specific characteristics or to regional differences in sediment delivery and attenuation tied to the broad scale geologic, climatic, and ecologic contexts. Notably, the active ponds and BDAs measured in my study more closely resembled the residual volumes documented in the UK with 49.4% and 52.5% V^*, respectively, indicating that beaver activity is critical for pond storage maintenance.

4.1.1 Post-fire sediment storage

Comparison of the residual pool volume indicates that burned ponds store greater relative volumes of sediment than unburned ponds. Additionally, the extent of burning in a watershed and the burn severity were both correlated with residual volume. These findings support Hypothesis 1 that burned ponds will store more sediment than unburned ponds due to greater sediment generation and transport in burned watersheds. Although I was unable to distinguish between pre- and post-fire sediment storage volumes, this result implies that beaver ponds effectively capture high volumes of post-fire sediment. Field observations further corroborate this finding. A pre-fire photo of a pond on Little Beaver Creek shows standing water and wetland vegetation, whereas the same pond was almost entirely full of sediment by 2022 (Figure 19). In addition to burn characteristics, I found that some vegetation, geomorphic, and pond characteristics significantly explained variation in pond sediment storage.

Figure 19: View of abandoned beaver pond (LBC-4) on Little Beaver Creek before and after the Cameron Peak Fire. Stars mark matching trees to aid comparison. Left: In June of 2020 (pre-fire), the pond is shallow but has a wide extent of standing water and wetland vegetation. Photo credit: Ellen Wohl. Right: After the fire, by July of 2022 the pond had filled in with dark, charcoal-rich sediment with little standing water remaining. Vegetation type shifted to dense grasses and sedges in the valley floor, contrasting the blackened hillslopes which had yet to recover.

4.1.2 Other controls on sediment storage

Pre-fire watershed vegetation cover correlated to pond sediment volumes normalized by drainage area. Areas with higher vegetation cover stored higher normalized volumes of sediment, which might reflect larger alterations to hillslope processes after fire when that vegetation is lost. Vegetation characteristics are also correlated with residual volume, and the local vegetation around the pond matters most. My findings suggest that areas with greater vegetation cover and higher magnitudes of vegetation recovery have higher residual volumes, meaning less sediment storage. Vegetation in the valley bottom might increase roughness and result in more sediment trapping across the floodplain rather than just in the pond (Bywater-Reyes et al., 2022). Roots may also stabilize alluvium, making it less likely to be reworked during high flows. Because these are processes that operate within the river corridor and not on surrounding hillslopes, it makes sense that local scale vegetation metrics show opposing trends with residual volume compared to the watershed scale. The magnitude of vegetation recovery is greatest in the areas surrounding beaver ponds. This corroborates the findings of Fairfax and Whittle (2020), who documented more rapid post-fire vegetation recovery in valley bottoms with beaver ponds. The authors attribute the vegetation recovery to the lower severity of fire in areas with abundant surface water, and the high water table that facilitates rapid regrowth of riparian species in comparison with surrounding hillslopes.

Geomorphic characteristics did not all correlate with pond sediment volumes normalized by drainage area or residual volume in the direction I expected. Lower relief ratios, steeper valley gradients, and narrower valleys stored significantly lower normalized volumes of sediment. Steeper valley gradients corresponded to lower residual volume, meaning more sediment is stored in ponds, as predicted based on the greater sediment transport capacity of steeper channels. However, larger drainage areas, higher mean watershed slopes, and wider valley bottoms corresponded to higher residual volumes, meaning less sediment in storage with more remaining volume available. Dams on large rivers might overtop more readily, be more permeable due to the higher water pressure, or might force more channel splitting and avulsion leading to less sediment deposited in the pond. I observed all three of these processes at work on a large dam across Fall River in Rocky Mountain National Park (Figure20).

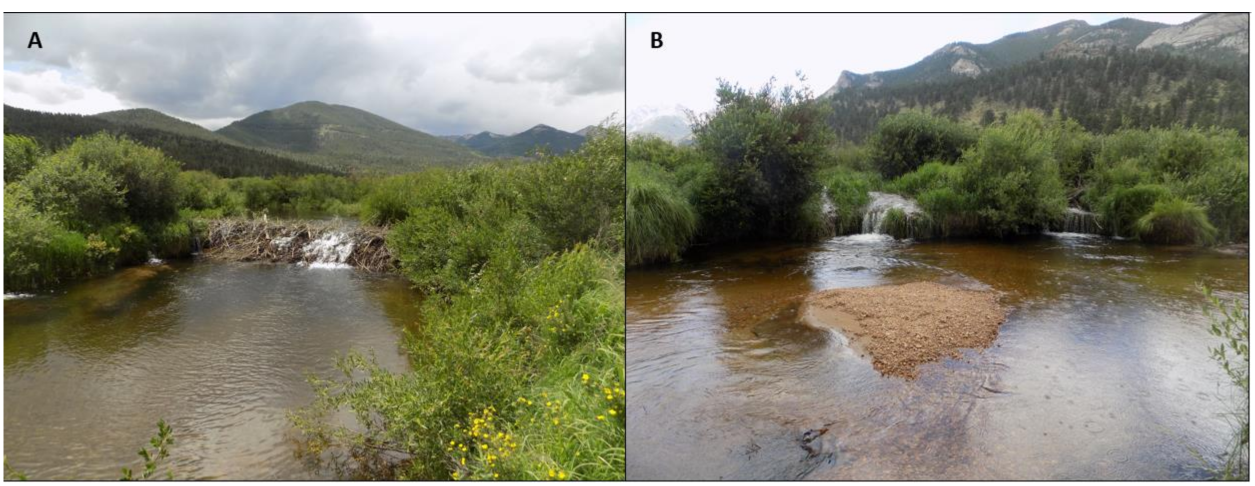

Figure 20: Beaver dam impacts on Fall River, Rocky Mountain National Park, 2022. (A) Flow overtops and spills over the ~1.5 m tall active beaver dam on the right, flows through a permeable portion of the dam

in the center, and forms multiple small avulsion channels across the flood plain to the left. (B) Larger channels formed by ponding on the floodplain spill across a meander bend into the main channel downstream of the pond. Dense riparian vegetation stabilizes the floodplain, however, steep ~0.5 m head cuts are formed at the juncture. Photos credit: Ellen Wohl.

The geomorphic trends might also indicate that dams built on larger rivers and in wider valleys are more likely to partially fail or breach entirely due to the higher discharges passing through. Dam breaches may result in flushing of sediments downstream, although they may also redistribute sediment across the floodplain or vegetation may stabilize it in place (Butler and Malanson, 2005; Westbrook et al., 2011). One breached dam observed on the mainstem of the Big Thompson River in Rocky Mountain National Park in July 2022 had been rebuilt by beavers by January 2023, providing evidence that dams and sediment storage on larger systems may be more transient (Figure 21). Persico and Meyer (2009) found charcoal-rich deposits in a beaver meadow dating to ~800 radiocarbon calibrated years before present that they interpret as evidence of post-fire flooding capable of destroying dams, suggesting that compounding disturbances may result in differences in sedimentation detectable over hundreds of years.

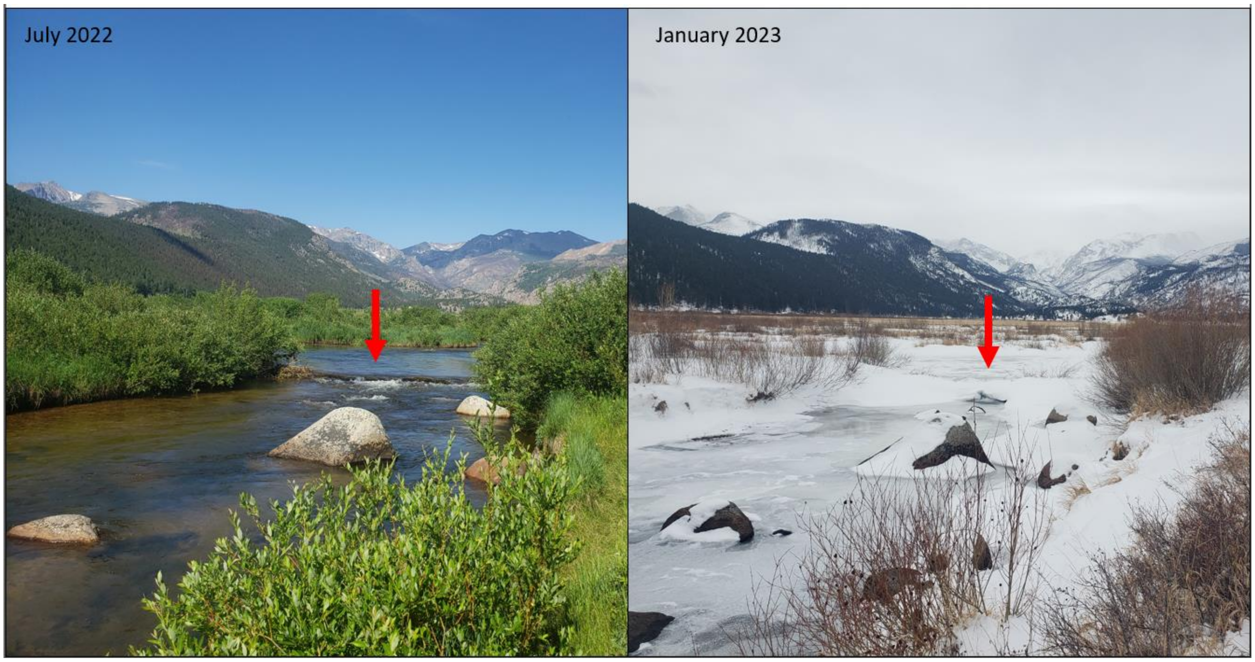

Figure 21: Partially breached dam on the Big Thompson River in Rocky Mountain National Park. In July 2022, the dam (indicated by the red arrow) was partially breached resulting in minimal ponding of water behind the dam and coarse bed scour around the structure. By January of 2023, the dam had been rebuilt, and though covered in snow, higher degrees of ponding behind the dam were observed. This pond was not included in my dataset because it was not intact during the time of initial survey.

Pond characteristics likely interact with the geomorphic and ecological context to determine sediment fate. Beaver maintenance emerged as a significant explanatory variable for normalized sediment volume and residual volume in my pairwise comparison, such that actively maintained beaver ponds store less sediment and have greater remaining storage capacities than abandoned ponds. BDAs stored the least sediment and had the greatest remaining storage capacity, implying that these structures are less effective at trapping sediment than natural dams. This may be due to intentional siting of BDAs on 'degraded' channel reaches experiencing incision and high sediment fluxes, where habitat is suboptimal for beaver (Nash et al., 2021). I found no significant difference between pond age and residual volume, but older ponds stored higher normalized volumes of sediment, which is consistent with previous research showing that sediment storage positively corresponds with beaver pond age (Butler and Malanson, 1995). Pond surface area strongly corresponded to sediment volumes and normalized sediment volumes: larger ponds stored more sediment. In contrast, larger pond surface areas non-significantly corresponded to higher residual volumes, likely because larger ponds have higher total volumes, so it takes greater volumes of sediment to fill them. Off-channel ponds stored greater sediment volumes and normalized sediment volumes than on-channel ponds. It is noteworthy that the channel position of the pond was not significant in the pairwise comparison with residual volume but emerged as a significant variable in the multiple linear regression model. It became significant when combined with the percent area burned and valley width, suggesting multiplicative effects between burn, vegetation, and pond characteristics.

Many of the study ponds were constructed across small tributaries and had been abandoned for at least a decade, as evidenced by satellite imagery and vegetation growth (Figure 22). These tributaries had small drainage areas and relatively narrow valley bottoms. The low stream power in these systems may allow dams to persist for longer than on larger streams (Persico and Meyer, 2009). The effects of beaver damming such as multithread channel planform, dense riparian vegetation, and spatial heterogeneity of geomorphic landforms likely persist even after dams are abandoned, and even after the dams have partially deteriorated. A study of surface water extent found that abandoned beaver ponds continued to store water and force new pond construction in less optimal areas, thereby maintaining comparable regional surface water extents through time (Johnson-Bice et al., 2022). There has been relatively little research quantifying the function and effects of abandoned beaver ponds for sediment storage, although there is evidence that beaver berms (vegetated relict dams) trap large wood, secondarily increasing backwater sediment storage (Wohl et al., 2022).

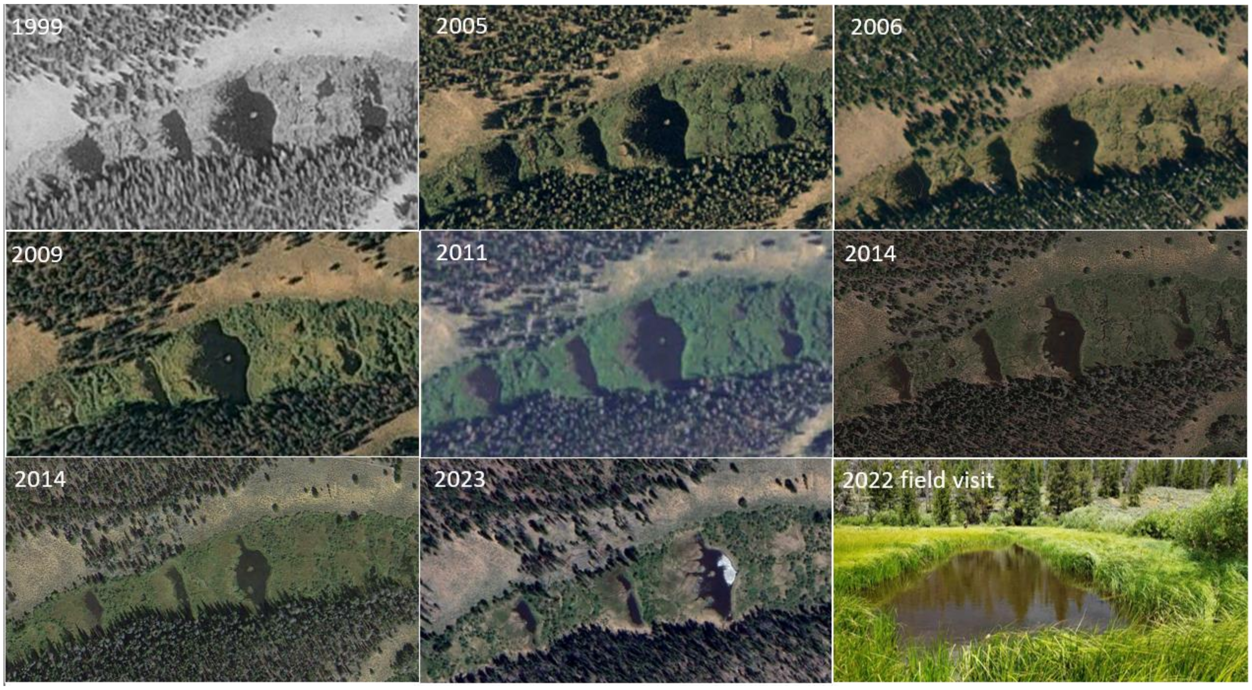

Figure 22: Satellite imagery of a beaver complex on a tributary to Boswell Creek, WY, 1999-2023. Ponds can be seen changing in size through time, with an overall shrinking trend. While some change in the surface water extent may be attributed to seasonal water availability, vegetation encroachment indicates long term infilling. The bottom right pane shows the pond to the left of the largest pond visible in the satellite imagery. The pond had dense wetland vegetation encroachment during our 2022 field visit where we found no evidence of current beaver occupation (person in distance for scale). Satellite imagery provided by Google Earth.

4.1.3 Assumptions

My analysis of sediment volume relied upon accurate interpretation of sediment probing results. I assumed that the depth to refusal is representative of the pond sediment thickness, but other sediment types such as floodplain deposits may be as easily penetrable and fine in texture, making them hard to distinguish. I found that coarse channel deposits could readily be detected by texture. I also assume that the water level at the time of survey represents the maximum depth of the pond. I surveyed many ponds during base-flow season, so some ponds might be able to retain greater volumes of water or sediment during higher flows. In actively maintained ponds, beavers may increase the dam height, resulting in pond enlargement and increased storage. Thus, the reported residual volumes should be taken as minimum values.

4.1.4 Comparison with empirical equations estimating sediment volume

Other studies have developed empirical equations relating the total sediment volume stored in beaver ponds to various predictor variables. In a 2017 review, Wohl and Scott found that these empirical equations are widely used to estimate sediment volume and sedimentation rates, with few studies directly measuring sediment volumes. Here, I review the available equations and test how well they describe the sediment volume data I collected.

Naiman et al. (1986) published the first sediment storage equation for beaver ponds developed from data collected in low gradient beaver meadows in Quebec, Canada. The authors relate sediment volume to the surface area of the pond. In their study, sediment volumes were estimated from valley and dam geometry, rather than probed, so the storage volumes are likely approximate. The equation is stated as

$$Sediment\ Volume = 47.3 + 0.39 * \ [Surface\ Area]$$

where sediment volume is in cubic meters and surface area is in square meters.

Bulter and Malanson (1995) probed beaver ponds on low-order streams in Montana, USA to develop equations relating sediment volume to pond surface area and age. Additionally, they found that age related to surface area, although their dataset consisted of ponds of similar age, and they used the oldest age estimate in their calculations. One pond exerted disproportionate leverage in these equations, which are stated as

$$Sediment\ Volume = \ -84.082 + 0.62502 * [Pond\ Area]$$

$$Volume = \ -457.0 + 169.9 * Age$$

$$Area = \ -514.8 + 261.9 * Age$$

where sediment volume is in cubic meters, surface area is in square meters, and age is in years.

I tested these equations using my pond surface area dataset, measured by RTK-GPS, and pond age dataset, estimated from satellite imagery. The limitations of the satellite imagery age-estimation method are discussed in the sedimentation rates section. The ponds in my study area more closely resemble those studied by Butler and Malanson in Montana in terms of pond surface area and sediment volume (Table 7). Additionally, the ecology of the Montana Rocky Mountains is likely more similar to the Colorado Rockies than is the Quebec boreal forest. Thus, I would expect the equations developed by Butler and Malanson to perform better than Naiman's for my ponds.

Table 7: Comparison of sediment volume datasets. The size and volumes of the ponds included in this study are more similar to those studied by Butler and Malanson, Montana, due to similar geomorphic settings.

Study	**Naiman et al., 1986**	**Bulter and Malanson, 1995**	**Current**
Location	Quebec, CN	Montana, USA	Colorado and Wyoming, USA
Fluvial setting	low gradient, multiple stream orders	low and high gradient, low stream orders	low and high gradient, low and high stream orders
Number of ponds	18	8	37
Range of ages (years)	*NA*	1-28	1-37
Range of pond surface areas (m^2)	100-14650	50-8200	16-6360
Range of sediment volumes (m^3)	35-6500	11.4-5064	3.8-4888

The performance of each equation is compared in Figure 23. I find that for my ponds, the area-based equations significantly underestimate sediment storage by a factor of 0.5 and account for less of the variability in the measured dataset. In contrast, the age-based equation significantly overestimates the sediment volume by a factor of 6 and produces more variable results than the measured dataset.

This trend holds true across groups, even when ponds are divided by burn status, channel location, and age (Table 8).

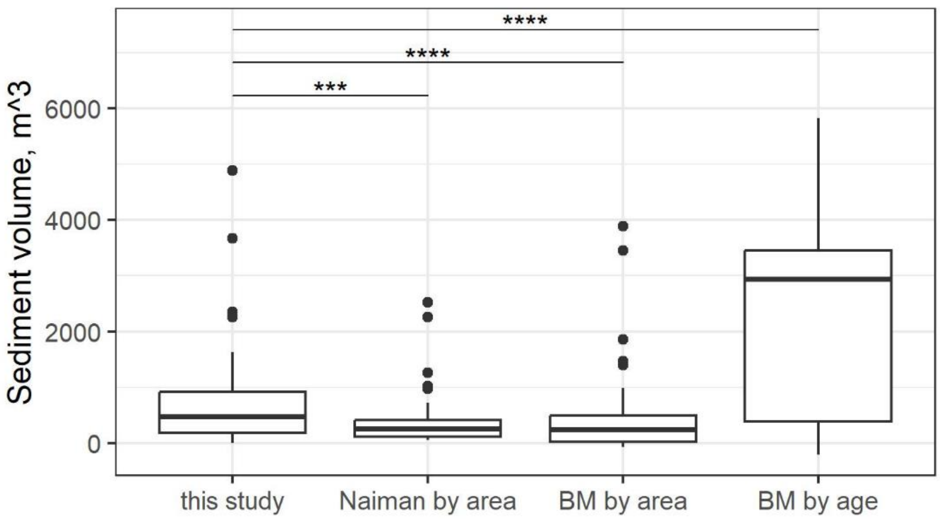

Figure 23: Pairwise comparison with of measured sediment volumes to volumes calculated from three empirical equations shown by boxplot. The connecting lines and asterisks indicate that each of the volumes estimated by empirical equations is significantly different than the measured sediment volumes. BM indicates Butler and Malanson.

Table 8: Comparison of measured and empirical equation estimated sediment volume and pond surface area. Results are shown for all ponds and as grouped by burn status, channel position, and pond age. Estimated results that are higher than the measured values are highlighted in red whole those than are lower are in blue.

	all	**Burn status**		**Channel position**		**Age**		
	all	**burned**	**unburned**	**on-channel**	**off-channel**	**recent**	**moderate**	**old**
Sediment volume source	***Median sediment volume, m^3***							
Measured	465	563	361	241	763	79	416	756
Estimated from age (Butler and Malanson 1995)	2941	3281	393	393	3451	308	2941	3451
Estimated from surface area (Butler and Malanson 1995)	241	310	107	65	495	-13	410	455
Estimated from surface area (Naiman 1986)	250	293	166	140	408	92	355	384
Pond surface area source	***Median pond surface area, m^2***							
Measured	520	631	306	238	926	114	790	863
Estimated from age (Butler and Malanson 1995)	4723	5247	795	795	5509	664	4723	5509

Fire disturbance does not account for the difference in measured and estimated results from the equations because both burned and unburned ponds show the same trends in difference. There may be regional factors such as geology, ecology, climate, and hydrology that account for the difference. Additionally, the majority of my ponds were abandoned, and it may be that sedimentation processes shift once beavers no longer occupy ponds. My finding of significant differences in residual volume based on beaver activity supports this interpretation. When estimating sediment volumes, additional factors such as disturbance regime, ecology, and pond characteristics may be necessary to improve accuracy. Pollock et al. (2003) hypothesized that the channel gradient and dam geometry govern the maximum sediment storage, but this has yet to be tested and does not predict the actual sediment storage because few ponds reach 100% infilling. In summary, beaver pond sediment volumes calculated from existing equations may drastically over or underestimate actual sediment volume, and equations should be used with care.

4.2 Sedimentation rates

The median lifetime sedimentation rate of the ponds (2.96 cm/yr) falls within the range of previously published data (0.2 – 45 cm/yr; Table 5) (Larsen et al., 2021). However, the lifetime sedimentation rate of one pond exceeded published rates at 52.2 cm/yr. Like other authors, I documented a wide spread in sedimentation rates, indicating that this is a highly variable and sensitive metric (Butler and Malanson, 1995; Puttock et al., 2018). Wildfire disturbance can increase sedimentation rates: I found that post-fire sedimentation rates were higher than lifetime rates and fall within the high end of the published literature, with a median of 19.8 cm/yr. Post-fire sedimentation rates did not show a meaningful relationship to any of the explanatory variables tested. This suggests that burning was the main control on sedimentation and other factors such as vegetation, geomorphology, and pond characteristics were overwhelmed in the short-term. Multivariate analysis indicates that of all the variables, valley gradient best accounts for the variation, but with quite low explanatory power.

4.2.1 Post-fire sedimentation

Burned ponds did not exhibit significantly different sedimentation rates than unburned ponds. However, sedimentation rates were significantly higher, by an order of magnitude, after fire in ponds with both pre- and post-fire sediments. Thus, Hypothesis 2 is partially supported: I found evidence that post-fire sedimentation rates exceed pre-fire rates, but sedimentation rates in burned ponds did not exceed rates in unburned ponds. Post-fire sedimentation rates in beaver ponds (median = 19.8 cm/yr) are similar to the post-fire sedimentation rates from Chambers Lake (median = 18.5 cm/yr). This corroborates the lack of relationship between pond surface area and sedimentation rate: smaller ponds, on average, accumulated sediment just as quickly as large ponds and even reservoirs.

Together, these findings suggest that although disturbances might contribute to some of the variability in the data, they do not overwhelm other factors controlling sedimentation over the lifespan of a pond. Additionally, I only evaluated one type of disturbance: fire. However, the ponds included may have been impacted by other disturbances throughout their existence including floods, debris flows, and vegetation shifts. An intense summer rainstorm in summer 2022 at Little Beaver Creek visually demonstrated how sedimentation and scour might be tied to specific precipitation events, although wildfire undoubtedly impacted how the landscape responded (Figure 24, Figure 25). Beaver activity may be considered a disturbance to sedimentation and ecological processes, resulting in an alternative stable state (Polvi and Wohl, 2013). The signals of these disturbances might confound the selected fire signal. Thus, sedimentation rates might not be a useful comparison tool across landscapes experiencing unique and compounding histories of disturbance.

Figure 24: Images of the July 15th, 2022 flood on Little Beaver Creek facing pond LBC-4. At 4:00 PM before the flood, shallow standing water is visible in the foreground with dark, charcoal-rich saturated sediments filling the majority of the pond. Small channels are incised into the sediment and patches of vegetation appear in the middle of the pond. By 5:30 PM, an intense rainstorm centered over the watershed caused flooding within the pond. By 7:30 PM, flood waters receded revealing a fresh sediment surface with lighter colors indicating more mineral sediment than charcoal. Channels shifted location and vegetation in the middle of the pond was either scoured or buried.

Figure 25: Images of the July 15th 2022 flood on Little Beaver Creek facing pond LBC-3. At 4:15 PM before the flood, thick vegetation surrounds the pond and patches have begun colonizing sediments in the middle of the pond where no standing water is visible. At bar of lighter colored coarse mineral sediment is visible in the mid-ground, behind which a small channel drains through the breached dam. Dark colored charcoal and organic rich sediments are visible in the foreground. Flood waters filled the pond nearly to capacity by 5:30 PM. By 7:30 PM, the pond had drained again leaving flattened vegetation along the margins and patches in the middle of the pond. A raindrop obscures the view, however, the sediment bar in the midground appears to have been scoured or covered with new sediment.

4.2.2 Other controls on sedimentation rates

Geomorphic setting describes much of the observed lifetime sedimentation. Watersheds that are larger, have lower relief ratios and lower watershed slopes, or steeper valley gradients and wider valleys at the reach scale demonstrated significantly higher sedimentation rates. These explanatory variables may increase stream power and sediment transport so that more sediment is available to be trapped in ponds. Relatedly, pond connection to the channel emerged as significant, which likely dictates sediment transport as described in the residual volume section.

Multivariate modeling indicates that pond age is the most critical variable for describing lifetime sedimentation rates, capable of explaining nearly two thirds of the variation. Sedimentation rates decline with pond age, which corroborates previous research (Butler and Malanson, 1995; Bigler et al., 2001). Rates may decline as a result of several processes impacting sediment delivery, sediment compaction, and sediment retention in ponds. Dams may force avulsion and enhance multithread planforms, stranding ponds off the channel and decreasing sediment supply to the pond (John and Klein, 2004; Polvi and Wohl, 2013). Beaver are ambitious dam builders and over time are more likely to construct ponds upstream, which may retain sediment before it can pass downstream (Puttock et al., 2018; Johnson-Bice et al., 2022). Beaver may be more likely to excavate their ponds to maintain swimming space as sediment infilling occurs. Stored sediment may compact over time in response to more loading, thus resulting in lower average sedimentation rates. As the pond fills, sediments are more prone to erosion due to a greater difference in baselevel compared to the downstream channel. The likelihood of a pond experiencing a high flow increases as it grows older, creating more opportunities for dam breaches and scour. More research is needed to explore these pathways and processes.

4.2.3 Assumptions

My method for calculating the post-fire sedimentation rate relied on charcoal stratigraphy to identify post-fire sediment. I assumed that observed charcoal in the upper parts of the stratigraphic column was deposited by 2020 fires. In some locations, I saw evidence of fuel-reduction burn piles and campfires that could introduce additional charcoal and muddy the signal. In most cases, however, fire occurrence was readily identified by sharp increases in charcoal content, especially where larger charcoal pieces like charred pine needles were present. The method also assumes that no reworking of sediment occurred after deposition, as that could move charcoal further down in the stratigraphic column, artificially increasing rates. Distinct stratigraphic units present in many burned ponds suggest that sediments are not mixed downwards (Figure 26). Unburned ponds also demonstrated distinct stratigraphy, but the units' boundaries were typically more gradational (Figure 27). Additionally, time lapse imagery documents scour and deposition during high flows, providing further evidence that post-fire sedimentation rates are not overestimates (Figure 24, Figure 25).

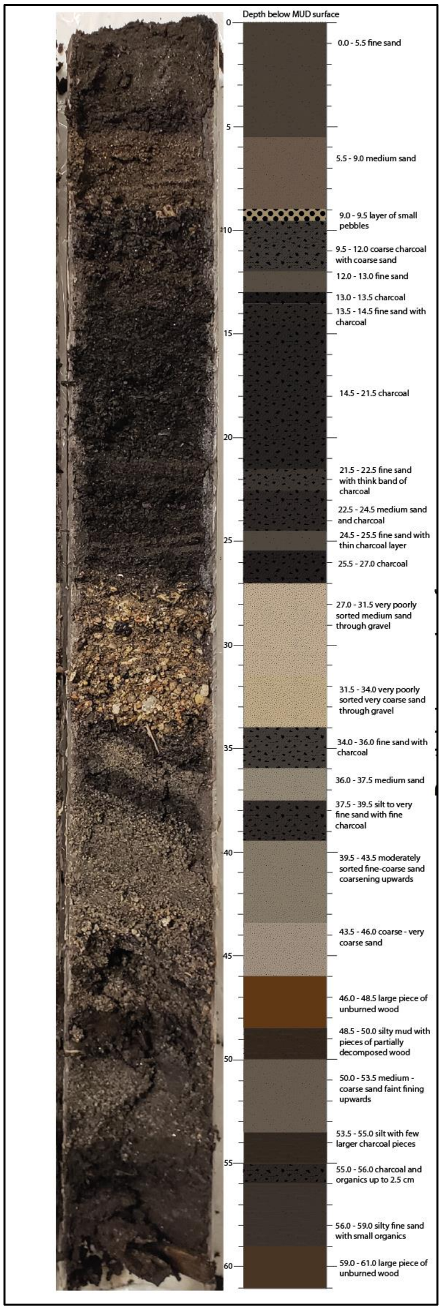

Figure 26: The LBC21-1A-1C core was collected from pond LBC-3 in October 2021. The pond burned in the Cameron Peak fire. On the left, a photograph of the core reveals distinct stratigraphic units defined by visible changes in color and grain size. On the right, a visual representation and description of each unit.

Figure 27: The GLC-2-2 core was collected from the GLC-2 pond in July 2022. The Glacier Creek watershed did not burn during recent wildfires. Stratigraphic units with both abrupt and gradational boundaries are visible along the core.

4.2.4 Sensitivity Analysis

4.2.4.1 Pond age

My assessment of the sensitivity of sedimentation rates to the method for measuring pond age and depth yielded mixed results. I found no significant difference between the mean sedimentation rate and the minimum and maximum rates for ponds with constrained imagery ($p = 0.49$) (Figure 28). However, there are significant differences in the mean sedimentation rates and the 50- and 100-year-old pond rates calculated for unconstrained ponds ($p < 0.05$). These results show that assigning the youngest or oldest date for ponds with constrained dates creates negligible differences, likely because the longest gap in imagery from 1985-1999 is only 14 years, whereas the unconstrained ponds first appeared in either 1985 or 1999, depending on the resolution of the imagery, with ages of 37 or 23 years. Arbitrarily assigning 50 and 100 year ages doubled or tripled the ages, resulting in significantly lower sedimentation rates.

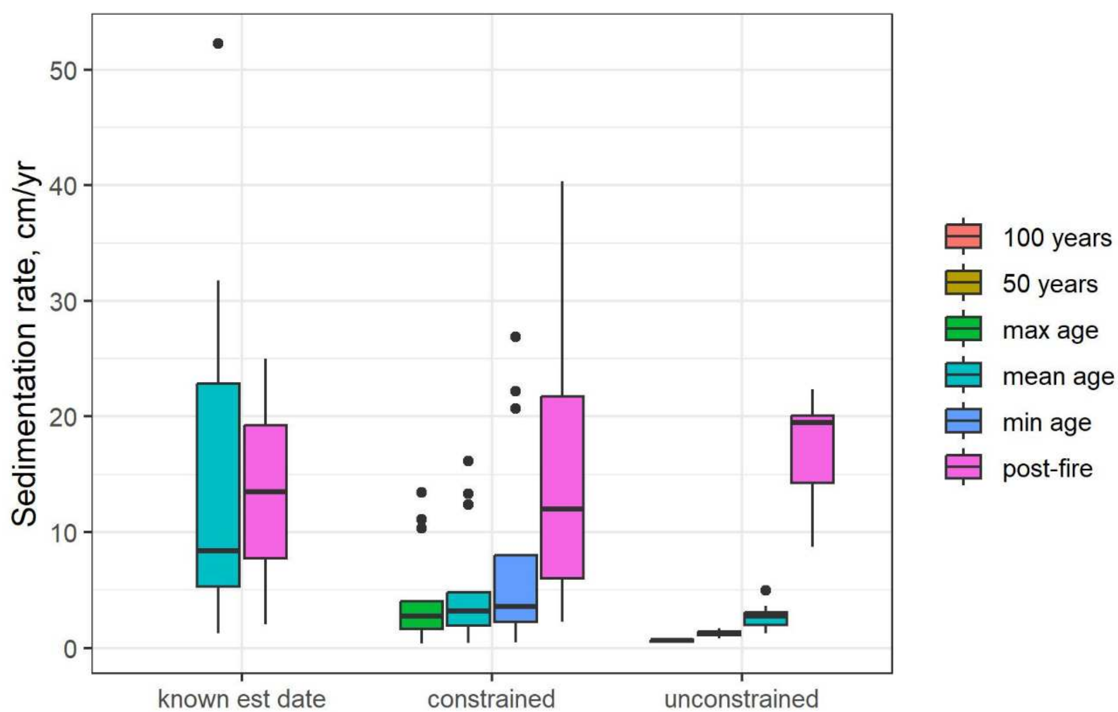

Figure 28: Comparison of sedimentation rate sensitivity to pond establishment year.

The results of hypothesis testing using sedimentation rates calculated from different ages are presented in Table 9. Overall, substitution of the constrained maximum and constrained minimum performed similarly to the mean age used in the full analysis. The only different outcome came from testing the channel position against the maximum age. The 50- and 100-year unconstrained substitution yielded greatly different results during hypothesis testing compared to the sedimentation rates used in the full analysis.

Table 9: Sensitivity of hypothesis testing results to using sedimentation rates calculated from different pond ages. Sedimentation rates were compared against three selected explanatory variables with statistical hypothesis testing. The results of the mean age used in the full analysis are highlighted in yellow. The results of each alternative sedimentation rate calculation are shown below, with results that match the mean age in green and those that differ in orange. S and N indicate significant or not significant results of hypothesis testing.

	Explanatory Variable				
Sedimentation rate method	**burn status**	**channel position**	**pond age, recent:moderate**	**pond age, recent:old**	**pond age, moderate:old**
mean age	S	S	S	S	N
constrained maximum age	S	N	S	S	N
constrained minimum age	S	S	S	S	N
unconstrained - 50 years old	N	S	N	S	N
unconstrained - 100 years old	N	S	N	S	S

I conclude from this analysis that ponds constrained by imagery on either side are not sensitive to whether the minimum and maximum age was selected, and my use of the mean age for these ponds is justified. However, ponds established before imagery is available prove more sensitive because their timing is completely unconstrained. My selection of 50- and 100- years may be unusually old, but beaver meadows may persist for long periods of time (Kramer et al., 2012). Therefore, my reported sedimentation rates for these ponds may be on the high end, representing maximum rates.

4.2.4.2 Sediment depth

I found a significant difference in median lifetime sedimentation rate depending on which sediment thickness method is used ($p < 0.05$) (Figure 29). The probed depths generated higher sedimentation rates than the core depth. This corroborates field experience that I was unable to retrieve the full thickness of the sediment column with the coring methods. I noted that sediments compressed during insertion of the tubing, an issue that other researchers have encountered (Butler and Malanson, 1995). In addition, at times some sediment was lost out of the bottom of the core during extraction. A different coring system, such as a Livingston corer, might be more appropriate for full retrieval of saturated sediments. Despite the differences in sedimentation rate, changing the method used for depth measurements did not result in any changes in hypothesis testing outcomes for selected variables (Table 10).

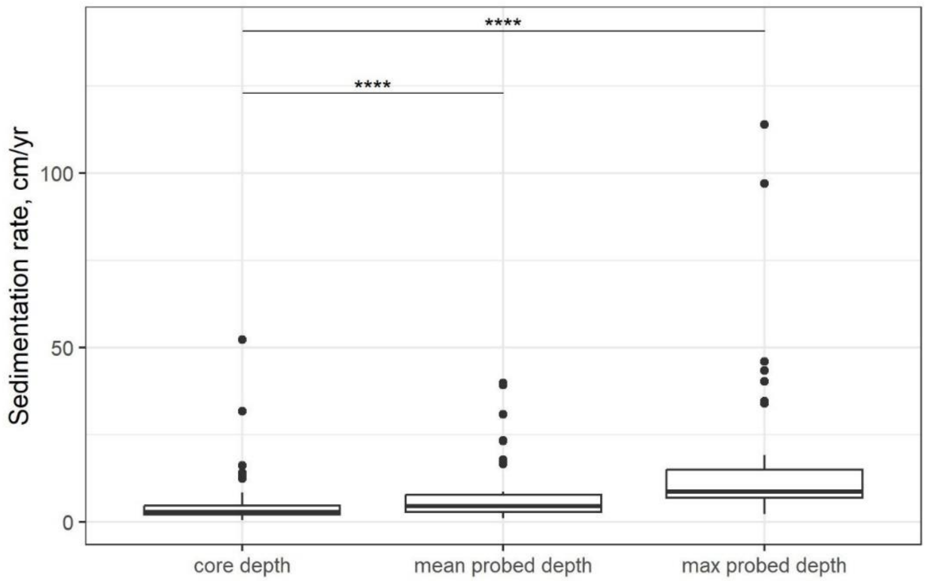

Figure 29: Comparison of lifespan sedimentation rates (cm/yr) calculated from three thickness sources: the sediment core depth, mean probed depth, and maximum probed depth.

Table 10: Sensitivity of hypothesis testing results to using sedimentation rates calculated from three thickness sources: the sediment core depth, mean probed depth, and maximum probed depth. Sedimentation rates were compared against three selected explanatory variables with statistical hypothesis testing. The results of the core depth used in the full analysis are highlighted in yellow. The results of each alternative sedimentation rate calculation are shown below, with results that match the core in green.

	Explanatory Variable				
Sedimentation rate method	**burn status**	**channel position**	**pond age, recent:moderate**	**pond age, recent:old**	**pond age, moderate:old**
core depth	NS	S	S	S	N
mean probed	NS	S	S	S	N
max probed	NS	S	S	S	N

From this analysis, I conclude that although sedimentation rate calculation is sensitive to the sediment thickness used, the uncertainty does not alter the results of hypothesis testing. Even though coring resulted in some, unquantified sediment loss, the loss may have been relatively consistent between ponds, thus incorporating method bias evenly. Therefore, sedimentation rates should be calculated using consistent methods through the study, and care must be taken when comparing to rates reported elsewhere. The sediment thickness method I used appears to underestimate sedimentation rates compared to using probed sediment thickness values.

4.3 Sediment composition

4.3.1 Grain size

I found that beaver ponds contain high abundances of fine sediments (median = 46.7% fines). The fine texture of beaver pond sediments is consistent with other research that has found high abundances of the silt and clay fractions stored in beaver ponds (Butler and Malanson, 1995; Bigler et al., 2001; Giriat et al., 2016). Additionally, beaver ponds contained finer sediments compared to all other geomorphic units measured in the similar valleys across the region (median = 12.01) (Sutfin and Wohl, 2017). The sediment texture of beaver ponds is variable (min = 5.9 %, max = 77.4 % fines), like other geomorphic units (min = 0, max = 48.19% (Sutfin and Wohl, 2017)). Sediment texture within beaver ponds likely depends on the sediment transport capacity of inflowing streams, the upstream sediment supply, and the trap efficiency of the dam. However, sediments may be reworked from floodplain deposits, or delivered atmospherically or directly from hillslopes. The diversity of potential transport pathways may partially explain the mixed results.

4.3.1.1 Post-fire grain size

Burn characteristics did not significantly relate to grain size but burned ponds in more severely burned watersheds contained finer sediments compared to unburned ponds or lower burn extents. I hypothesized that burned ponds would contain coarser mineral sediment due to the increased post-fire sediment transport capacity of watersheds, but this hypothesis is not supported. I qualitatively observed more sharply defined stratigraphy in burned ponds than in unburned ponds. Units commonly alternated between large (>1 cm) pieces of charcoal and sand (i.e., Figure 26). The boundaries between units in unburned ponds were more diffuse and typically defined by the concentration of fibrous plant roots, perhaps recording wetting and drying cycles, or periods of pond abandonment and reoccupation by beaver (i.e., Figure 27). However, my statistical analyses did not find a significant difference in grain size variation within burned and unburned ponds. I had also hypothesized that post-fire sediment would be coarser than pre-fire sediment, but this hypothesis is not supported either. Instead, I found no significant difference in grain size between pre-and post-fire sediment, suggesting that sediment texture is governed by other factors besides wildfire.

4.3.1.2 Other controls on grain size

Geomorphic characteristics corresponded to grain size, as I predicted. Large drainage areas, steep watershed slopes, high relief ratios, steep valley gradients, and narrow valley bottom widths corresponded with coarser sediments in beaver ponds. These findings suggest that the geomorphic context plays a critical role in sediment generation, transport, and attenuation, which furthers a large body of previous research on the geomorphic impacts of sediment transport on fire-impacted landscapes (e.g., Moody et al., 2008; Wohl, 2018; Wohl et al., 2020).

Relatedly, pond position in relation to the channel and other ponds corresponded with grain size. On-channel and solitary ponds contained coarser sediment than off-channel ponds and ponds that were near others. Coarse sediment delivery is possible to ponds on the channel whereas off-channel ponds may only be connected during high overbank flows when energy is dispersed across the floodplain, and finer grain sizes are deposited. Off-channel ponds may also receive sediment inputs directly from surrounding hillslopes from diffuse sediment migration, rilling and gullying, and debris flows. At a field site on Little Beaver Creek, I saw alluvial fans fed by ephemeral hillslope gullies splaying coarse sediments into an off-channel beaver pond (Figure 30).

Figure 30: Alluvial span spilling into LBC-1 pond near Little Beaver Creek, CO. White arrows mark the same piece of burned wood in the fan. (A) Looking to the south down the alluvial fan in October 2021, very coarse sand and gravels are seen in transport further into the pond, carried by flow from an ephemeral hillslope gully. The pond is not connected to the mainstem channel. (B) View of the pond looking east in July 2022. Water levels were lower during this visit, exposing fine sediments deposited at the distal end of the fan toward the right.

Sediment delivery and trapping likely changes over the lifetime of a pond. I found that mid-aged and old ponds contain finer sediments than recently constructed ponds. Likewise, inactive ponds contained finer sediment than ponds actively maintained by beaver. BDAs contained the coarsest sediment of any grouping, with a median of 7.5% fines. Inactive dams may be the least permeable due to dense vegetation growth along the dam, which would facilitate greater trapping of fine sediment. Active ponds may also be relatively permeable, but beavers actively excavate and rework sediment, potentially resuspending and transporting fine sediments. BDAs are not maintained and thus likely become the most permeable over time as they typically are not stabilized by vegetation or rebuilt by beaver. This might explain the lower trapping ability of BDAs, along with the higher stream power of the sites on which they are typically placed.

4.3.1.3 Assumptions

My analytical methods might have skewed samples high in organic material toward finer grain sizes. I heated samples to 550°C to remove organic matter, but this combustion produced ashy by-products and these could be quite significant in samples with high abundances of organic material. Additionally, PyC resembles inorganic carbon in its chemical and thermal properties, so that heating to 950 °C might be more appropriate for full removal (Santisteban et al., 2004; Masiello, 2004). Incompletely combusted by-products are fragile and may have deteriorated to silt-size during the physical de-aggregation processing step, which could artificially inflate the silt-size class. As such, the reported grain size might not reflect the texture of material transported and found in the pond and may skew burn data toward finer textures. A dissolution method for organic removal was initially considered, but was deemed infeasibly time-consuming.

4.3.2 Total Organic Carbon (TOC)

I found that beaver pond sediments contain high abundances of organic matter, with a median of 6.4% TOC across all ponds. This value falls within the range of 4.9-17.5% TOC (9.7 – 35.0% organic matter) reported for beaver ponds in Montana but is less than the 14.7% total carbon documented for beaver pond sediments in England (Butler and Malanson, 1995; Puttock et al., 2018). The median TOC value from our ponds is similar to the TOC storage documented in ponds recently constructed by reintroduced beaver in Washington State (median = 5.7% TOC) (McCreesh et al., 2019). Pond TOC values are higher than other valley deposit types in the region (median = 3.50% TOC), but they fall within the range of observed values (0.16 – 41.9% TOC) (Sutfin and Wohl, 2017). Additionally, beaver ponds contribute to a suite of processes that result in highly heterogenous floodplains and enhanced carbon storage (Polvi and Wohl, 2012; Wohl et al., 2018; Laurel and Wohl, 2019). Beaver ponds sediments contain significant carbon stocks, placing them in the same class as wetland soils that store an estimated 20-30% of global soil carbon (Mitsch and Gosselink, 2007).

4.3.2.1 Post-fire TOC

My hypothesis that burned ponds would contain greater abundances of TOC due to the influx of post-fire PyC was not supported as I did not find significant differences in TOC by burn characteristics. Burned ponds did contain slightly higher median TOC than unburned ponds, but the insignificance of this relationship suggests that other carbon sources are important. Additionally, burned ponds had significantly higher variation in TOC content between stratigraphic units, suggesting that carbon cycling pathways shift and become more variable after fire, even while overall TOC storage remains similar. Furthermore, I only quantified particulate carbon stored in the pond sediments, which does not account for pathways of carbon loss through fluvial transport, decomposition and biotic cycling, or atmospheric off-gassing. The speed of these cycles might be altered by fire in unexpected and conflicting ways.

4.3.2.2 Other controls on TOC

Of the vegetation characteristics, only post-fire NDVI at the local scale showed a significant negative relationship to TOC. Ponds surrounded by more vegetation after fire contained less TOC than ponds with less vegetation. This could indicate greater input of PyC to the pond relative to leaf litter and plant detritus. It could also indicate a difference in how carbon is cycled within ponds; PyC is recalcitrant whereas other forms of organic carbon are biologically available. More riparian vegetation might indicate an overall more productive ecosystem capable of cycling carbon into organisms and the atmosphere.

Geomorphic setting also matters for TOC accumulation in beaver ponds. Laurel and Wohl (2019) found that carbon stock, derived from TOC, did not vary significantly between beaver meadows abandoned at different times, which they interpret as indicative of geology controlling the persistence of floodplain carbon over longer scales. I found that larger watersheds with greater relief correlated with lower TOC abundances in beaver ponds. Given the relationship between drainage area and discharge, it is reasonable to assume that TOC from primary production is reduced in swifter waters. Indeed, I noticed that the large drainage area sites had much cooler, clearer water than the warm, stagnant, and murky green ponds on small tributaries. I did not measure water temperatures in this study, but other researchers have documented thermal gradients within beaver ponds (Gran et al., 2022).

Relatedly, off-channel ponds contained higher abundances of TOC than on-channel ponds. I interpret this as further evidence that moving water lowers temperatures, flushes out nutrients and carbon, and results in lower primary production. Off-channel ponds are disconnected from high flows and may experience greater levels of nutrient cycling. There also appear to be longitudinal effects along a reach, as downstream ponds have more TOC than upstream ponds. This trend might be discharge-related as well because upstream ponds might diffuse and disperse flows, allowing downstream ponds to be more productive. Lower velocities might result in more TOC deposition because most organic material is lower in density than mineral sediment. Younger ponds contained less TOC than older ponds, which might indicate more anaerobic preservation of TOC through the lifespan of a pond as more sediment is buried, limiting nutrient cycling.

4.3.2.3 Assumptions

My analysis of TOC relied on a commercial Loss on Ignition (LOI) protocol that was not designed for burned sediments (Ward, 2022). The LOI temperature was relatively low, and likely did not result in combustion of most PyC products. Therefore, the TOC results may not fully account for the carbon storage within ponds. Instead, the reported TOC results describe the unburned, bio-available carbon in the system. Although this is critical for comprehending nutrient cycling, it leaves the question of PyC storage in beaver ponds inconclusively addressed.

4.4 Management implications

The findings of this study may help managers better understand sediment dynamics in beaver ponds after wildfire. In addition to being shaped by physical processes, every watershed is guided by a suite of management goals which often include sediment attenuation, infrastructure protection, long-term sediment storage, water quality improvement, habitat creation and/or protection, and more. As managers balance these overlapping goals, beavers may prove invaluable partners in promoting resilience. Below I summarize and discuss a few of my key findings in the context of post-wildfire river and sediment management.

4.4.1 Beaver ponds capture and store post-fire sediment and carbon.

Burned ponds had lower residual volumes than unburned ponds, meaning they stored more sediment. Additionally, sedimentation rates were higher after fire compared to before. In the study area, the majority of beaver ponds were located upstream of water supply infrastructure, so their sediment storage function likely reduced downstream delivery and buffered some of the post-fire effects in the two years following the 2020 fires. Overall, beaver ponds contained high abundances of total organic carbon.

4.4.2 Large ponds store higher volumes of sediment.

Managers attempting to store post-fire sediment in river corridors rather than in reservoirs might prioritize the creation, maintenance, and protection of large beaver ponds. Beavers build and maintain dams that impound larger ponds than BDAs. Even though BDAs create smaller ponds that store less sediment than natural dams, they may still be useful management tools where beaver reintroduction is costly or infeasible. BDAs may store comparable residual volumes of sediment to ponds actively maintained by beaver. BDA performance might be enhanced through adaptive management such as modifying designs to more closely mimic beaver structures and revisiting structures after installation to perform maintenance (like a beaver does daily). In addition to attenuating sediment, BDAs may also create suitable habitat that entices beavers to inhabit a reach. Beavers built natural dams proximal to BDAs on three of my study reaches (FALL, COW, FC). BDAs may offer beavers a toehold in areas with habitat degradation, and the structures can provide additional sediment storage.

4.4.3 More ponds mean more sediment storage.

I generally found that reaches with greater numbers of ponds stored higher volumes of sediment. In addition to each individual pond simply providing more storage space, additional ponds on a reach may promote non-linear responses with multiplicative effects. For example, if an upstream dam breaches, the released sediment may be partially trapped in ponds further down on the reach. Beaver damming may alter valley geomorphology resulting in an alternative stable state with more sediment storage and resilience to disturbance (Polvi and Wohl, 2013, Fairfax and Whittle, 2020).

4.4.4 Beaver pond sediment dynamics are shaped by nested contexts.

Geology, climate, and ecology are well established as high-level regional drivers of sediment dynamics and processes within rivers (Wohl, 2018; Wohl et al., 2020), and I found evidence that they drive beaver pond sedimentation as well. Reach characteristics such as channel planform, valley confinement and gradient influence whether a location is likely to be transport, erosion, or deposition dominated. Pond characteristics determine how likely the pond is to intercept and retain sediment traveling through a reach. Sediment dynamics depend on multiple scales of interaction, however, pond characteristics may be of relevance to engineers and managers tasked with protecting water supply in fire-prone landscapes, as these parameters might be more easily adjusted within a project than the larger context. Ponds located in wide, low-gradient reaches that are constructed directly on the channel accumulate sediment the most rapidly, thus offering the greatest benefit for dampening downstream sediment fluxes in the post-fire “window of disturbance” while other watershed processes recover.

4.4.5 Sediment dynamics change as ponds age.

Young ponds accumulate sediment more rapidly but store low normalized volumes of sediment and higher residual volumes meaning more remaining storage capacity. Conversely, older ponds stored greater normalized volumes of sediment and higher relative volumes of sediment but exhibited lower sedimentation rates. Older dams must have some level of stability to withstand flooding and breaching, so sediments stored in these ponds are more likely to persist than sediments stored in younger ponds. Protecting older ponds may increase the persistence of sediment on the landscape even after the “window of disturbance” has closed. Constructing ponds and introducing beaver over longer time periods may ensure a variety of pond ages that diversifies and balances the short-term rapid accumulation provided by young ponds and the longer-term storage provided by old ponds. Reoccupied or restored abandoned ponds offer opportunities for combining these benefits.

4.4.6 Beaver-based restoration can be implemented prior to fire.

All the ponds I visited were established before the 2020 fires and provide sediment storage both before and after fire. Beaver-based restoration may be a proactive rather than reactive response to disturbance. Indeed, the presence of beaver in river corridors make those areas less likely to burn (Fairfax and Whittle, 2020). In addition to being prepared for potential fire impacts, beaver restoration or mimicry may benefit other ecosystem functions including hydrology, sediment dynamics, water quality, and habitat improvement (Westbrook et al., 2006; Nash et al., 2021). In the event of fire, beaver ponds provide critical post-fire sediment storage, thus enhancing watershed resilience and recovery.

5. CONCLUSION

In 2020, large wildfires burned in the Colorado Rocky Mountains, and in the following "window of disturbance" managers documented elevated levels of charcoal-laden sediment traveling through rivers. The influx of sediment challenged water supply infrastructure and aquatic habitat; the blackened waters are a familiar yet distressing sight as fires are growing increasingly common across the American West. Forested regions throughout North America are facing increasingly frequent wildfires that are impacting more communities each year, compounding the risks posed by global climate change (Williams et al., 2019). Yet, we find ourselves in an exciting moment of accelerated growth in beaver research and, relatedly, beaver-based restoration. Understanding beaver pond contributions to sediment and carbon dynamics following fire is a necessary component for improving river management and restoration practices, maintaining river corridor ecosystem diversity and function, and partnering with beaver to adaptively increase resilience of natural and human systems challenged by climate change (Dittbrenner, 2019; Jordan and Fairfax, 2022).

In this study, I analyzed sediment storage and composition in 45 beaver ponds to test hypotheses regarding the effectiveness of sediment attenuation in beaver ponds. I used sediment proving surveys, sediment cores, stratigraphic analysis, TOC and grain size analyses, and geospatial datasets to quantify sediment storage and characterize composition. Results indicate that beaver ponds in the Rocky Mountains store high volumes of sediment (mean = 796 m^3). A comparison of residual volume indicates that burned ponds have less remaining storage than unburned ponds, indicating that beaver ponds are storing significant amounts of post-fire sediments. In ponds with both pre- and post-fire sediments present, sedimentation rates were an order of magnitude higher after fire. Sediment volumes, normalized sediment volumes, sedimentation rates, grain size, and TOC content did not vary significantly between burned and unburned ponds, indicating that geomorphic, ecologic, and pond characteristics exerted greater control on the rate of sediment deposition and the composition of sediments.

Human-constructed BDAs and active beaver ponds both had high sedimentation rates with high residual volumes of remaining storage, indicating they these ponds also quickly retain sediment with additional space available, compared to inactive ponds. Relatedly, larger ponds tended to have more remaining storage capacity and lower sedimentation rates. I found that the position of ponds in relation to each other along a reach also impacts sedimentation. Ponds that are solitary along a reach experience the highest sedimentation rates and have the greatest remaining storage capacity, whereas ponds that are upstream of other ponds have the least remaining storage capacity and low sedimentation rates. Downstream ponds have moderate amounts of remaining storage and low sedimentation rates. These results suggest that beaver ponds work in concert with each other to provide storage along a river reach. Upstream ponds initially may do most of the work, but the effects likely compound downstream as velocities are progressively lowered. Additionally, downstream dams might provide redundancy in the event of a dam blowout, capturing remobilized sediment before it leaves the reach. Therefore, although individual ponds provide large benefits, multiple ponds may reduce the transiency of sediment. Younger ponds had more remaining storage and higher sedimentation rates compared to older ponds, but older ponds still functioned to store sediment. In the event of fire, beaver ponds of varied characteristics provide critical post-fire sediment storage, thus enhancing watershed resilience and recovery.

5.1 Ideas for future research

I documented that beaver ponds store high volumes of sediment, much of which is generated after wildfire. However, the question remains: how much of total post-fire sediment moving through rivers is captured and stored in beaver ponds? One approach for approximating this value would be constructing a pre- and post-fire a DEM of differencing (DoD) to volumetrically estimate sediment loss from hillslopes. Alternatively, discharge, turbidity, suspended sediment, and bedload monitoring of streams post-fire could be used to determine sediment volumes. This method could also potentially link discharge events to deposition and scour within ponds if paired with continuous pond monitoring. Sediment transport modeling could provide another path forward, especially if paired with monitoring data.

My sensitivity analysis of sedimentation rates demonstrates the importance of constraining pond establishment ages and obtaining complete sediment cores. Unconstrained ages varied significantly and are less reliable for calculating sedimentation rates. This limitation will diminish as high-resolution satellite imagery becomes increasingly available, but analysis of historical ponds could benefit from alternative dating methods. Depending on the estimated age of the pond, using radionuclides, radiocarbon, or vegetation growth might be appropriate options (Levine and Meyer, 2019). These methods rely on complete and representative sediment core retrieval, as does accurate characterization of sedimentation rates. Sediment core retrieval might be improved by using a different coring system such as a Livingston corer.

The age question could be circumvented entirely by measuring sedimentation rates in situ. This could involve installing sediment traps, monitored at an established interval or after large discharge events. An alternative method would be to install a camera facing a staff gage in a pond to capture stage through time. This would only work in ponds with little standing water. Although more time intensive, researchers could make repeat measurements of sediment depths to back-calculate sedimentation rates. Depth measurement data could also be used to refine estimates of residual volume through time.

Therein lies another broad knowledge gap and area for future research: time. My study, like most, used a point-in-time method for sediment surveys, assuming that field observations were representative of overall post-fire sediment conditions in beaver ponds. However, ponds are clearly dynamic and transient on multiple timescales. Future research is needed to track the fate and quantify the longevity of sediments in beaver ponds (Larsen et al., 2021). Repeat surveys of beaver pond sediments multiple years after disturbance and the use of sediment clast tracers could help fill these gaps. New technologies to survey pond bathymetry and estimate sediment thickness could facilitate faster field measurements (Bradbury et al., 2022).

Spatial scale and regional patterns constitute additional areas for research. Thus far, estimates of current and historical sediment storage in beaver ponds rely on limited data and generalizing calculations (Butler and Malanson, 2005; Scamardo et al., 2022). But it seems likely that the sediment storage function of beaver ponds depends on the geologic, climatic, and ecological template of a region. An active area of research is leveraging remote sensing and machine learning to map and track beaver ponds through time at large spatial scales (Fairfax et al., 2022). Once these datasets are readily available, it will be more feasible to scale-up field studies, although field truthing will remain important, especially given the heterogeneity and variability inherent to beaver-modified river systems.

Refined TOC measurement techniques could help distinguish between bioavailable organic carbon and pyrogenic carbon, lending insight into both the carbon storage and ecosystem function of beaver ponds. Transdisciplinary work might span the fields of ecology, hydraulics, fisheries, and biogeochemistry to trace nutrient fluxes, chemical cycling, and system structure across tropic levels. Wetlands have been the focus of much of this transdisciplinary work, but beaver ponds likely function differently and there has been relatively little research in this realm (Naiman et al., 1986; Puttock et al., 2018; Larsen et al., 2021; Fegel and Rhoades, 2022).

Furthermore, land and wildlife management practices such as beaver removal, reintroduction, willow protection, fuels thinning, and wolf reintroduction all might impact the sediment dynamics, but by what pathways and by how much remain unknown. Considering the human dimension prompts additional questions including the cost, both monetary and social, of the services provided by beaver dams, and the political possibilities of beaver restoration. Research addressing these questions could help managers better preserve ecosystem function and protect critical drinking water supplies.

REFERENCES

Anderson, S.W., Anderson, S.P., and Anderson, R.S., 2015, Exhumation by debris flows in the 2013 Colorado Front Range storm: Geology, v. 43, p. 391–394, doi:10.1130/G36507.1.

Arkle, R.S., Pilliod, D.S., and Strickler, K., 2010, Fire, flow and dynamic equilibrium in stream macroinvertebrate communities: Freshwater Biology, v. 55, p. 299–314, doi:10.1111/j.1365-2427.2009.02275.x.

Baker, B.W., 2003, Beaver (Castor canadensis) in heavily browsed environments: , p. 9.

Battige, K., Wright, B., Carroll, C., Fairchild, M., and Geiger, R., 2022, Evaluating the resiliency for Cutthroat Trout following large wildfires in the Front Range:

Benavides-Solorio, J. de D., and MacDonald, L.H., 2005, Measurement and prediction of post-fire erosion at the hillslope scale, Colorado Front Range: International Journal of Wildland Fire, v. 14, p. 457, doi:10.1071/WF05042.

Bigler, W., Butler, D.R., and Dixon, R.W., 2001, Beaver-Pond Sequence Morphology and Sedimentation in Northwestern Montana: Physical Geography, v. 22, p. 531–540, doi:10.1080/02723646.2001.10642758.

Birkeland, P.W., Shroba, R.R., Burns, S.F., Price, A.B., and Tonkin, P.J., 2003, Integrating soils and geomorphology in mountains—an example from the Front Range of Colorado: Geomorphology, v. 55, p. 329–344, doi:10.1016/S0169-555X(03)00148-X.

Bladon, K.D., Emelko, M.B., Silins, U., and Stone, M., 2014, Wildfire and the Future of Water Supply: Environmental Science & Technology, v. 48, p. 8936–8943, doi:10.1021/es500130g.

Blount, K., Ruybal, C.J., Franz, K.J., and Hogue, T.S., 2020, Increased water yield and altered water partitioning follow wildfire in a forested catchment in the western United States: Ecohydrology, v. 13, p. e2170, doi:10.1002/eco.2170.

Boot, C.M., Haddix, M., Paustian, K., and Cotrufo, M.F., 2015, Distribution of black carbon in ponderosa pine forest floor and soils following the High Park wildfire: Biogeosciences, v. 12, p. 3029–3039, doi:10.5194/bg-12-3029-2015.

Bozek, M., and Young, M., 1994, Fish mortality resulting from delayed effects of fire in the Greater Yellowstone ecosystem: The Great Basin Naturalist, v. 54, p. 91–95, doi:10.2307/41712815.

Bradbury, G., Puttock, A., Coxon, G., Clarke, S., and Brazier, R.E., 2022, Testing a novel sonar-based approach for measuring water depth and monitoring sediment storage in beaver ponds: River Research and Applications, v. n/a, doi:10.1002/rra.4082.

Brazier, R.E., Puttock, A., Graham, H.A., Auster, R.E., Davies, K.H., and Brown, C.M.L., 2021, Beaver: Nature's ecosystem engineers: Wires. Water, v. 8, p. e1494, doi:10.1002/wat2.1494.

Brogan, D.J., MacDonald, L.H., Nelson, P.A., and Morgan, J.A., 2019a, Geomorphic complexity and sensitivity in channels to fire and floods in mountain catchments: Geomorphology, v. 337, p. 53–68, doi:10.1016/j.geomorph.2019.03.031.

Brogan, D.J., Nelson, P.A., and MacDonald, L.H., 2019b, Spatial and temporal patterns of sediment storage and erosion following a wildfire and extreme flood: Earth Surface Dynamics, v. 7, p. 563–590, doi:10.5194/esurf-7-563-2019.

Burchsted, D., Daniels, M., Thorson, R., and Vokoun, J., 2010, The River Discontinuum: Applying Beaver Modifications to Baseline Conditions for Restoration of Forested Headwaters: BioScience, v. 60, p. 908–922, doi:10.1525/bio.2010.60.11.7.

Butler, D.R., and Malanson, G.P., 1995, Sedimentation rates and patterns in beaver ponds in a mountain environment: Geomorphology, v. 13, p. 255–269, doi:10.1016/0169-555X(95)00031-Y.

Butler, D.R., and Malanson, G.P., 2005, The geomorphic influences of beaver dams and failures of beaver dams: Geomorphology, v. 71, p. 48–60, doi:10.1016/j.geomorph.2004.08.016.

Bywater-Reyes, S., Diehl, R.M., Wilcox, A.C., Stella, J.C., and Kui, L., 2022, A Green New Balance: Interactions among riparian vegetation plant traits and morphodynamics in alluvial rivers: Earth Surface Processes and Landforms, v. 47, p. 2410–2436, doi:10.1002/esp.5385.

Castro, J., Pollock, M., Jordan, C., Lewallen, G., and Woodruff, K., 2015, The Beaver Restoration Guidebook: Working with Beaver to Restore Streams, Wetlands, and Floodplains. Version 1.02.: United States Fish and Wildlife Service, 188 p., https://www.fws.gov/media/beaver-restoration-guidebook (accessed April 2022).

Chapman, S.S., Griffith, G.E., Omernik, J.M., Price, A.B., Freeof, J., and Schrupp, D.L., 2006, Ecoregions of Colorado: U.S. Geological Survey Level IV Ecoregions 2 sided color poster with map, descriptive text, summary tables, and photographs, http://www.ecologicalregions.info/data/co/co_front.pdf (accessed January 2023).

Chow, A.T., Tsai, K.-P., Fegel, T.S., Pierson, D.N., and Rhoades, C.C., 2019a, Lasting Effects of Wildfire on Disinfection By-Product Formation in Forest Catchments: Journal of Environmental Quality, v. 48, p. 1826–1834, doi:10.2134/jeq2019.04.0172.

Coalition for the Poudre River Watershed-Post-Fire Water Quality Protection Coalition for the Poudre River Watershed, https://www.poudrewatershed.org/post-fire-water-quality-protection (accessed December 2022).

Colorado Parks and Wildlife Living with Beavers: Colorado Parks and Wildlife, https://cpw.state.co.us/learn/Pages/LivingwithWildlifeBeaver.aspx (accessed January 2023).

Core Processing Continental Scientific Drilling, https://cse.umn.edu/csd/core-processing (accessed February 2022).

Cotrufo, M.F. et al., 2016, Redistribution of pyrogenic carbon from hillslopes to stream corridors following a large montane wildfire: Global Biogeochemical Cycles, v. 30, p. 1348–1355, doi:10.1002/2016GB005467.

Cribari-Neto, F., and Zeileis, A., 2010, Beta Regression in *R*: Journal of Statistical Software, v. 34, doi:10.18637/jss.v034.i02.

De Girolamo, A.M., Cerdan, O., Grangeon, T., Ricci, G.F., Vandromme, R., and Lo Porto, A., 2022, Modelling effects of forest fire and post-fire management in a catchment prone to erosion: Impacts on sediment yield: CATENA, v. 212, p. 106080, doi:10.1016/j.catena.2022.106080.

DeBano, L.F., 2000, The role of fire and soil heating on water repellency in wildland environments: a review: Journal of Hydrology, v. 231–232, p. 195–206, doi:10.1016/S0022-1694(00)00194-3.

Dennison, P.E., Brewer, S.C., Arnold, J.D., and Moritz, M.A., 2014, Large wildfire trends in the western United States, 1984–2011: Geophysical Research Letters, v. 41, p. 2928–2933, doi:10.1002/2014GL059576.

Dittbrenner, B.J., 2019, Restoration potential of beaver for hydrological resilience in a changing climate: University of Washington, 149 p.

Doesken, N.J., Pielke, R.A., Sr., and Bliss, O.A.P., 2003, Climatography of the United States No. 60: Colorado Climate Center, https://climate.colostate.edu/climate_long.html (accessed January 2023).

Dunham, J.B., Young, M.K., Gresswell, R.E., and Rieman, B.E., 2003, Effects of fire on fish populations: landscape perspectives on persistence of native fishes and nonnative fish invasions: Forest Ecology and Management, v. 178, p. 183–196, doi:10.1016/S0378-1127(03)00061-6.

Dunn, O.J., 1961, Multiple Comparisons Among Means: Journal of the American Statistical Association, v. 56, p. 52–64, doi:10.2307/2282330.

Dunnette, P.V., Higuera, P.E., McLauchlan, K.K., Derr, K.M., Briles, C.E., and Keefe, M.H., 2014, Biogeochemical impacts of wildfires over four millennia in a Rocky Mountain subalpine watershed: New Phytologist, v. 203, p. 900–912, doi:10.1111/nph.12828.

Ebel, B.A., 2020, Temporal evolution of measured and simulated infiltration following wildfire in the Colorado Front Range, USA: Shifting thresholds of runoff generation and hydrologic hazards: Journal of Hydrology, v. 585, p. 124765, doi:10.1016/j.jhydrol.2020.124765.

Ebel, B.A., and Moody, J.A., 2017, Synthesis of soil-hydraulic properties and infiltration timescales in wildfire-affected soils: Hydrological Processes, v. 31, p. 324–340, doi:10.1002/hyp.10998.

Eidmann, J.S., Rathburn, S.L., White, D., and Huson, K., 2022, Channel Response and Reservoir Delta Evolution From Source to Sink Following an Extreme Flood: Journal of Geophysical Research: Earth Surface, v. 127, p. e2020JF006013, doi:10.1029/2020JF006013.

Emelko, M.B., Silins, U., Bladon, K.D., and Stone, M., 2011, Implications of land disturbance on drinking water treatability in a changing climate: Demonstrating the need for “source water supply and protection” strategies: Water Research, v. 45, p. 461–472, doi:10.1016/j.watres.2010.08.051.

Fairfax, E., and Whittle, A., 2020, Smokey the Beaver: beaver-dammed riparian corridors stay green during wildfire throughout the western United States: Ecological Applications, v. 30, p. e02225, doi:10.1002/eap.2225.

Fairfax, E., Zhu, E., Clinton, N., Maiman, S., Ackerstein, D., and Corwin, E., 2022, EEAGER: A neural network model for automatically identifying beaver complexes in satellite and aerial imagery, *in* Geological Society of America Abstracts with Programs, Denver, CO, v. 54, No. 5, doi:10.1130/abs/2022AM-377687.

Fegel, T., and Rhoades, C.C., 2022, Impact of beaver ponds on biogeochemistry of organic carbon and nitrogen along a fire-impacted stream: Environmental Science Processes and Impacts. https://doi.org/10.1039/d2em00184e., doi:10.1039/d2em00184e.

Ferrari, S., and Cribari-Neto, F., 2004, Beta Regression for Modelling Rates and Proportions: Journal of Applied Statistics, v. 31, p. 799–815, doi:10.1080/0266476042000214501.

Foster, M.A., Anderson, R.S., Wyshnytzky, C.E., Ouimet, W.B., and Dethier, D.P., 2015, Hillslope lowering rates and mobile-regolith residence times from in situ and meteoric 10Be analysis, Boulder Creek Critical Zone Observatory, Colorado: GSA Bulletin, v. 127, p. 862–878, doi:10.1130/B31115.1.

Gannon, B.M., 2020, Wildfire-water supply risk in montane watersheds of Colorado: Baseline assessment and evaluation of mitigation strategies [Doctoral]: Colorado State University, 196 p.

Gannon, B.M., Wei, Y., Thompson, M.P., Scott, J.H., and Short, K.C., 2021 System Analysis of Wildfire-Water Supply Risk in Colorado, USA with Monte Carlo Wildfire and Rainfall Simulation: Risk Analysis, v. n/a, doi:10.1111/risa.13762.

Gardner, J.J., and Whitlock, C., 2001, Charcoal accumulation following a recent fire in the Cascade Range, northwestern USA, and its relevance for fire-history studies: The Holocene, v. 11, p. 541–549, doi:10.1191/095968301680223495.

Giriat, D., Gorczyca, E., and Sobucki, M., 2016, Beaver ponds' impact on fluvial processes (Beskid Niski Mts., SE Poland): Science of The Total Environment, v. 544, p. 339–353, doi:10.1016/j.scitotenv.2015.11.103.

Graham, R.T., 2003, Hayman Fire Case Study: Gen. Tech. Rep. RMRS-GTR-114. Ogden, UT: U.S. Department of Agriculture, Forest Service, Rocky Mountain Research Station. 396 p., v. 114, doi:10.2737/RMRS-GTR-114.

Gran, K., Behar, H., Burgeson, E., Dymond, S.F., Mitchell, S., and Nazzaro, A., 2022, Beaver removal impacts on low flow hydrology, *in* Denver, CO, doi:10.1130/abs/2022AM-380927.

Harrison, H.N., Hammond, J.C., Kampf, S., and Kiewiet, L., 2021, On the hydrological difference between catchments above and below the intermittent-persistent snow transition: Hydrological Processes, v. 35, p. e14411, doi:10.1002/hyp.14411.

Hauer, F.R., and Spencer, C.N., 1998, Phosphorus and Nitrogen Dynamics in Streams Associated With Wildfire: a Study of Immediate and Longterm Effects: International Journal of Wildland Fire, v. 8, p. 183–198, doi:10.1071/wf9980183.

Heiri, O., Lotter, A.F., and Lemcke, G., 2001, Loss on ignition as a method for estimating organic and carbonate content in sediments: reproducibility and comparability of results: Journal of Paleolimnology, v. 25, p. 101–110, doi:10.1023/A:1008119611481.

Higuera, P.E., Cook, M.C., Balch, J.K., Stavros, E.N., Mahood, A.L., and St. Denis, L.A., 2023, Shifting social-ecological fire regimes explain increasing structure loss from Western wildfires: PNAS Nexus, v. 2, p. pgad005, doi:10.1093/pnasnexus/pgad005.

Higuera, P.E., Shuman, B.N., and Wolf, K.D., 2021, Rocky Mountain subalpine forests now burning more than any time in recent millennia: Proceedings of the National Academy of Sciences, v. 118, p. e2103135118, doi:10.1073/pnas.2103135118.

Horton, J.D., 2017, The State Geologic Map Compilation (SGMC) Geodatabase of the Conterminous United States:, doi:10.5066/F7WH2N65.

IPCC, 2022, Global Warming of 1.5°C: IPCC Special Report on Impacts of Global Warming of 1.5°C above Pre-industrial Levels in Context of Strengthening Response to Climate Change, Sustainable Development, and Efforts to Eradicate Poverty: Cambridge University Press, doi:10.1017/9781009157940.

John, S., and Klein, A., 2004, Hydrogeomorphic effects of beaver dams on floodplain morphology: avulsion processes and sediment fluxes in upland valley floors (Spessart, Germany) [Les effets hydro-géomorphologiques des barrages de castors sur la morphologie de la plaine alluviale : processus d'avulsions et flux sédimentaires des vallées intra-montagnardes (Spessart, Allemagne).]: Quaternaire, v. 15, p. 219–231, doi:10.3406/quate.2004.1769.

Johnson-Bice, S.M., Gable, T.D., Windels, S.K., and Host, G.E., 2022, Relics of beavers past: time and population density drive scale-dependent patterns of ecosystem engineering: Ecography, v. 2022, doi:10.1111/ecog.05814.

Jordan, C.E., and Fairfax, E., 2022, Beaver: The North American freshwater climate action plan: WIREs Water, v. 9, p. e1592, doi:10.1002/wat2.1592.

Kassambara, A., 2022, rstatix: Pipe-Friendly Framework for Basic Statistical Tests:, https://CRAN.R-project.org/package=rstatix.

Kayranli, B., Scholz, M., Mustafa, A., and Hedmark, Å., 2010, Carbon Storage and Fluxes within Freshwater Wetlands: a Critical Review: Wetlands, v. 30, p. 111–124, doi:10.1007/s13157-009-0003-4.

Keeley, J.E., 2009, Fire intensity, fire severity and burn severity: a brief review and suggested usage: International Journal of Wildland Fire, v. 18, p. 116–126, doi:10.1071/WF07049.

Kieschnick, R., and McCullough, B.D., 2003, Regression analysis of variates observed on (0, 1): percentages, proportions and fractions: Statistical Modelling, v. 3, p. 193–213, doi:10.1191/1471082X03st053oa.

Kirchner, J.W., Finkel, R.C., Riebe, C.S., Granger, D.E., Clayton, J.L., King, J.G., and Megahan, W.F., 2001, Mountain erosion over 10 yr, 10 k.y., and 10 m.y. time scales: Geology, v. 29, p. 591–594, doi:10.1130/0091-7613.

Kramer, N., 2011, An investigation into beaver-induced Holocene sedimentation using ground penetrating radar and seismic refraction: Beaver Meadows, Rocky Mountain National Park, Colorado [M.S.]: Colorado State University, 109 p., https://www.proquest.com/docview/889138896/abstract/23D1838438FF42E3PQ/1 (accessed November 2021).

Kramer, N., Wohl, E.E., and Harry, D.L., 2012, Using ground penetrating radar to 'unearth' buried beaver dams: Geology, v. 40, p. 43–46, doi:10.1130/G32682.1.

Kruskal, W.H., and Wallis, W.A., 1952, Use of Ranks in One-Criterion Variance Analysis: Journal of the American Statistical Association, v. 47, p. 583–621, doi:10.2307/2280779.

Kunze, M.D., and Stednick, J.D., 2006, Streamflow and suspended sediment yield following the 2000 Bobcat fire, Colorado: Hydrological Processes, v. 20, p. 1661–1681, doi:10.1002/hyp.5954.

Larsen, A., Larsen, J.R., and Lane, S.N., 2021, Dam builders and their works: Beaver influences on the structure and function of river corridor hydrology, geomorphology, biogeochemistry and ecosystems: Earth-Science Reviews, v. 218, p. 103623, doi:10.1016/j.earscirev.2021.103623.

Laurel, D., and Wohl, E., 2019, The persistence of beaver-induced geomorphic heterogeneity and organic carbon stock in river corridors: Earth Surface Processes and Landforms, v. 44, p. 342–353, doi:10.1002/esp.4486.

Lenth, R.V., 2023, emmeans: Estimated Marginal Means, aka Least-Squares Means:, https://CRAN.R-project.org/package=emmeans.

Levine, R., and Meyer, G.A., 2019, Beaver-generated disturbance extends beyond active dam sites to enhance stream morphodynamics and riparian plant recruitment: Scientific Reports, v. 9, p. 8124, doi:10.1038/s41598-019-44381-2.

Lininger, K.B., Wohl, E., and Rose, J.R., 2018, Geomorphic Controls on Floodplain Soil Organic Carbon in the Yukon Flats, Interior Alaska, From Reach to River Basin Scales: Water Resources Research, v. 54, p. 1934–1951, doi:10.1002/2017WR022042.

Lisle, T.E., and Hilton, S., 1992, The Volume of Fine Sediment in Pools: An Index of Sediment Supply in Gravel-Bed Streams1: JAWRA Journal of the American Water Resources Association, v. 28, p. 371–383, doi:10.1111/j.1752-1688.1992.tb04003.x.

Lyon, J.P., and O'Connor, J.P., 2008, Smoke on the water: Can riverine fish populations recover following a catastrophic fire-related sediment slug? Austral Ecology, v. 33, p. 794–806, doi:10.1111/j.1442-9993.2008.01851.x.

Macfarlane, W. et al., 2020, CALIFORNIA BEAVER RESTORATION ASSESSMENT TOOL Building Realistic Expectations for Partnering with Beaver in Conservation and Restoration Recommended Citation:, doi:10.13140/RG.2.2.20316.00644.

Macfarlane, W., Meier, M., and Wheaton, J., 2019, John Day Basin BRAT Final Report:, doi:10.13140/RG.2.2.29252.27520.

Macfarlane, W.W., Wheaton, J.M., Bouwes, N., Jensen, M.L., Gilbert, J.T., Hough-Snee, N., and Shivik, J.A., 2017, Modeling the capacity of riverscapes to support beaver dams: Geomorphology, v. 277, p. 72–99, doi:10.1016/j.geomorph.2015.11.019.

Macfarlane, W., Wheaton, J., and Jensen, M., 2014, The Utah Beaver Restoration Assessment Tool: A Decision Support & Planning Tool:

Madole, R.F., VanSistine, D.P., and Michael, J.A., 1998, Pleistocene glaciation in the upper Platte River drainage basin, Colorado: IMAP, doi:10.3133/i2644.

Maiolo-Heath, M., 2021, Aerial Mulching Operations to Resume in Cameron Peak Burn Area:, https://www.fcgov.com/utilities//img/site_specific/uploads/press-release_-aerial_mulching_july2022.pdf?1658513862.

Malone, D., Rondeau, R., and Decker, K., 2019, Rocky Mountain Subalpine-Montane Riparian Shrubland: Colorado Natural Heritage Program, https://cnhp.colostate.edu/projects/ecological-systems-of-colorado/details/ (accessed January 2023).

Masiello, C.A., 2004, New directions in black carbon organic geochemistry: Marine Chemistry, v. 92, p. 201–213, doi:10.1016/j.marchem.2004.06.043.

McCreesh, R.K., Fox-Dobbs, K., Wimberger, P., Woodruff, K., Holtgrieve, G., and Pool, T.K., 2019, Reintroduced Beavers Rapidly Influence the Storage and Biogeochemistry of Sediments in Headwater Streams (Methow River, Washington): Northwest Science, v. 93, p. 112–121, doi:10.3955/046.093.0203.

McDaniel, J., 2021, Forests, Fire, and Faucets: What We Are Learning About Lingering Water Quality Effects of High-Severity Wildfires: Rocky Mountain Research Station: Science You Can Use Bulletin, p. 1–12.

McGuire, L.A., Rengers, F.K., Kean, J.W., Staley, D.M., Tang, H., and Youberg, A.M., 2019, Looking through the window of disturbance at post-wildfire debris flow hazards: Contained in: Proceedings of the Seventh International Conference on Debris-Flow Hazards Mitigation, Golden, Colorado, USA, June 10-13, 2019, https://hdl.handle.net/11124/173051, doi:10.25676/11124/173177.

McWethy, D.B. et al., 2019, Rethinking resilience to wildfire: Nature Sustainability, v. 2, p. 797–804, doi:10.1038/s41893-019-0353-8.

Meentemeyer, R.K., and Butler, D.R., 1999, Hydrogeomorphic effects of beaver dams in glacier national park, montana: Physical Geography, v. 20, p. 436–446, doi:10.1080/02723646.1999.10642688.

Minckley, T.A., Shriver, R.K., and Shuman, B., 2012, Resilience and regime change in a southern Rocky Mountain ecosystem during the past 17 000 years: Ecological Monographs, v. 82, p. 49–68, doi:10.1890/11-0283.1.

Mitsch, W.J., and Gosselink, J.G., 2007, Wetlands: John Wiley & Sons, 602 p.

Moody, J.A., and Martin, D.A., 2001, Initial hydrologic and geomorphic response following a wildfire in the Colorado Front Range: Earth Surface Processes and Landforms, v. 26, p. 1049–1070, doi:10.1002/esp.253.

Moody, J.A., Martin, D.A., and Cannon, S.H., 2008, Post-wildfire erosion response in two geologic terrains in the western USA: Geomorphology, v. 95, p. 103–118, doi:10.1016/j.geomorph.2007.05.011.

Morrison, A., Westbrook, C.J., and Bedard-Haughn, A., 2015, Distribution of Canadian Rocky Mountain Wetlands Impacted by Beaver: Wetlands, v. 35, p. 95–104, doi:10.1007/s13157-014-0595-1.

Naiman, R.J., Melillo, J.M., and Hobbie, J.E., 1986, Ecosystem Alteration of Boreal Forest Streams by Beaver (Castor Canadensis): Ecology, v. 67, p. 1254–1269, doi:10.2307/1938681.

Nash, C.S., Grant, G.E., Charnley, S., Dunham, jason B., Gosnell, H., Hausner, M.B., Pilliod, D.S., and Taylor, J.D., 2021, Great Expectations: Deconstructing the Process Pathways Underlying Beaver-Related Restoration: BioScience, v. 71, p. 249–267, doi:10.1093/biosci/biaa165.

Nolan, R.H., Collins, L., Leigh, A., Ooi, M.K.J., Curran, T.J., Fairman, T.A., Resco de Dios, V., and Bradstock, R., 2021, Limits to post-fire vegetation recovery under climate change: Plant, Cell & Environment, v. 44, p. 3471–3489, doi:10.1111/pce.14176.

Nyssen, J., Pontzeele, J., and Billi, P., 2011, Effect of beaver dams on the hydrology of small mountain streams: Example from the Chevral in the Ourthe Orientale basin, Ardennes, Belgium: Journal of Hydrology, v. 402, p. 92–102, doi:10.1016/j.jhydrol.2011.03.008.

Oropeza, J., and Heath, J., 2013, Effects of the 2012 Hewlett & High Park Wildfires on Water Quality of the Poudre River and Seaman Reservoir: City of Fort Collins, 33 p., https://www.fcgov.com/utilities/img/site_specific/uploads/2012__Wildfire_Effects_on_Water_Quality_in_the_Poudre_River.pdf (accessed February 2022).

Persico, L., and Meyer, G., 2009, Holocene beaver damming, fluvial geomorphology, and climate in Yellowstone National Park, Wyoming: Quaternary Research, v. 71, p. 340–353, doi:10.1016/j.yqres.2008.09.007.

Pollock, M.M., Beechie, T.J., and Jordan, C.E., 2007, Geomorphic changes upstream of beaver dams in Bridge Creek, an incised stream channel in the interior Columbia River basin, eastern Oregon: Earth Surface Processes and Landforms, v. 32, p. 1174–1185, doi:10.1002/esp.1553.

Pollock, M., Heim, M., and Werner, D., 2003, Hydrologic and Geomorphic Effects of Beaver Dams and Their Influence on Influence on Fishes, *in* American Fisheries Society Symposium, v. 2003.

Polvi, L.E., and Wohl, E., 2013, Biotic Drivers of Stream Planform: Implications for Understanding the Past and Restoring the Future: BioScience, v. 63, p. 439–452, doi:10.1525/bio.2013.63.6.6.

Polvi, L.E., and Wohl, E., 2012, The beaver meadow complex revisited – the role of beavers in post-glacial floodplain development: Earth Surface Processes and Landforms, v. 37, p. 332–346, doi:10.1002/esp.2261.

Pribyl, D.W., 2010, A critical review of the conventional SOC to SOM conversion factor: Geoderma, v. 156, p. 75–83, doi:10.1016/j.geoderma.2010.02.003.

Puttock, A., Graham, H.A., Carless, D., and Brazier, R.E., 2018, Sediment and nutrient storage in a beaver engineered wetland: Earth Surface Processes and Landforms, v. 43, p. 2358–2370, doi:10.1002/esp.4398.

R Core Team, 2022, R: A Language and Environment for Statistical Computing:, https://www.R-project.org/.

Rathburn, S., Shahverdian, S., and Ryan, S., 2018, Post-disturbance sediment recovery: Implications for watershed resilience: Geomorphology, v. 305, doi:10.1016/j.geomorph.2017.08.039.

Rhoades, C.C., Chow, A.T., Covino, T.P., Fegel, T.S., Pierson, D.N., and Rhea, A.E., 2019, The Legacy of a Severe Wildfire on Stream Nitrogen and Carbon in Headwater Catchments: Ecosystems, v. 22, p. 643–657, doi:10.1007/s10021-018-0293-6.

Rhoades, C.C., Entwistle, D., Butler, D., Rhoades, C.C., Entwistle, D., and Butler, D., 2011, The influence of wildfire extent and severity on streamwater chemistry, sediment and temperature following the Hayman Fire, ColoradoA: International Journal of Wildland Fire, v. 20, p. 430–442, doi:10.1071/WF09086.

Robichaud, P.R., Beyers, J.L., and Neary, D.G., 2000, Evaluating the effectiveness of postfire rehabilitation treatments: U.S. Department of Agriculture, Forest Service, Rocky Mountain Research Station RMRS-GTR-63, RMRS-GTR-63 p., doi:10.2737/RMRS-GTR-63.

Robichaud, P.R., Wagenbrenner, J.W., Brown, R.E., Wohlgemuth, P.M., and Beyers, J.L., 2008, Evaluating the effectiveness of contour-felled log erosion barriers as a post-fire runoff and erosion mitigation treatment in the western United States: International Journal of Wildland Fire, v. 17, p. 255, doi:10.1071/WF07032.

Robichaud, P.R., Wagenbrenner, J.W., Lewis, S.A., Ashmun, L.E., Brown, R.E., and Wohlgemuth, P.M., 2013, Post-fire mulching for runoff and erosion mitigation Part II: Effectiveness in reducing runoff and sediment yields from small catchments: CATENA, v. 105, p. 93–111, doi:10.1016/j.catena.2012.11.016.

Rosell, F., Bozsér, O., Collen, P., and Parker, H., 2005, Ecological impact of beavers Castor fiber and Castor canadensis and their ability to modify ecosystems: Mammal Review, v. 35, p. 248–276, doi:10.1111/j.1365-2907.2005.00067.x.

Rust, A.J., Hogue, T.S., Saxe, S., McCray, J., Rust, A.J., Hogue, T.S., Saxe, S., and McCray, J., 2018, Post-fire water-quality response in the western United States: International Journal of Wildland Fire, v. 27, p. 203–216, doi:10.1071/WF17115.

Santisteban, J.I., Mediavilla, R., López-Pamo, E., Dabrio, C.J., Zapata, M.B.R., García, M.J.G., Castaño, S., and Martínez-Alfaro, P.E., 2004, Loss on ignition: a qualitative or quantitative method for organic matter and carbonate mineral content in sediments? Journal of Paleolimnology, v. 32, p. 287–299, doi:10.1023/B:JOPL.0000042999.30131.5b.

Scamardo, J.E., Marshall, S., and Wohl, E., 2022, Estimating widespread beaver dam loss: Habitat decline and surface storage loss at a regional scale: Ecosphere, v. 13, p. e3962, doi:10.1002/ecs2.3962.

Schmadel, N.M., Harvey, J.W., Schwarz, G.E., Alexander, R.B., Gomez-Velez, J.D., Scott, D., and Ator, S.W., 2019, Small Ponds in Headwater Catchments Are a Dominant Influence on Regional Nutrient and Sediment Budgets: Geophysical Research Letters, v. 46, p. 9669–9677, doi:10.1029/2019GL083937.

Schmeer, S.R., Kampf, S.K., MacDonald, L.H., Hewitt, J., and Wilson, C., 2018, Empirical models of annual post-fire erosion on mulched and unmulched hillslopes: CATENA, v. 163, p. 276–287, doi:10.1016/j.catena.2017.12.029.

Shakesby, R.A., and Doerr, S.H., 2006, Wildfire as a hydrological and geomorphological agent: Earth-Science Reviews, v. 74, p. 269–307, doi:10.1016/j.earscirev.2005.10.006.

Smith, H.G., Sheridan, G.J., Lane, P.N.J., Nyman, P., and Haydon, S., 2011, Wildfire effects on water quality in forest catchments: A review with implications for water supply: Journal of Hydrology, v. 396, p. 170–192, doi:10.1016/j.jhydrol.2010.10.043.

Stoof, C.R., Vervoort, R.W., Iwema, J., van den Elsen, E., Ferreira, A.J.D., and Ritsema, C.J., 2012, Hydrological response of a small catchment burned by experimental fire: Hydrology and Earth System Sciences, v. 16, p. 267–285, doi:10.5194/hess-16-267-2012.

Sutfin, N.A., and Wohl, E., 2017, Substantial soil organic carbon retention along floodplains of mountain streams: Journal of Geophysical Research: Earth Surface, v. 122, p. 1325–1338, doi:10.1002/2016JF004004.

USDA Forest Service, Geospatial Technology and Applications Center, BAER Imagery Support Program, 2020a, Soil Burn Severity Dataset for the CAMERON PEAK Fire occurring on the Arapaho & Roosevelt National Forests/Pawnee National Grassland National Forest: USDS Forest Service raster digital data, https://fsapps.nwcg.gov/afm/baer/download.php (accessed November 2022).

USDA Forest Service, Geospatial Technology and Applications Center, BAER Imagery Support Program, 2021, Soil Burn Severity Dataset for the EAST TROUBLESOME Fire occurring on the Arapaho & Roosevelt National Forest National Forest: USDS Forest Service raster digital data, https://fsapps.nwcg.gov/afm/baer/download.php (accessed November 2022).

USDA Forest Service, Geospatial Technology and Applications Center, BAER Imagery Support Program, 2020b, Soil Burn Severity Dataset for the MULLEN Fire occurring on the Medicine Bow National

Forest National Forest: USDS Forest Service raster digital data, https://fsapps.nwcg.gov/afm/baer/download.php (accessed November 2022).

USGS 1/3 Arc Second n41w106 20230314 - ScienceBase-Catalog, 2023a, https://www.sciencebase.gov/catalog/item/6413f42dd34eb496d1cea115 (accessed April 2023).

USGS 1/3 Arc Second n41w107 20230314 - ScienceBase-Catalog, 2023b, https://www.sciencebase.gov/catalog/item/6413f42cd34eb496d1cea113 (accessed April 2023).

USGS 1/3 Arc Second n42w107 20230314 - ScienceBase-Catalog, 2023c, https://www.sciencebase.gov/catalog/item/6413f42ad34eb496d1cea10d (accessed April 2023).

Wagenbrenner, J.W., MacDonald, L.H., and Rough, D., 2006, Effectiveness of three post-fire rehabilitation treatments in the Colorado Front Range: Hydrological Processes, v. 20, p. 2989–3006, doi:10.1002/hyp.6146.

Ward, 2022, Standard Operating Procedure: Organic Matter:

Westbrook, C.J., Cooper, D.J., and Baker, B.W., 2011, Beaver assisted river valley formation: River Research and Applications, v. 27, p. 247–256, doi:10.1002/rra.1359.

Westbrook, C.J., Cooper, D.J., and Baker, B.W., 2006, Beaver dams and overbank floods influence groundwater–surface water interactions of a Rocky Mountain riparian area: Water Resources Research, v. 42, doi:10.1029/2005WR004560.

WFIGS Wildland Fire Perimeters Full History Wildland Fire Interagency Geospatial Services Group REST layer, https://services3.arcgis.com/T4QMspbfLg3qTGWY/arcgis/rest/services/Fire_History_Perimeters_Public/FeatureServer (accessed January 2023).

Wickham, H. et al., 2019, Welcome to the tidyverse: Journal of Open Source Software, v. 4, p. 1686, doi:10.21105/joss.01686.

Wilcoxon, F., 1945, Individual Comparisons by Ranking Methods: Biometrics Bulletin, v. 1, p. 80–83, doi:10.2307/3001968.

Wilkinson, S.N., Wallbrink, P.J., Hancock, G.J., Blake, W.H., Shakesby, R.A., and Doerr, S.H., 2009, Fallout radionuclide tracers identify a switch in sediment sources and transport-limited sediment yield following wildfire in a eucalypt forest: Geomorphology, v. 110, p. 140–151, doi:10.1016/j.geomorph.2009.04.001.

Williams, A.P., Abatzoglou, J.T., Gershunov, A., Guzman-Morales, J., Bishop, D.A., Balch, J.K., and Lettenmaier, D.P., 2019, Observed Impacts of Anthropogenic Climate Change on Wildfire in California: Earth’s Future, v. 7, p. 892–910, doi:10.1029/2019EF001210.

Wohl, E., 2018, Geomorphic context in rivers: Progress in Physical Geography: Earth and Environment, v. 42, p. 841–857, doi:10.1177/0309133318776488.

Wohl, E., 2013, Landscape-scale carbon storage associated with beaver dams: Geophysical Research Letters, v. 40, p. 3631–3636, doi:10.1002/grl.50710.

Wohl, E., Lininger, K.B., Rathburn, S.L., and Sutfin, N.A., 2020, How geomorphic context governs the influence of wildfire on floodplain organic carbon in fire-prone environments of the western United States: Earth Surface Processes and Landforms, v. 45, p. 38–55, doi:10.1002/esp.4680.

Wohl, E., Lininger, K.B., and Scott, D.N., 2018, River beads as a conceptual framework for building carbon storage and resilience to extreme climate events into river management: Biogeochemistry, v. 141, p. 365–383, doi:10.1007/s10533-017-0397-7.

Wohl, E., Marshall, A.E., Scamardo, J., White, D., and Morrison, R.R., 2022, Biogeomorphic influences on river corridor resilience to wildfire disturbances in a mountain stream of the Southern Rockies, USA: Science of The Total Environment, p. 153321, doi:10.1016/j.scitotenv.2022.153321.

Wohl, E., and Scott, D.N., 2017, Wood and sediment storage and dynamics in river corridors: Earth Surface Processes and Landforms, v. 42, p. 5–23, doi:10.1002/esp.3909.

Yi, C., and Jackson, N., 2021, A review of measuring ecosystem resilience to disturbance: Environmental Research Letters, v. 16, p. 053008, doi:10.1088/1748-9326/abdf09.

APPENDIX I

Table 11: Data table of pond locations, GPS survey method, and burn and vegetation characteristics of the pond's watershed.

Site				**Burn**			**Vegetation**					
Site ID	**latitude**	**longitude**	**GPS method**	**percent burned**	**percent burned (severity)**	**burn status**	**median pre-fire watershed vegetation cover (NDVI)**	**median pre-fire local vegetation cover (NDVI)**	**median post-fire watershed vegetation cover (NDVI)**	**median post-fire local vegetation cover (NDVI)**	**median post-fire watershed vegetation recovery (ΔNDVI)**	**median post-fire local vegetation recovery (ΔNDVI)**
BRC-2	41.0605	-106.134	RTK	47.6	14.2	burned	0.19	0.19	0.18	0.19	0.03	0.02
BRC-3	41.0604	-106.134	RTK	47.6	14.2	burned	0.19	0.19	0.18	0.19	0.03	0.02
BRC-4	41.0604	-106.134	RTK	47.4	14.1	burned	0.19	0.18	0.18	0.19	0.03	0.02
BVB-1	40.367	-105.593	phone	19.2	4.4	unburned	0.21	0.25	0.19	0.20	0.00	-0.02
COW-1	40.4332	-105.494	satellite	0.0	0.0	unburned	0.20	0.21	0.20	0.22	-0.01	0.00
COW-2	40.433	-105.495	satellite	0.0	0.0	unburned	0.20	0.22	0.19	0.22	-0.01	0.00
CUB-3	40.3502	-105.621	InReach	22.9	17.5	unburned	0.17	0.24	0.15	0.24	-0.02	0.01
FALL-1	40.4012	-105.61	RTK	0.0	0.0	unburned	0.20	0.34	0.18	0.31	0.02	-0.01
FC-1	40.3285	-105.52	RTK	0.0	0.0	unburned	0.15	0.29	0.16	0.25	0.00	-0.02
FC-10	40.3297	-105.517	RTK	0.0	0.0	unburned	0.16	0.25	0.16	0.22	0.01	-0.02
FC-2	40.3288	-105.519	RTK	0.0	0.0	unburned	0.15	0.28	0.16	0.24	0.00	-0.03
FC-3	40.3287	-105.519	RTK	0.0	0.0	unburned	0.36	0.29	0.34	0.25	0.05	-0.03

FC-4	40.3289	-105.519	RTK	0.0	0.0	unburned	0.15	0.28	0.16	0.24	0.00	-0.04
FC-5	40.3291	-105.519	RTK	0.0	0.0	unburned	0.15	0.27	0.16	0.22	0.00	-0.04
FC-6	40.3293	-105.519	RTK	0.0	0.0	unburned	0.15	0.26	0.16	0.22	0.00	-0.04
FC-7	40.3298	-105.518	RTK	0.0	0.0	unburned	0.15	0.23	0.16	0.21	0.00	-0.02
FC-8	40.3298	-105.517	RTK	0.0	0.0	unburned	0.16	0.26	0.16	0.22	0.01	-0.03
FC-9	40.3295	-105.517	RTK	0.0	0.0	unburned	0.27	0.26	0.23	0.23	0.04	-0.04
GLC-2	40.3186	-105.62	RTK	0.0	0.0	unburned	0.22	0.20	0.21	0.20	-0.02	-0.01
LBC-1	40.6386	-105.612	RTK	100.0	65.5	burned	0.19	0.24	0.12	0.13	0.04	0.02
LBC-2	40.6384	-105.612	RTK	100.0	65.8	burned	0.19	0.24	0.12	0.13	0.04	0.01
LBC-3	40.638	-105.611	RTK	100.0	61.4	burned	0.21	0.25	0.11	0.13	0.04	-0.02
LBC-4	40.6378	-105.61	RTK	100.0	61.5	burned	0.21	0.24	0.11	0.13	0.04	-0.02
LRR-1	40.6619	-105.859	RTK	87.9	56.8	burned	0.12	0.29	0.10	0.30	0.03	0.05
LRR-10	40.6806	-105.855	RTK	11.5	0.0	unburned	0.19	0.32	0.19	0.30	0.01	-0.02
LRR-2	40.6698	-105.856	RTK	99.7	10.0	burned	0.18	0.30	0.13	0.29	0.02	0.01
LRR-3	40.6702	-105.857	RTK	99.5	8.7	burned	0.18	0.32	0.14	0.31	0.02	0.00
LRR-4	40.6706	-105.856	RTK	100.0	8.9	burned	0.36	0.32	0.36	0.31	0.01	-0.01
LRR-5	40.6707	-105.858	RTK	88.5	54.3	unburned	0.16	0.33	0.11	0.33	0.03	0.00
LRR-6	40.6716	-105.856	RTK	38.9	0.0	unburned	0.21	0.30	0.22	0.29	0.00	-0.01
LRR-7	40.6719	-105.855	RTK	77.8	13.0	unburned	0.18	0.27	0.11	0.27	0.01	-0.01
LRR-8	40.6726	-105.855	RTK	66.7	11.1	unburned	0.18	0.26	0.12	0.26	0.01	-0.01
LRR-9	40.6802	-105.854	RTK	0.0	0.0	unburned	0.21	0.30	0.22	0.29	0.01	-0.01

MOR -1	40.3533	-105.585	RTK	13.8	8.6	unburned	0.06	0.33	0.05	0.30	0.00	-0.04
OF-1	40.6383	-105.562	RTK	100.0	67.9	burned	0.20	0.24	0.11	0.16	0.04	0.02
OF-2	40.6382	-105.562	RTK	99.9	67.9	burned	0.20	0.26	0.11	0.18	0.04	0.02
PDR-1	40.7047	-105.758	RTK	36.8	17.9	burned	0.18	0.26	0.17	0.28	0.01	0.03
RRC-1	40.7294	-105.75	iPad	18.3	13.4	burned	0.20	0.25	0.18	0.18	0.00	0.05
RRC-2	40.7293	-105.75	iPad	18.4	13.5	burned	0.20	0.26	0.18	0.18	0.00	0.05
SWP-1	40.7402	-105.627	RTK	0.0	0.0	burned	0.23	0.22	0.16	0.16	0.00	-0.03
SWP-2	40.7401	-105.626	RTK	0.0	0.0	burned	0.23	0.22	0.16	0.16	0.00	-0.04
SWP-3	40.7408	-105.625	RTK	0.0	0.0	burned	0.23	0.22	0.17	0.15	0.00	-0.04
SWP-4	40.7437	-105.624	RTK	0.0	0.0	burned	0.23	0.24	0.16	0.17	0.00	-0.03
SWP-5	40.7438	-105.623	RTK	0.0	0.0	burned	0.23	0.24	0.16	0.15	0.00	-0.02
WLD-1	40.2112	-105.548	RTK	0.0	0.0	unburned	0.24	0.26	0.16	0.21	-0.07	-0.05

Table 12: Data table of geomorphology and pond characteristics.

	Geomorphology						Pond						
Site ID	**current drainage area, km^2**	**historical drainage area, km^2**	**mean water-shed slope**	**relief ratio**	**valley gradient**	**valley width, m**	**channel position**	**position in sequence**	**reach position**	**beaver activity**	**pond surface area m^2**	**pond age, years**	**age class**
BRC-2	4.7	4.7	5	0.07	0.023	43	on-channel	3	downstream	inactive	216	23	old
BRC-3	4.7	4.7	5	0.07	0.018	45	on-channel	4	downstream	inactive	322	22	moderate
BRC-4	4.7	4.7	5	0.07	0.016	56	on-channel	5	downstream	inactive	685	23	old
BVB-1	13.5	13.5	31	0.17	0.028	181	on-channel	1	single	BDA	16	2	recent
COW-1	23.5	23.5	37	0.14	0.023	41	on-channel	2	downstream	active	240	1.5	recent
COW-2	23.4	23.4	37	0.14	0.024	45	on-channel	1	upstream	BDA	62	2	recent
CUB-3	2.3	2.3	43	0.23	0.018	150	off-channel	3	downstream	inactive	1715	37	old
FALL-1	80.9	80.9	45	0.16	0.003	257	on-channel	1	single	active	5661	2	recent
FC-1	10.2	10.2	35	0.24	0.079	120	on-channel	1	upstream	BDA	54	5	recent
FC-10	10.5	10.5	34	0.23	0.052	137	on-channel	8	downstream	BDA	77	5	recent
FC-2	10.3	10.3	35	0.09	0.069	97	on-channel	2	downstream	BDA	32	5	recent
FC-3	0.0	10.3	10	0.24	0.066	97	on-channel	1	upstream	active	371	4	recent
FC-4	10.3	10.3	35	0.23	0.068	98	on-channel	3	downstream	BDA	30	5	recent
FC-5	10.3	10.3	35	0.23	0.052	100	on-channel	4	downstream	BDA	114	5	recent
FC-6	10.3	10.3	35	0.23	0.046	97	on-channel	5	downstream	BDA	45	5	recent
FC-7	10.4	10.4	34	0.23	0.034	115	on-channel	6	downstream	BDA	173	5	recent
FC-8	10.5	10.5	34	0.25	0.051	145	on-channel	7	downstream	BDA	41	5	recent
FC-9	0.1	10.4	24	0.23	0.049	115	on-channel	3	downstream	active	634	20	moderate
GLC-2	0.0	34.0	22	0.24	0.011	72	off-channel	2	downstream	inactive	737	37	old
LBC-1	1.6	1.6	22	0.17	0.028	87	on-channel	1	upstream	inactive	315	23	old
LBC-2	1.6	3.7	22	0.17	0.032	92	off-channel	2	downstream	inactive	332	23	old
LBC-3	17.7	17.7	25	0.16	0.044	69	on-channel	3	downstream	inactive	520	23	old
LBC-4	17.7	17.7	25	0.16	0.034	76	off-channel	4	downstream	inactive	1199	23	old
LRR-1	25.2	25.2	28	0.21	0.002	162	on-channel	1	single	inactive	1095	13	moderate
LRR-10	0.4	66.2	42	0.23	0.008	392	off-channel	2	downstream	inactive	822	20	moderate

LRR-2	0.4	26.7	32	0.43	0.014	266	on-channel	1	upstream	inactive	2372	20	moderate
LRR-3	0.0	26.7	40	0.07	0.009	307	on-channel	2	downstream	inactive	790	20	moderate
LRR-4	0.0	26.7	6	0.18	0.012	391	on-channel	3	downstream	inactive	405	20	moderate
LRR-5	26.8	26.7	28	0.24	0.010	394	on-channel	1	single	active	215	1.5	recent
LRR-6	0.0	26.9	35	0.39	0.002	317	off-channel	4	downstream	inactive	863	23	old
LRR-7	0.0	27.0	41	0.39	0.000	311	off-channel	5	downstream	inactive	1370	23	old
LRR-8	0.0	27.0	36	0.25	0.001	307	off-channel	6	downstream	inactive	1547	23	old
LRR-9	0.1	65.6	39	0.36	0.008	394	off-channel	1	upstream	inactive	3099	20	moderate
MOR-1	103.0	103.0	45	0.10	0.004	148	on-channel	1	single	active	860	4.5	recent
OF-1	3.4	3.4	19	0.13	0.036	72	on-channel	1	upstream	inactive	140	4.5	recent
OF-2	3.5	3.5	19	0.12	0.035	87	on-channel	2	downstream	inactive	236	4.5	recent
PDR-1	10.6	10.6	16	0.14	0.000	652	on-channel	2	downstream	active	6361	11	old
RRC-1	21.6	21.6	23	0.13	0.068	57	on-channel	1	upstream	inactive	645	4.5	recent
RRC-2	21.6	21.6	23	0.13	0.057	52	on-channel	2	downstream	inactive	66	4.5	recent
SWP-1	1.8	1.8	9	0.08	0.033	86	off-channel	1	upstream	inactive	803	23	old
SWP-2	1.9	1.9	9	0.08	0.018	98	off-channel	2	downstream	inactive	1462	23	old
SWP-3	2.2	2.2	8	0.08	0.015	129	off-channel	3	downstream	inactive	926	23	old
SWP-4	3.0	3.0	9	0.08	0.021	120	off-channel	4	downstream	inactive	425	23	old
SWP-5	3.0	3.0	9	0.08	0.021	59	off-channel	5	downstream	inactive	631	21	moderate
WLD-1	0.0	82.3	36	0.41	0.011	276	off-channel	1	single	inactive	2482	37	old

Table 13: Data table of sediment response metrics at each pond.

		Response											
Site ID	**total pond volume m^3**	**sediment volume m^3**	**water volume m^3**	**sediment volume m^3/ drainage area km^2**	**percent residual volume**	**lifetime sediment-ation rate, cm/yr**	**post-fire sediment-ation rate, cm/yr**	**mean percent TOC**	**percent gravel**	**percent sand**	**percent fines**	**median grainsize (d50)**
BRC-2	260	0	35	50	13.0	2.8	0.0	3.8	NA	NA	NA	NA
BRC-3	440	340	95	75	22.1	3.5	21.5	6.3	3.5	48.2	48.3	124.8
BRC-4	900	640	255	135	28.4	3.3	22.3	6.8	0.9	45.8	53.3	61.8
BVB-1	10	5	5	0	34.2	8.0	0.0	0.8	59.7	34.4	5.9	1921.9
COW-1	270	130	140	5	51.4	31.8	25.0	3.7	11.8	46.5	41.7	135.7
COW-2	35	15	20	0	54.3	14.0	2.0	0.5	32.0	59.0	9.1	808.1
CUB-3	1385	915	465	395	33.7	2.0	12.5	6.8	20.9	43.7	35.4	223.0
FALL-1	9465	3665	5775	45	61.2	52.3	0.0	0.2	0.3	92.4	7.3	264.8
FC-1	0	10	5	0	41.9	NA	NA	NA	NA	NA	NA	NA
FC-10	55	25	30	5	50.8	8.4	0.0	NA	NA	NA	NA	NA
FC-2	0	5	5	0	66.3	NA	NA	NA	NA	NA	NA	NA
FC-3	NA	NA	NA	NA	NA	NA	NA	NA	NA	NA	NA	NA
FC-4	NA	NA	NA	NA	NA	NA	NA	NA	NA	NA	NA	NA
FC-5	0	20	45	0	70.2	2.6	0.0	7.9	0.0	22.6	77.4	33.6
FC-6	NA	NA	NA	NA	NA	NA	NA	NA	NA	NA	NA	NA
FC-7	NA	NA	NA	NA	NA	NA	NA	NA	NA	NA	NA	NA
FC-8	NA	NA	NA	NA	NA	NA	NA	NA	NA	NA	NA	NA
FC-9	355	195	455	1890	70.2	1.3	0.0	7.2	NA	NA	NA	NA
GLC-2	575	360	215	10555	37.1	1.3	0.0	5.1	13.9	45.6	40.5	132.9
LBC-1	445	445	0	285	0.1	2.7	20.2	7.8	11.0	37.0	52.0	144.5
LBC-2	665	660	0	420	0.3	2.7	19.8	10.5	2.7	42.2	55.0	124.5
LBC-3	2290	2260	25	130	1.2	3.1	22.3	5.7	17.1	48.2	34.8	1031.4
LBC-4	1570	1550	20	90	1.3	2.2	14.2	6.0	9.5	46.9	43.6	187.4

LRR-1	630	270	360	10	57.1	2.8	10.5	2.3	11.4	54.8	33.8	217.7
LRR-10	605	415	185	1045	30.7	0.4	0.0	8.0	NA	NA	NA	NA
LRR-2	2250	1620	615	3955	27.5	1.3	2.3	3.7	3.0	29.8	67.2	37.5
LRR-3	785	495	285	11995	36.3	2.1	0.0	6.4	2.7	28.7	68.5	37.4
LRR-4	315	240	70	53640	22.5	1.7	5.5	NA	*NA*	*NA*	*NA*	*NA*
LRR-5	195	145	50	5	25.8	NA	NA	NA	NA	NA	NA	NA
LRR-6	970	615	350	42665	36.4	3.0	0.0	6.9	4.6	31.8	63.6	43.8
LRR-7	1250	750	490	34655	39.7	2.0	19.8	*10.5*	*5.7*	*23.7*	*70.6*	*40.1*
LRR-8	1390	755	630	29995	45.4	*1.8*	*0.0*	*7.5*	*0.3*	*29.2*	*70.5*	*39.0*
LRR-9	3260	2355	890	40850	27.5	1.9	0.0	3.4	3.3	28.5	68.2	50.9
MOR-1	800	420	375	5	47.4	4.5	0.0	2.4	4.8	54.7	40.5	106.2
OF-1	155	140	15	40	10.9	13.3	24.8	8.9	12.0	50.4	37.6	437.7
OF-2	410	310	100	90	24.4	12.4	21.8	12.0	1.3	47.9	50.8	55.5
PDR-1	9055	4890	4140	460	45.9	5.0	19.3	4.8	17.7	31.9	50.4	317.6
RRC-1	585	565	20	25	3.4	16.1	40.3	2.9	14.3	41.6	44.1	580.4
RRC-2	25	25	0	0	4.2	4.8	12.0	1.2	75.8	17.3	6.9	11763.2
SWP-1	1545	1420	120	795	7.7	3.3	17.5	16.6	2.1	28.4	69.6	36.9
SWP-2	1770	1445	320	750	18.1	3.6	19.8	23.2	2.6	36.2	61.2	47.1
SWP-3	1560	1320	240	600	15.3	3.1	21.5	20.8	8.6	39.3	52.1	174.7
SWP-4	565	485	80	165	13.9	2.9	8.8	20.4	8.0	53.8	38.2	123.7
SWP-5	945	765	180	255	18.9	3.2	6.0	15.0	9.6	45.5	44.8	103.9
WLD-1	1505	915	580	56545	38.7	1.6	0.0	3.6	16.6	38.3	45.0	102.2

Table 14: Site name abbreviations and general locations.

Site Code	Name
BOS	Boswell Creek
BRC	Bear Creek
BVB	Beaver Brook
COW	Cow Creek
CUB	Cub Lake, unnamed valley
ELK	Elkhorn Creek
FALL	Fall River
FC	Fish Creek
GLC	Glacier Creek
LBC	Little Beaver Creek
LRR	Laramie River
MOR	Big Thompson, in Moraine Park
OF	Old Flowers Road, unnamed tributary to Little Beaver Creek
PDR	Poudre River
RRC	Roaring Creek
SWP	Swamp Creek
WLD	North St. Vrain, Wild Basin

Table 15: Reach burn and vegetation characteristics.

		Burn		Vegetation					
reach	**number of ponds measured**	**percent burned**	**percent burned (severity)**	**pre-fire watershed vegetation cover (NDVI)**	**mean pre-fire local vegetation cover (NDVI)**	**post-fire watershed vegetation cover (NDVI)**	**mean post-fire local vegetation cover (NDVI)**	**post-fire watershed vegetation recovery (ΔNDVI)**	**mean post-fire local vegetation recovery (ΔNDVI)**
BOS	1	0	0	0.18	0.17	0.18	0.17	0.01	0.01
BRC	3	47	14	0.19	0.19	0.18	0.19	0.03	0.02
BVB	1	19	4	0.21	0.25	0.19	0.20	0.00	-0.02
COW	2	0	0	0.20	0.22	0.20	0.22	-0.01	0.00
CUB	1	23	18	0.17	0.24	0.15	0.24	-0.02	0.01
FALL	1	0	0	0.20	0.34	0.18	0.31	0.02	-0.01
FC	5	0	0	0.16	0.27	0.16	0.23	0.01	-0.03
GLC	1	0	0	0.22	0.20	0.21	0.20	-0.02	-0.01
LBC	4	100	61	0.21	0.24	0.11	0.13	0.04	0.00
LRR - lower	2	12	0	0.19	0.31	0.19	0.30	0.01	-0.02
LRR - middle	7	88	54	0.16	0.30	0.11	0.29	0.03	0.00
LRR - upper	1	88	57	0.12	0.29	0.10	0.30	0.03	0.05
MOR	1	14	9	0.06	0.33	0.05	0.30	0.00	-0.04
OF	2	100	68	0.20	0.25	0.11	0.17	0.04	0.02
PDR	1	37	18	0.18	0.26	0.17	0.28	0.01	0.03
RRC	2	18	13	0.20	0.25	0.18	0.18	0.00	0.05
SWP	5	0	0	0.23	0.23	0.16	0.16	0.00	-0.03
WLD	1	0	0	0.24	0.26	0.16	0.21	-0.07	-0.05

Table 16: Reach geomorphic and sediment characteristics.

	Geomorphology					Reach sediment	
reach	**current drainage area, km2**	**relief ratio**	**mean valley gradient**	**mean valley width, m**	**mean watershed slope**	**sediment volume, m^3**	**sediment volume/ drainage area, m^3/km^2**
BOS	1	0.05	0.03	47	10	* 316	* 215
BRC	5	0.07	0.02	48	5	1210	257
BVB	14	0.17	0.03	181	31	6	0.5
COW	23	0.14	0.02	43	37	147	6
CUB	2	0.23	0.02	150	43	913	393
FALL	81	0.16	0.00	257	45	3665	45
FC	11	0.23	0.06	114	34	251	24
GLC	0	0.24	0.01	72	22	361	** 10555
LBC	18	0.16	0.03	81	25	4918	278
LRR - lower	0	0.23	0.01	393	42	2769	** 6944
LRR - middle	27	0.24	0.01	328	28	4625	173
LRR - upper	25	0.21	0.00	162	28	268	11
MOR	103	0.10	0.00	148	45	418	4
OF	3	0.12	0.04	79	19	448	129
PDR	11	0.14	0.00	652	16	4888	462
RRC	22	0.13	0.06	54	23	586	27
SWP	3	0.08	0.02	98	9	5434	1825
WLD	0	0.41	0.01	276	36	916	** 56546

* excluded due to fire history

** excluded from analysis as outlier

APPENDIX II

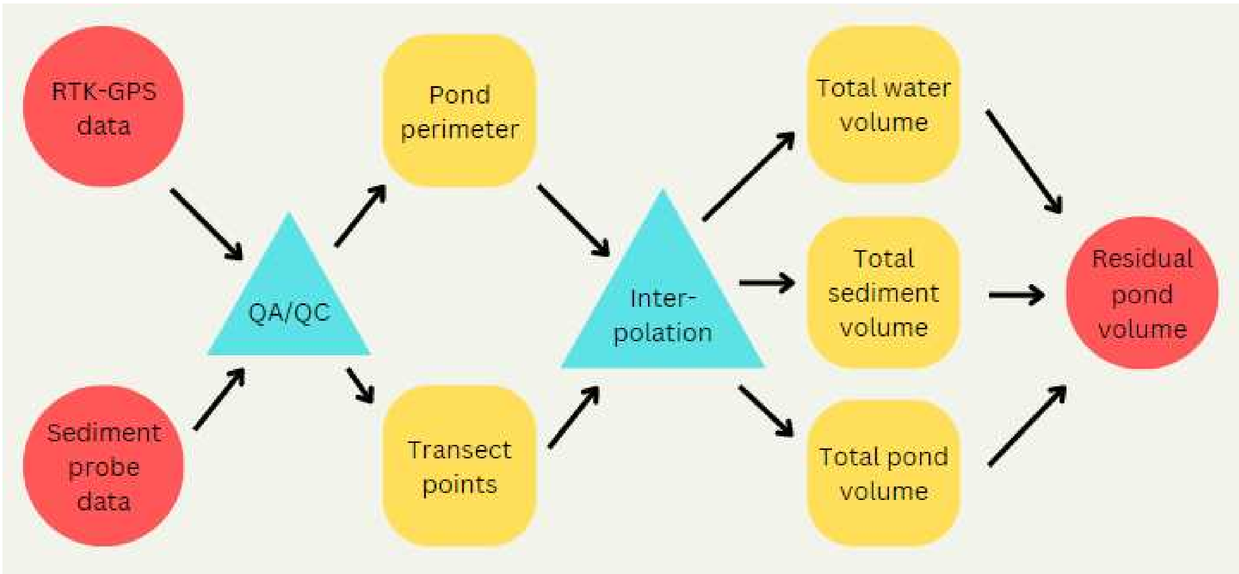

Figure 31: Simplified workflow for calculating residual pond volume from field data.

APPENDIX III

GEE NDVI code

```
/** NDVI compilation
 *
 * Code compiled by Bri Rick, February 2021; updated D. McGrath/L. Zeller, February 2023; modified by
S. Triantafillou and S. Dunn, March 2023  ***/

// Zoom to a location.
Map.setCenter(-105.65955327884019,40.643662247514754, 9); // Center map

//Create a function to mask clouds based on the pixel_qa band of Landsat 8 SR data.
function cloudMaskL8(image) {
  // Bits 3 and 5 are cloud shadow and cloud, respectively.
  var cloudShadowBitMask = (1 << 3);
  var cloudsBitMask = (1 << 5);
  // Get the pixel QA band.
  var qa = image.select('QA_PIXEL');
  // Both flags should be set to zero, indicating clear conditions.
  var mask = qa.bitwiseAnd(cloudShadowBitMask).eq(0)
              .and(qa.bitwiseAnd(cloudsBitMask).eq(0));
  return image.updateMask(mask);
}



// ----------------CREATING MOSAICS----------------------------------------------------
/** Create an image for every year between 2017 and 2022
// Landsat 8 is available for 2013 - 2023, Landsat 5 available for 1984 - 2012
// For each year we call the image collection (Landsat 5 or 8 surface reflectance)
// Then we filter by date, choosing the likely snow-free months of each year of interest
// Then we apply the cloud mask -- finds all cloud-free pixels during the date range
// Takes the median value of all clear images for each pixel and creates one cloud-free mosaic
*/
var L8_2022 = ee.ImageCollection('LANDSAT/LC08/C02/T1_L2')  // Open the image collection of all
Landsat 8 SR images
    .filterDate('2022-07-01', '2022-09-30')               // Filter by date for images in 2022
    .map(cloudMaskL8)                                   // Apply the cloud mask to only keep cloud-free pixels
    .median();

var L8_2021 = ee.ImageCollection('LANDSAT/LC08/C02/T1_L2')  // Open the image collection of all
Landsat 8 SR images
    .filterDate('2021-07-01', '2021-09-30')               // Filter by date for images in 2021
    .map(cloudMaskL8)                                   // Apply the cloud mask to only keep cloud-free pixels
    .median();
```

```
var L8_2020 = ee.ImageCollection('LANDSAT/LC08/C02/T1_L2')  // Open the image collection of all
Landsat 8 SR images
   .filterDate('2020-07-01', '2020-09-30')              // Filter by date for images in 2020
   .map(cloudMaskL8)                           // Apply the cloud mask to only keep cloud-free pixels
   .median();                              // Take the median of all the cloud-free pixels to create one
image

var L8_2019 = ee.ImageCollection('LANDSAT/LC08/C02/T1_L2')  // Open the image collection of all
Landsat 8 SR images
   .filterDate('2019-07-01', '2019-09-30')              // Filter by date for images in 2019
   .map(cloudMaskL8)                           // Apply the cloud mask to only keep cloud-free pixels
   .median();

var L8_2018 = ee.ImageCollection('LANDSAT/LC08/C02/T1_L2')  // Open the image collection of all
Landsat 8 SR images
   .filterDate('2018-07-01', '2018-09-30')              // Filter by date for images in 2018
   .map(cloudMaskL8)                           // Apply the cloud mask to only keep cloud-free pixels
   .median();

var L8_2017 = ee.ImageCollection('LANDSAT/LC08/C02/T1_L2')  // Open the image collection of all
Landsat 8 SR images
   .filterDate('2017-07-01', '2017-09-30')              // Filter by date for images in 2017
   .map(cloudMaskL8)                           // Apply the cloud mask to only keep cloud-free pixels
   .median();                              // probably finds the median pixel value

//----------------VISUALIZING & INDICIES--------------------------------------------------------------

// The following code adds the mosaics created in the previous steps to the map
// We identify which bands to display, using [B4, B3, B2] for a true color Landsat 8 image

// Create a visualization scheme for L8
var L8_RGBViz = {bands: ['SR_B4', 'SR_B3', 'SR_B2'], min: 5000, max: 25000, gamma: 1.3};



// Add layers to the map
Map.addLayer(L8_2022, L8_RGBViz, 'L8_2022')
Map.addLayer(L8_2021, L8_RGBViz, 'L8_2021')
Map.addLayer(L8_2020, L8_RGBViz, 'L8_2020')
Map.addLayer(L8_2019, L8_RGBViz, 'L8_2019')
Map.addLayer(L8_2018, L8_RGBViz, 'L8_2018')
Map.addLayer(L8_2017, L8_RGBViz, 'L8_2017')


// Calculate the NDVI for each time step using the 'normalized difference' function
// Create a new variable for each year, renaming the band 'NDVI'
```

```
var L8_2022_ndvi = L8_2022.normalizedDifference(['SR_B5', 'SR_B4']).rename('NDVI')
var L8_2021_ndvi = L8_2021.normalizedDifference(['SR_B5', 'SR_B4']).rename('NDVI')
var L8_2020_ndvi = L8_2020.normalizedDifference(['SR_B5', 'SR_B4']).rename('NDVI')
var L8_2019_ndvi = L8_2019.normalizedDifference(['SR_B5', 'SR_B4']).rename('NDVI')
var L8_2018_ndvi = L8_2018.normalizedDifference(['SR_B5', 'SR_B4']).rename('NDVI')
var L8_2017_ndvi = L8_2017.normalizedDifference(['SR_B5', 'SR_B4']).rename('NDVI')


// Using the images created above,
// Mask the polygon.
var ndvi2022 = L8_2022_ndvi.updateMask(L8_2022_ndvi.clip(geometry));
var ndvi2021 = L8_2021_ndvi.updateMask(L8_2021_ndvi.clip(geometry));
var ndvi2020 = L8_2020_ndvi.updateMask(L8_2020_ndvi.clip(geometry));
var ndvi2019 = L8_2019_ndvi.updateMask(L8_2019_ndvi.clip(geometry));
var ndvi2018 = L8_2018_ndvi.updateMask(L8_2018_ndvi.clip(geometry));
var ndvi2017 = L8_2017_ndvi.updateMask(L8_2017_ndvi.clip(geometry));


// Add these NDVI images
// Note: palette recognizes both common color names and CSS-style color strings
 Map.addLayer(ndvi2022)

// Export these as GeoTIFFs
Export.image.toDrive({
  image: ndvi2022,    // Name of image to export
  description: 'ndvi2022',   // Export name for file
  scale: 30,              // Define scale, in meters
  region: geometry,         // Define region to export
  fileFormat: 'GeoTIFF'})    // Define desired file format
  //crs: 'ESPG:3857'         // Define projection based on EPSG code. Default is WGS84
Export.image.toDrive({
  image: ndvi2021,    // Name of image to export
  description: 'ndvi2021',   // Export name for file
  scale: 30,              // Define scale, in meters
  region: geometry,         // Define region to export
  fileFormat: 'GeoTIFF'})    // Define desired file format
Export.image.toDrive({
  image: ndvi2020,    // Name of image to export
  description: 'ndvi2020',   // Export name for file
  scale: 30,              // Define scale, in meters
  region: geometry,         // Define region to export
  fileFormat: 'GeoTIFF'})    // Define desired file format
Export.image.toDrive({
  image: ndvi2019,    // Name of image to export
  description: 'ndvi2019',   // Export name for file
  scale: 30,              // Define scale, in meters
  region: geometry,         // Define region to export
  fileFormat: 'GeoTIFF'})    // Define desired file format
```

```
Export.image.toDrive({
  image: ndvi2018,    // Name of image to export
  description: 'ndvi2018',   // Export name for file
  scale: 30,              // Define scale, in meters
  region: geometry,         // Define region to export
  fileFormat: 'GeoTIFF'})    // Define desired file format
Export.image.toDrive({
  image: ndvi2017,    // Name of image to export
  description: 'ndvi2017',   // Export name for file
  scale: 30,              // Define scale, in meters
  region: geometry,         // Define region to export
  fileFormat: 'GeoTIFF'})    // Define desired file format
```

APPENDIX IV

Pond Sediment Volume

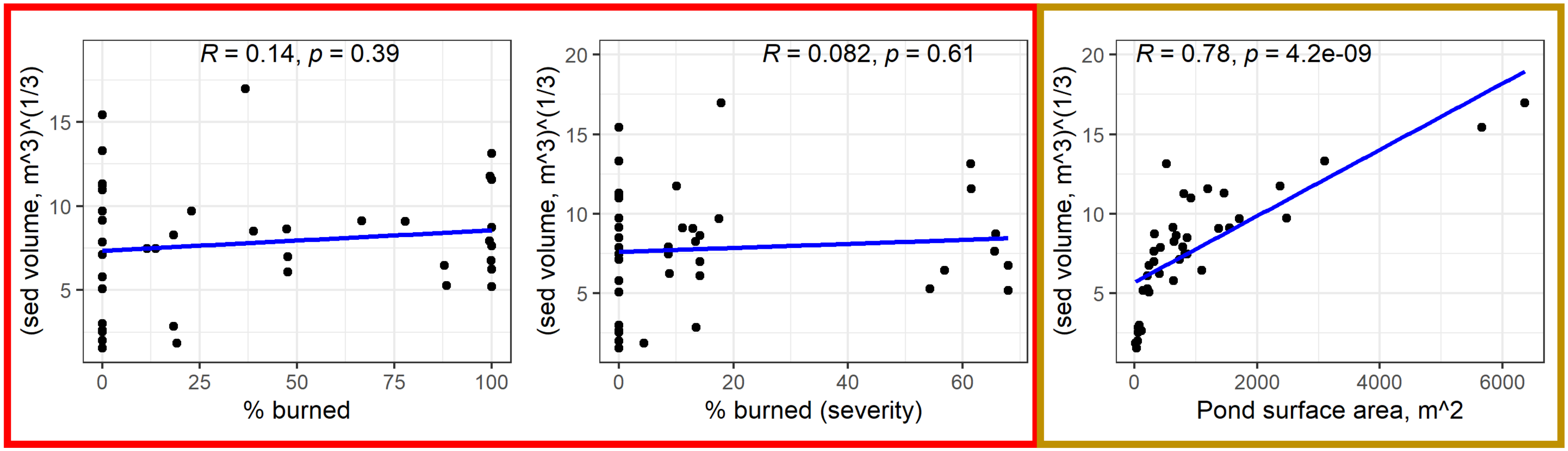

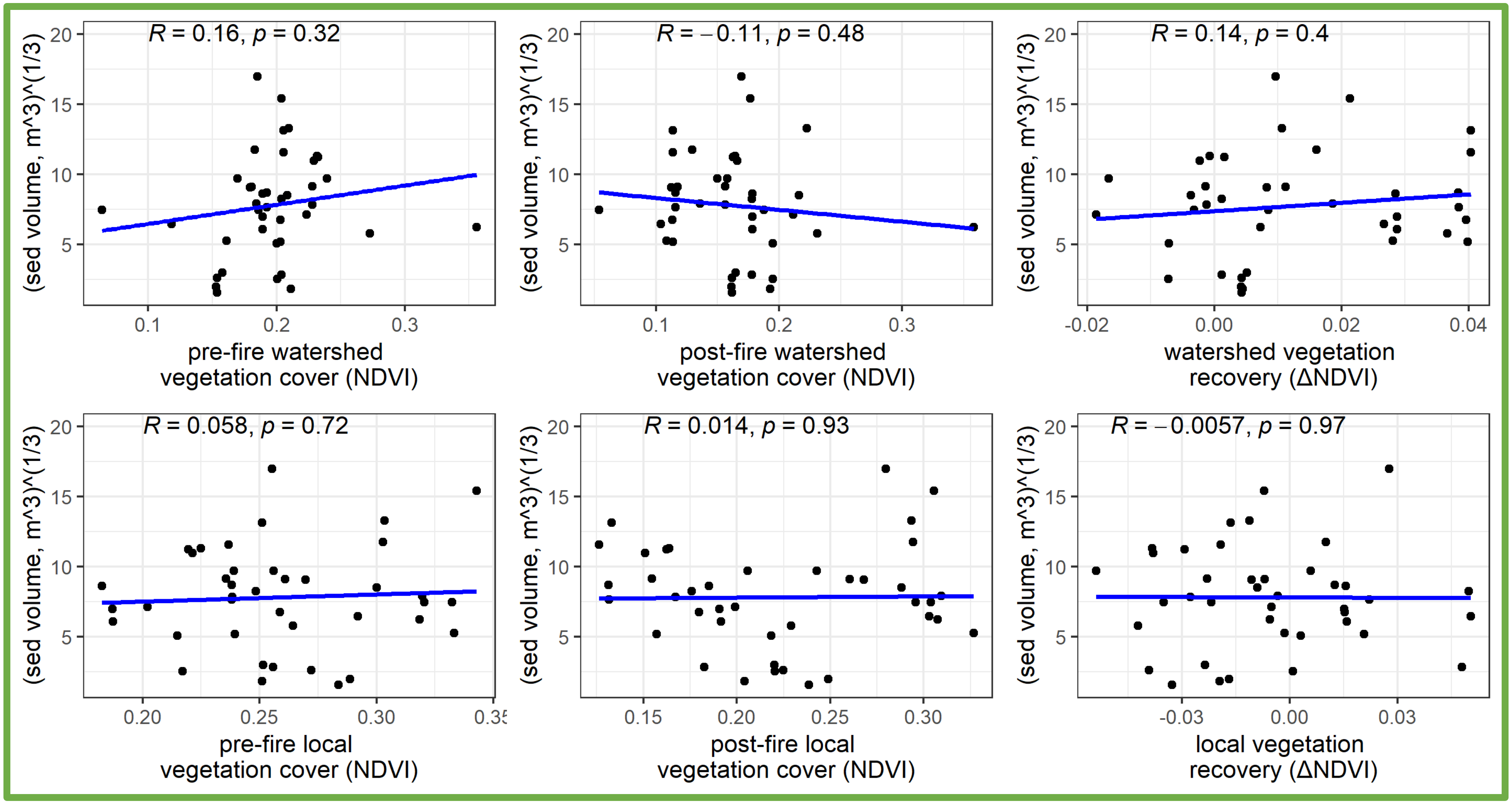

R = 0.16, p = 0.32
R = −0.11, p = 0.48
R = 0.14, p = 0.4
R = 0.058, p = 0.72
R = 0.014, p = 0.93
R = −0.0057, p = 0.97
(sed volume, m^3)^(1/3)
pre-fire watershed vegetation cover (NDVI)
post-fire watershed vegetation cover (NDVI)
watershed vegetation recovery (ΔNDVI)
pre-fire local vegetation cover (NDVI)
post-fire local vegetation cover (NDVI)
local vegetation recovery (ΔNDVI)

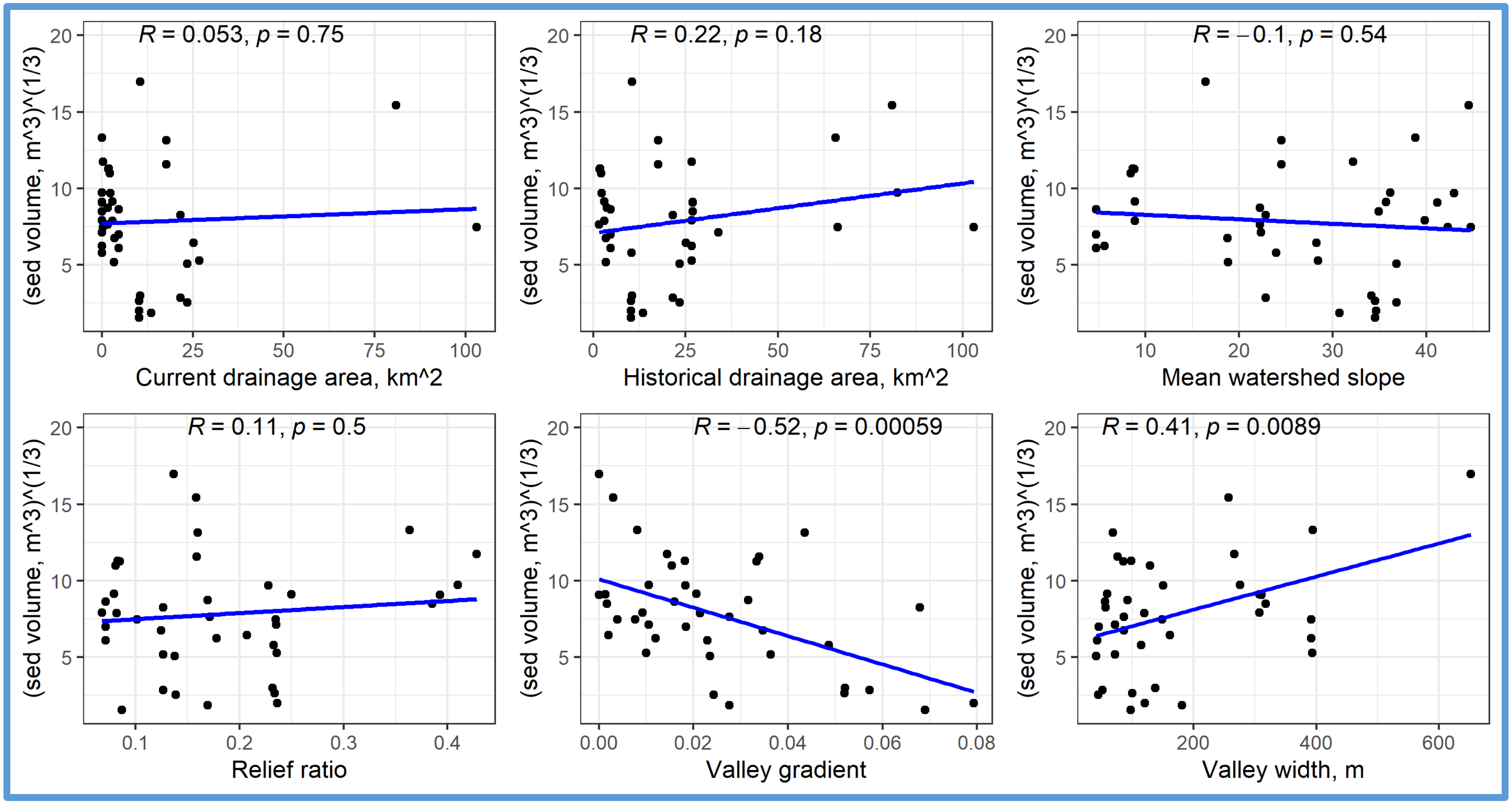

Figure 32: Results of pairwise analyses of explanatory variables and total pond sediment volumes. The linear relationship between continuous explanatory variables and transformed total pond sediment volume (m^3) is indicated by the blue line. The R value describes the direction and goodness of fit of the model, and the p-value is used to evaluate model significance. Burn characteristic comparisons are boxed in red, pond in gold, vegetation in green, and geomorphology in blue.

Normalized Pond Sediment Volume

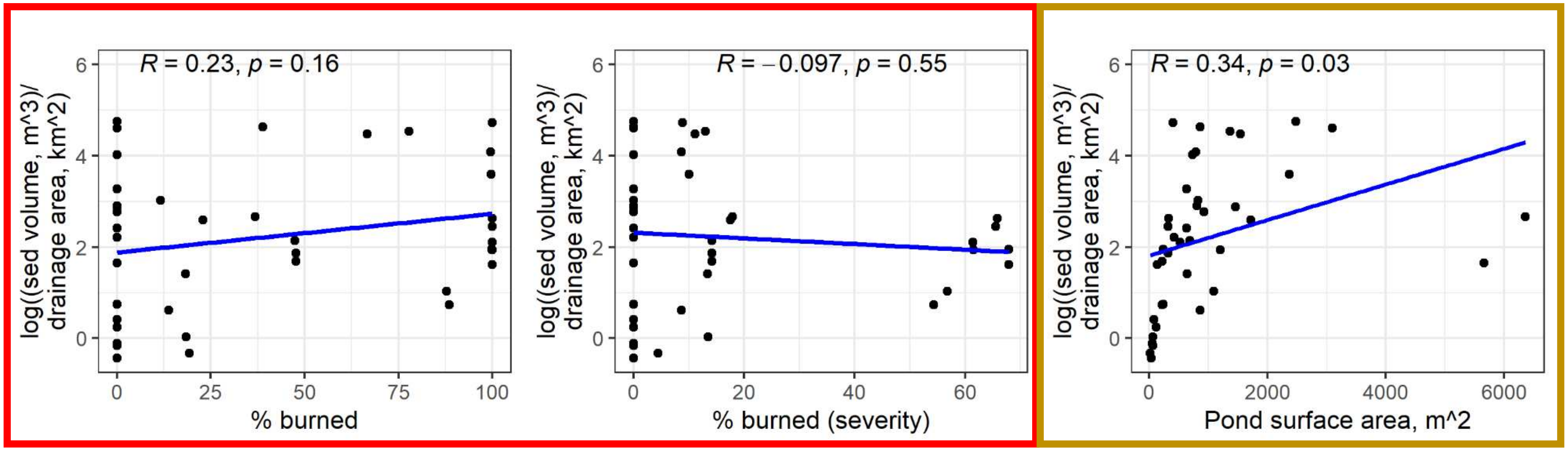

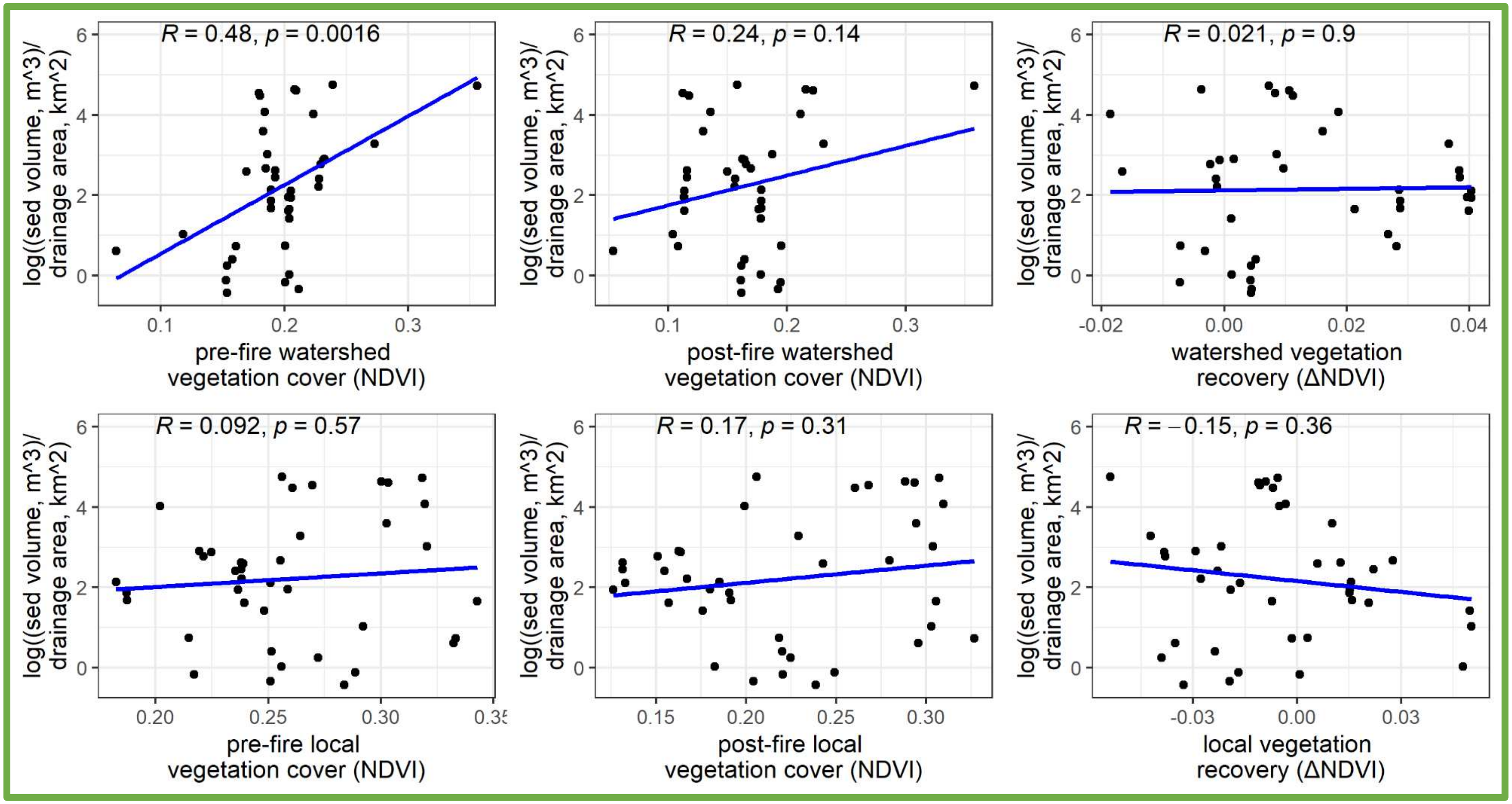
R = 0.48, p = 0.0016
R = 0.24, p = 0.14
R = 0.021, p = 0.9
R = 0.092, p = 0.57
R = 0.17, p = 0.31
R = –0.15, p = 0.36
log((sed volume, m^3)/ drainage area, km^2)
pre-fire watershed vegetation cover (NDVI)
post-fire watershed vegetation cover (NDVI)
watershed vegetation recovery (ΔNDVI)
pre-fire local vegetation cover (NDVI)
post-fire local vegetation cover (NDVI)
local vegetation recovery (ΔNDVI)

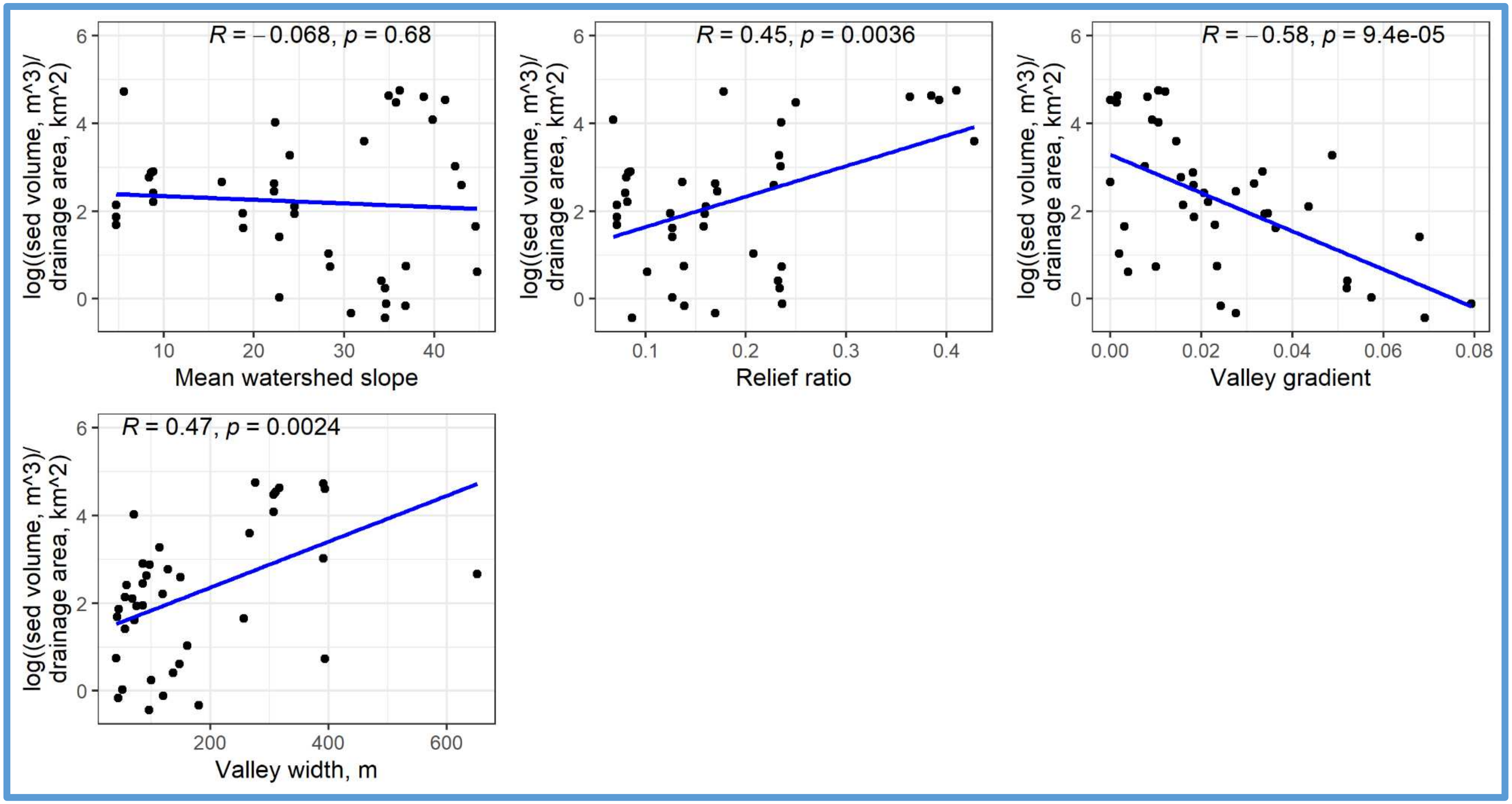

Figure 33: Results of pairwise analyses of explanatory variables and pond sediment volumes normalized by drainage area. The linear relationship between continuous explanatory variables and transformed normalized pond sediment volume (m^3/km^2) is indicated by the blue line. The R value describes the direction and goodness of fit of the model, and the p-value is used to evaluate model significance. Burn characteristic comparisons are boxed in red, pond in gold, vegetation in green, and geomorphology in blue.

Reach Sediment Volume

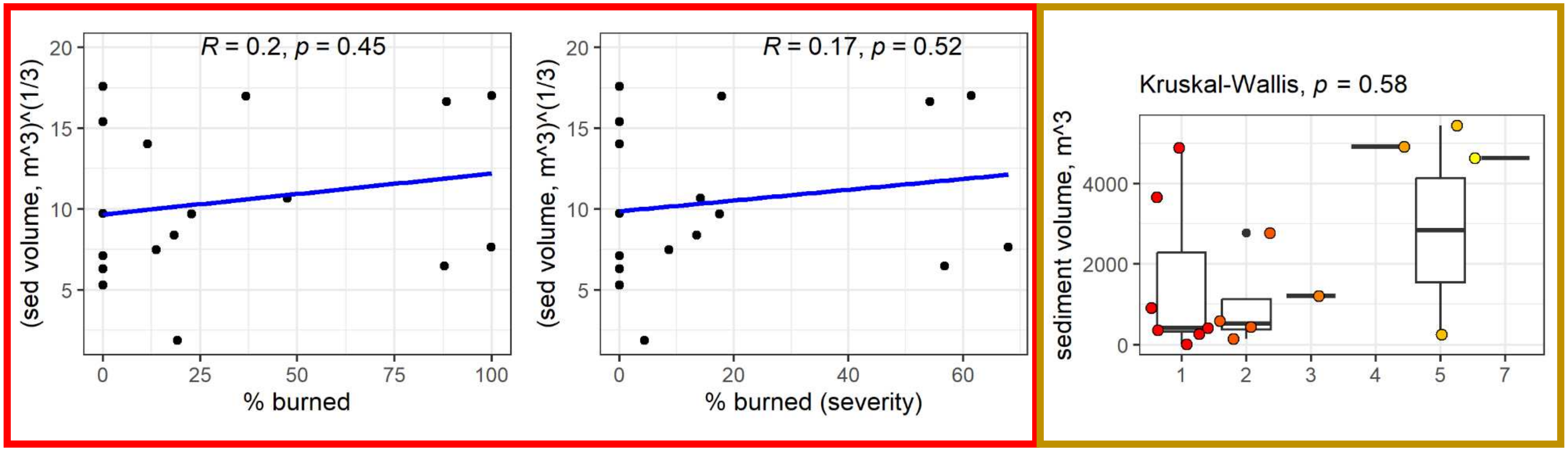

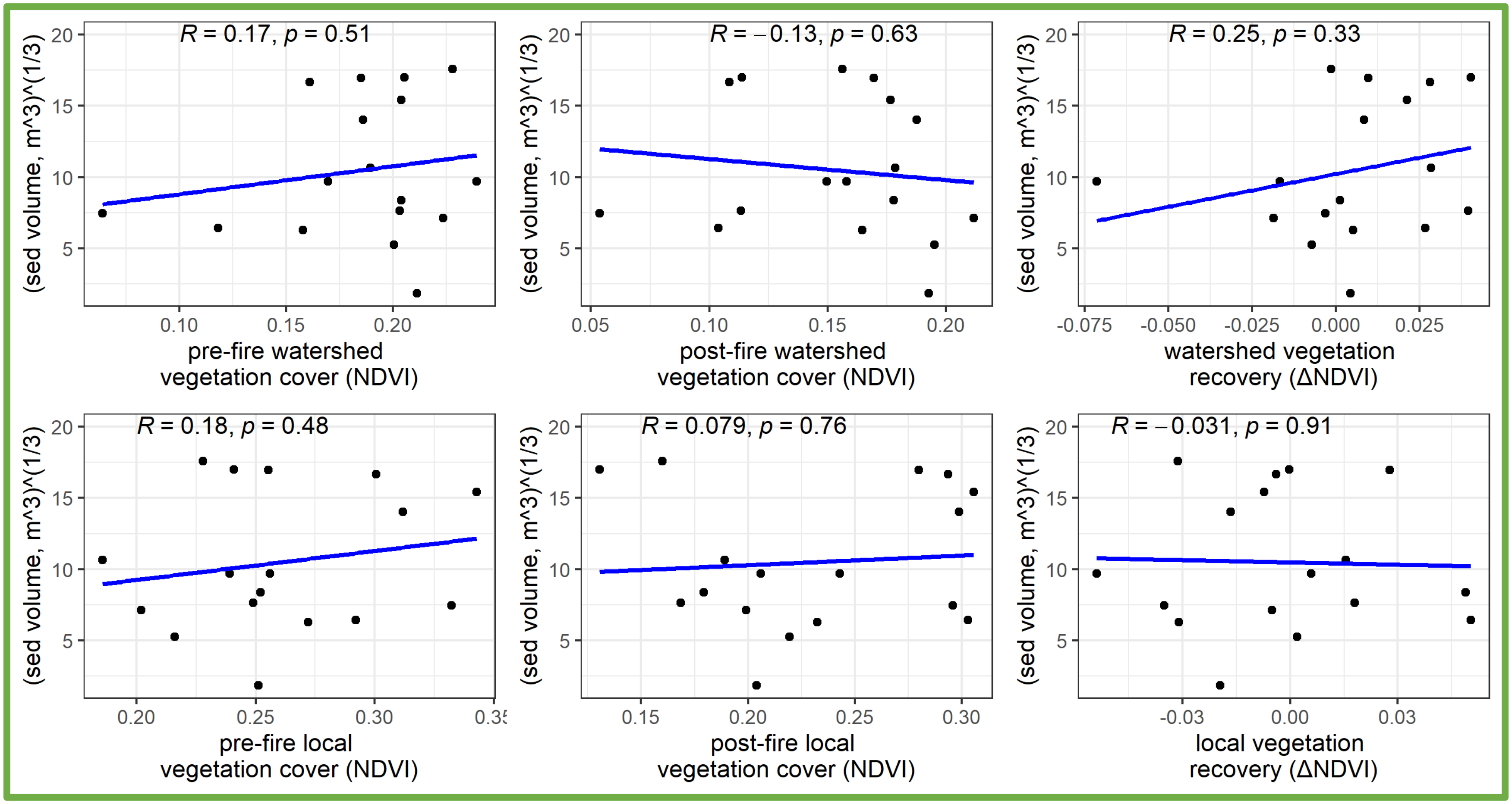
R = 0.17, p = 0.51
R = −0.13, p = 0.63
R = 0.25, p = 0.33
R = 0.18, p = 0.48
R = 0.079, p = 0.76
R = −0.031, p = 0.91
(sed volume, m^3)^(1/3)
pre-fire watershed vegetation cover (NDVI)
post-fire watershed vegetation cover (NDVI)
watershed vegetation recovery (ΔNDVI)
pre-fire local vegetation cover (NDVI)
post-fire local vegetation cover (NDVI)
local vegetation recovery (ΔNDVI)

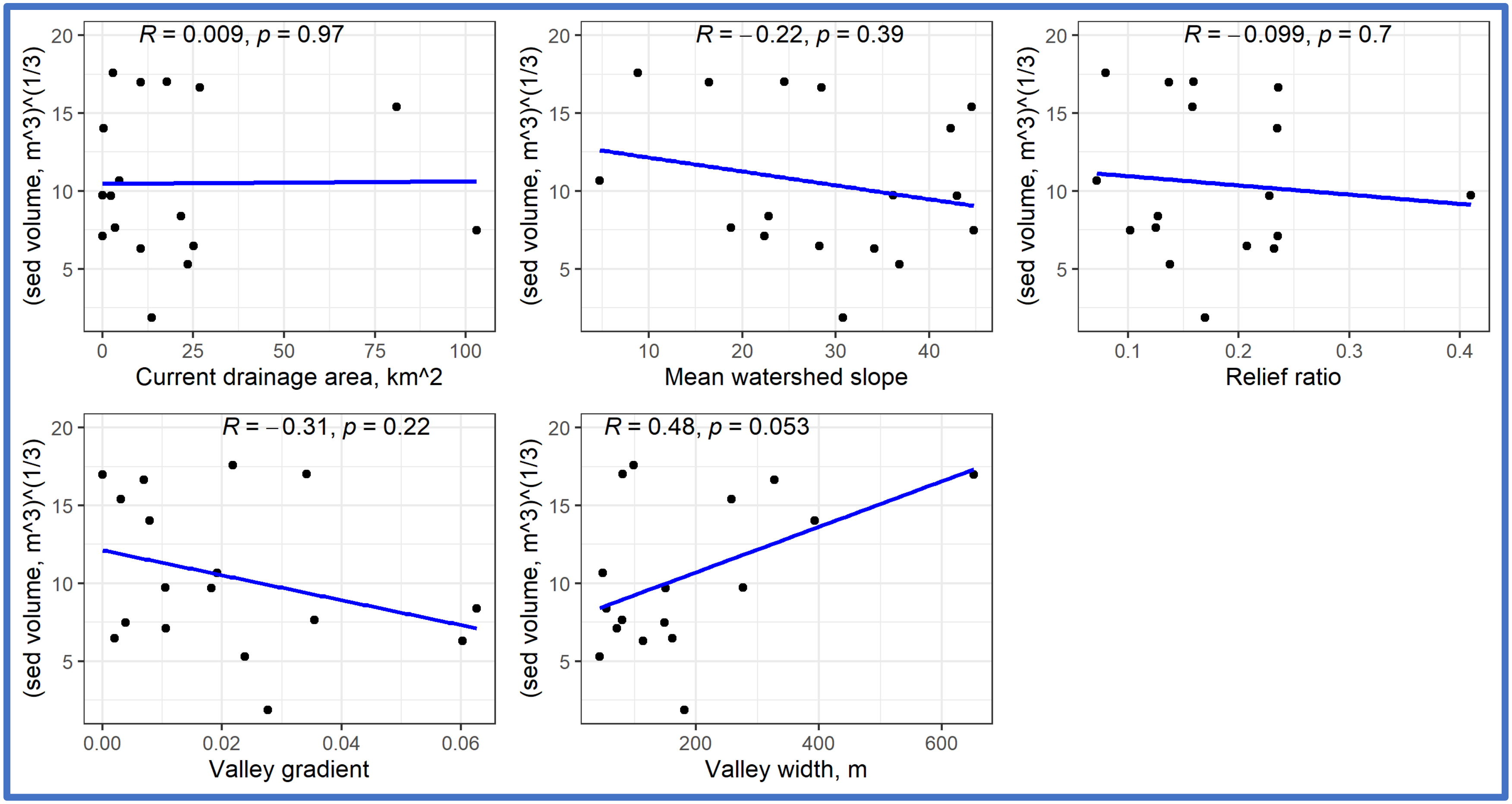

Figure 34: Results of pairwise analyses of explanatory variables and reach summed sediment volumes. The linear relationship between continuous explanatory variables and transformed reach summed sediment volume (m^3) is indicated by the blue line. The R value describes the direction and goodness of fit of the model, and the p-value is used to evaluate model significance. Burn characteristic comparisons are boxed in red, pond in gold, vegetation in green, and geomorphology in blue.

Normalized Reach Sediment Volume

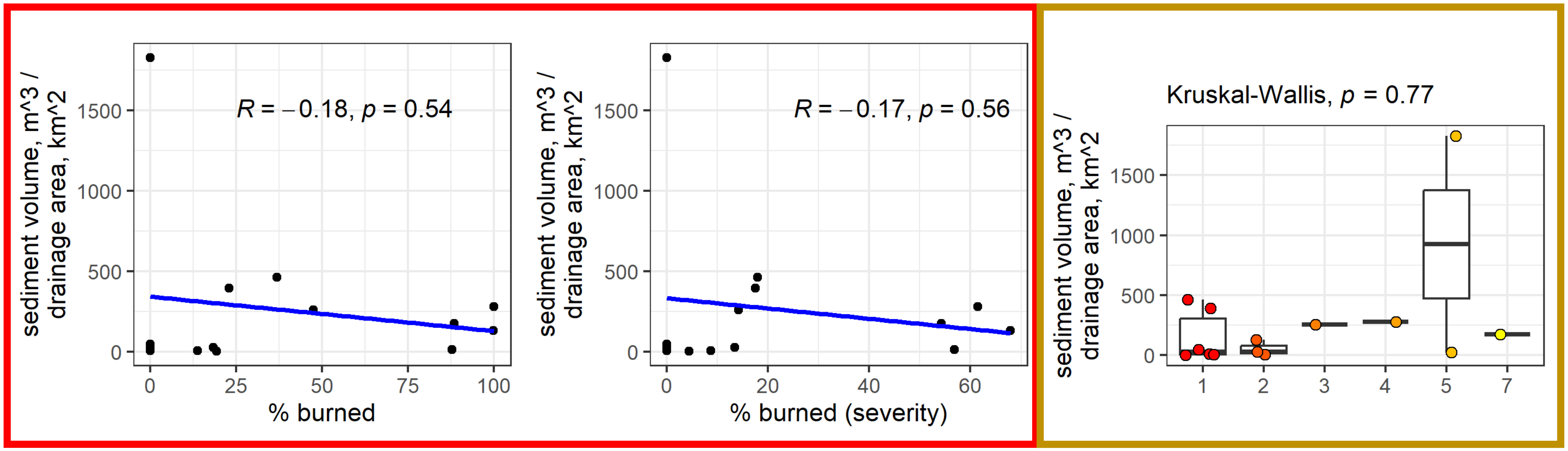

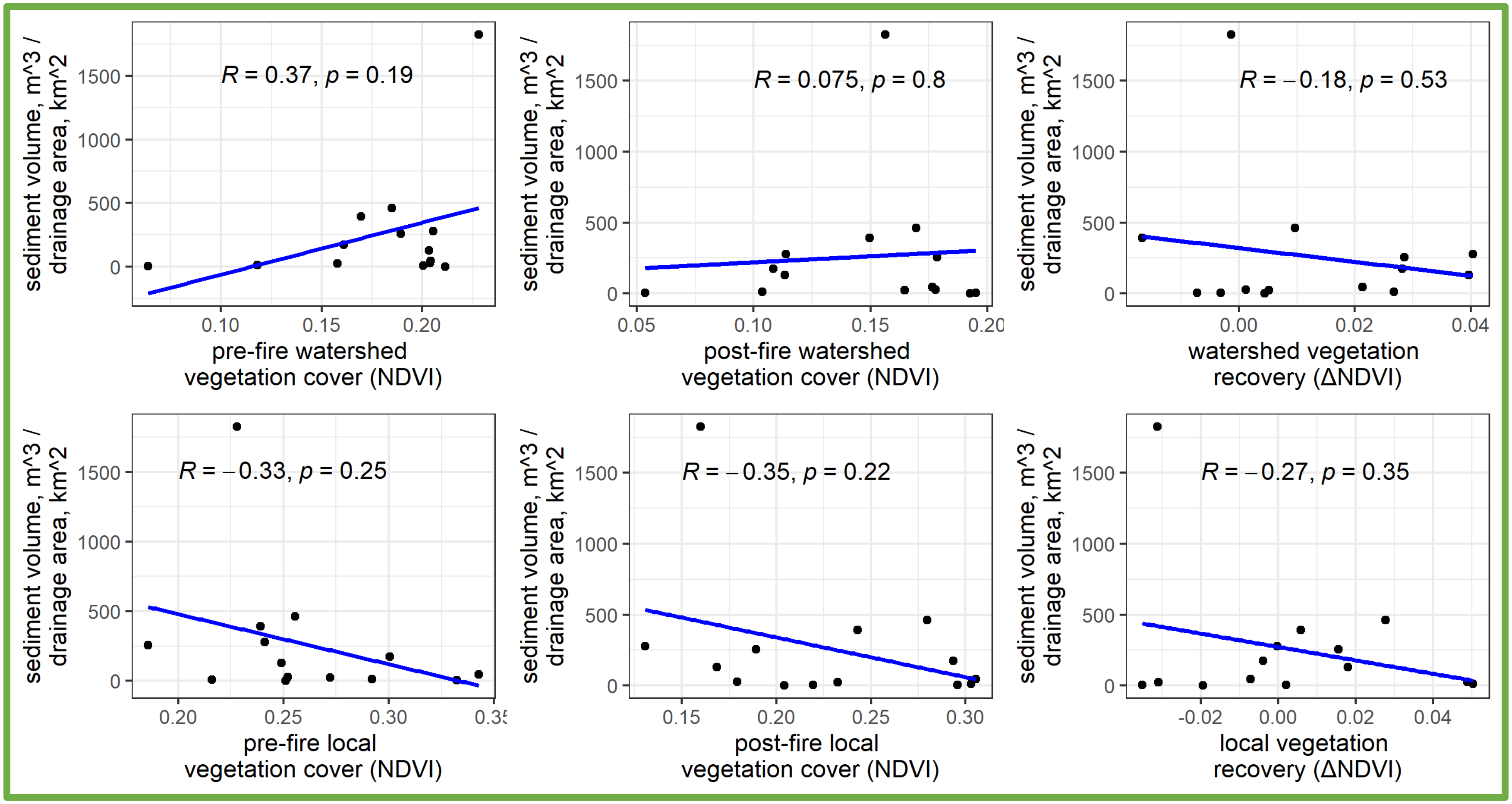
R = 0.37, p = 0.19
pre-fire watershed vegetation cover (NDVI)
R = 0.075, p = 0.8
post-fire watershed vegetation cover (NDVI)
R = –0.18, p = 0.53
watershed vegetation recovery (ΔNDVI)
R = –0.33, p = 0.25
pre-fire local vegetation cover (NDVI)
R = –0.35, p = 0.22
post-fire local vegetation cover (NDVI)
R = –0.27, p = 0.35
local vegetation recovery (ΔNDVI)
sediment volume, m^3 / drainage area, km^2

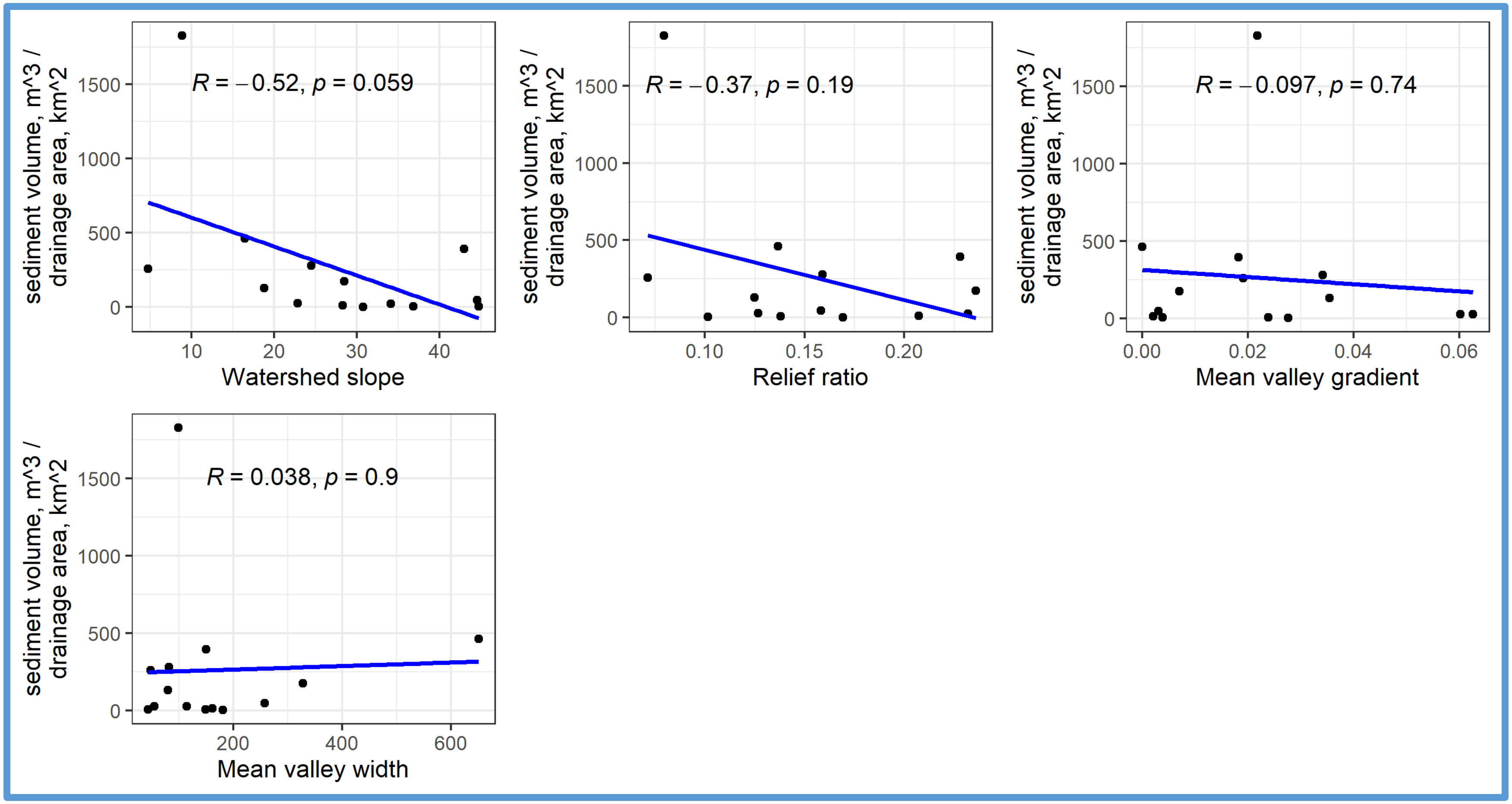

Figure 35: Results of pairwise analyses of explanatory variables and reach summed sediment volumes normalized by drainage area. The linear relationship between continuous explanatory variables and normalized reach summed sediment volume (m^3/km^2) is indicated by the blue line. The R value describes the direction and goodness of fit of the model, and the p-value is used to evaluate model significance. Burn characteristic comparisons are boxed in red, pond in gold, vegetation in green, and geomorphology in blue.

Residual Volume

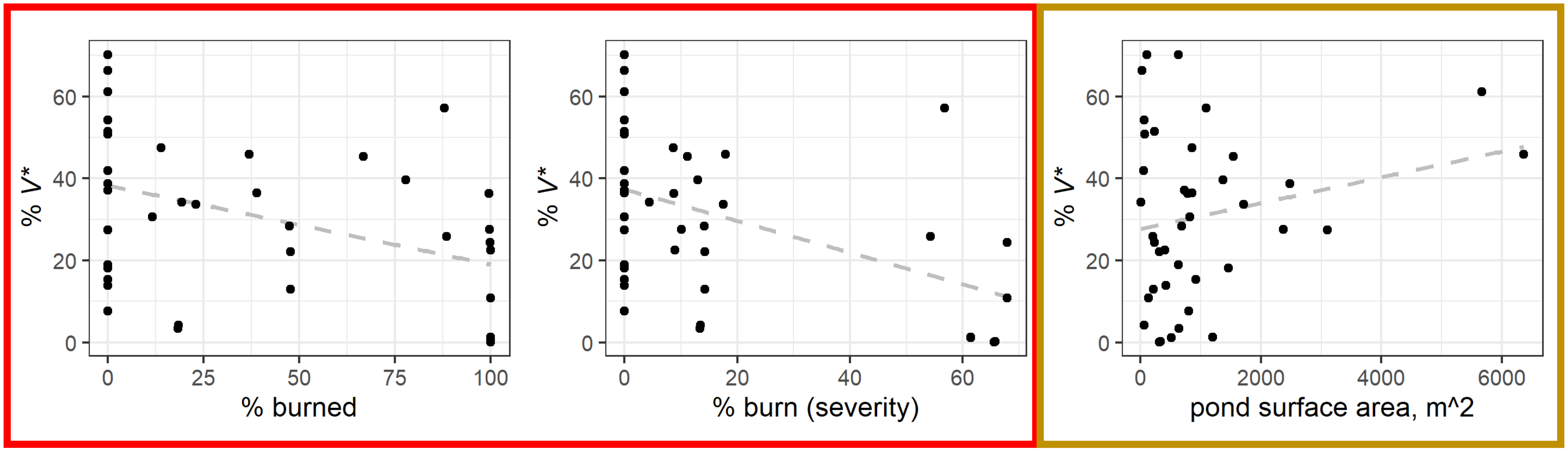

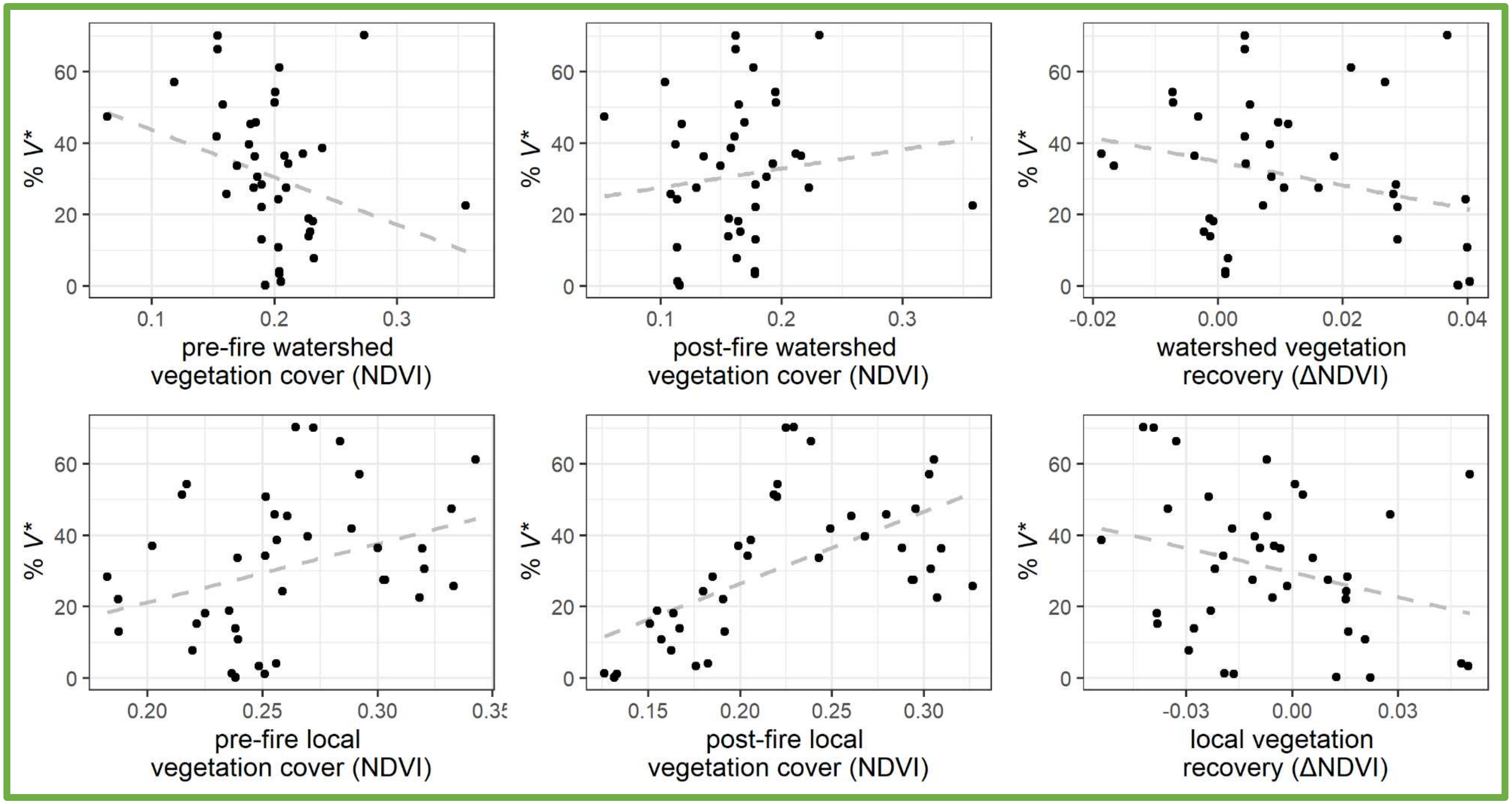

% V*
pre-fire watershed vegetation cover (NDVI)
post-fire watershed vegetation cover (NDVI)
watershed vegetation recovery (ΔNDVI)
pre-fire local vegetation cover (NDVI)
post-fire local vegetation cover (NDVI)
local vegetation recovery (ΔNDVI)

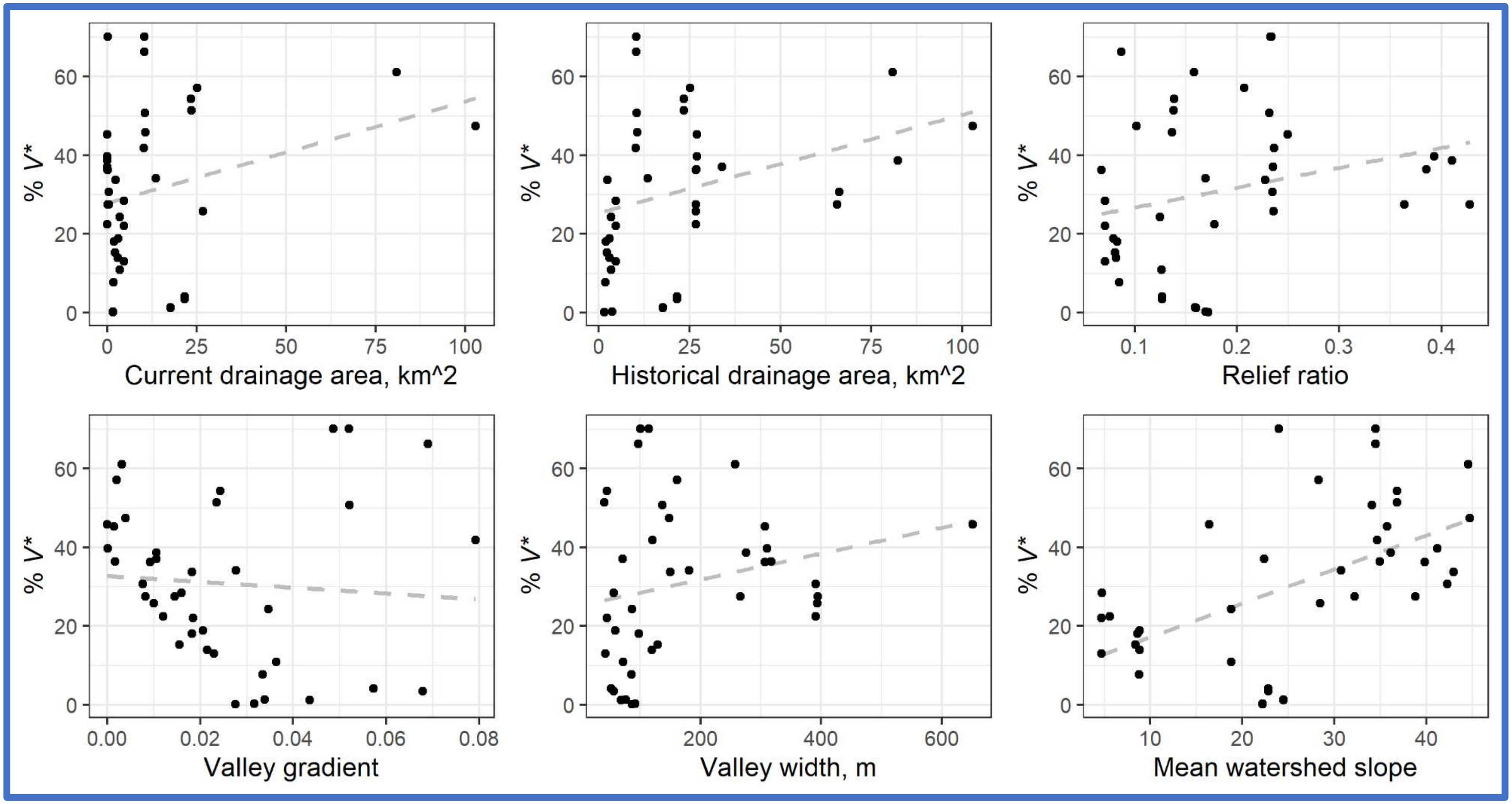

Figure 36: Results of pairwise analyses of explanatory variables and residual volume, V. The linear relationship between continuous explanatory variables and residual volume is indicated by the dotted grey line. Because beta regression rather than linear regression was used for assessing these relationships, the linear correlation and equation are not shown. Burn characteristic comparisons are boxed in red, pond in gold, vegetation in green, and geomorphology in blue.*

Lifetime Sedimentation Rates

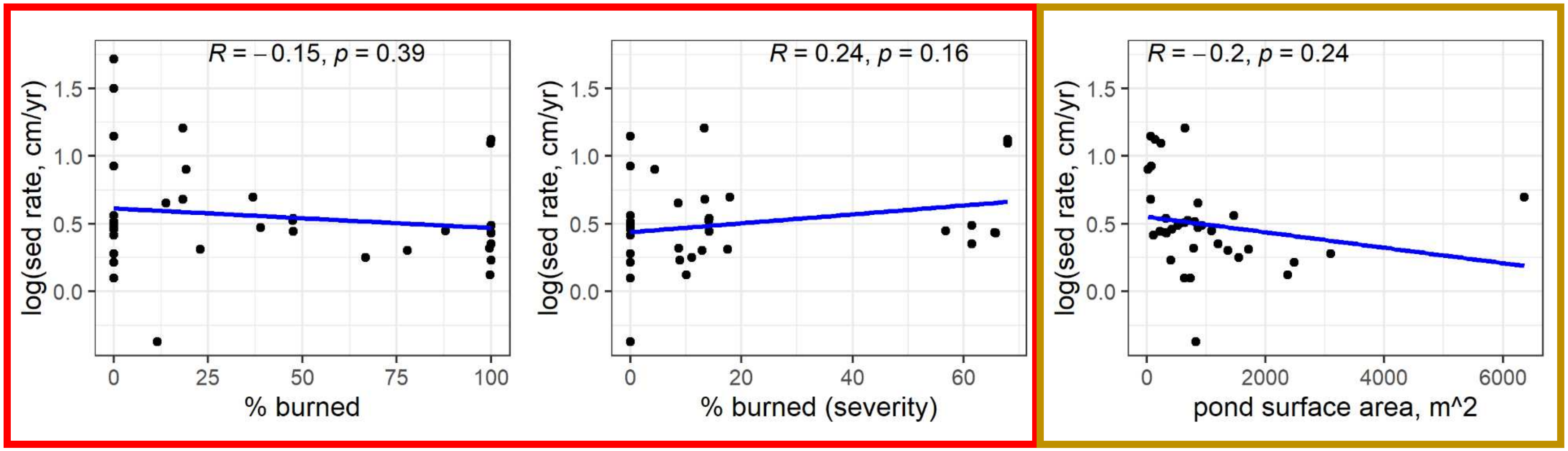

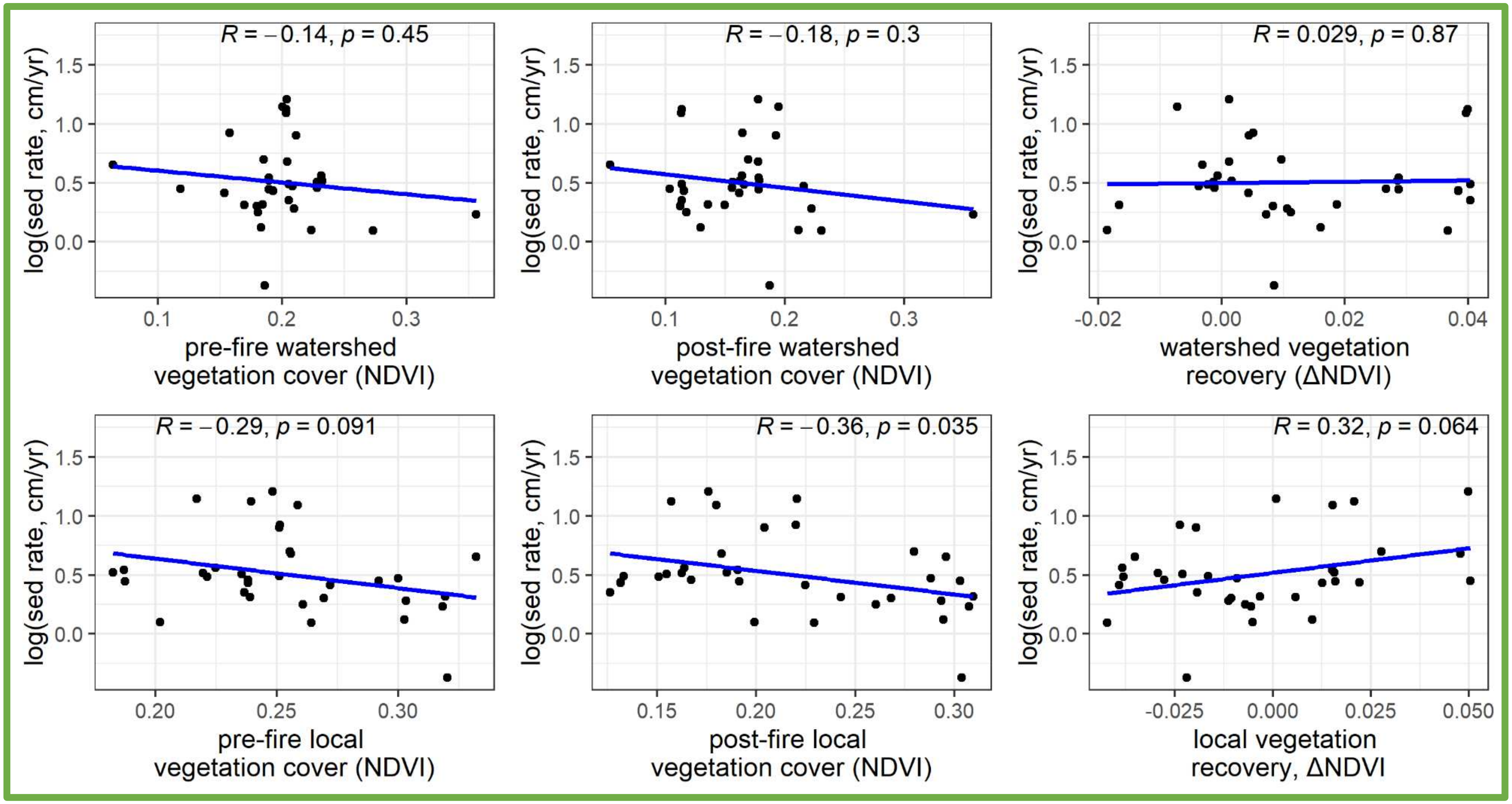
R = −0.14, p = 0.45
R = −0.18, p = 0.3
R = 0.029, p = 0.87
R = −0.29, p = 0.091
R = −0.36, p = 0.035
R = 0.32, p = 0.064
log(sed rate, cm/yr)
pre-fire watershed vegetation cover (NDVI)
post-fire watershed vegetation cover (NDVI)
watershed vegetation recovery (ΔNDVI)
pre-fire local vegetation cover (NDVI)
post-fire local vegetation cover (NDVI)
local vegetation recovery, ΔNDVI

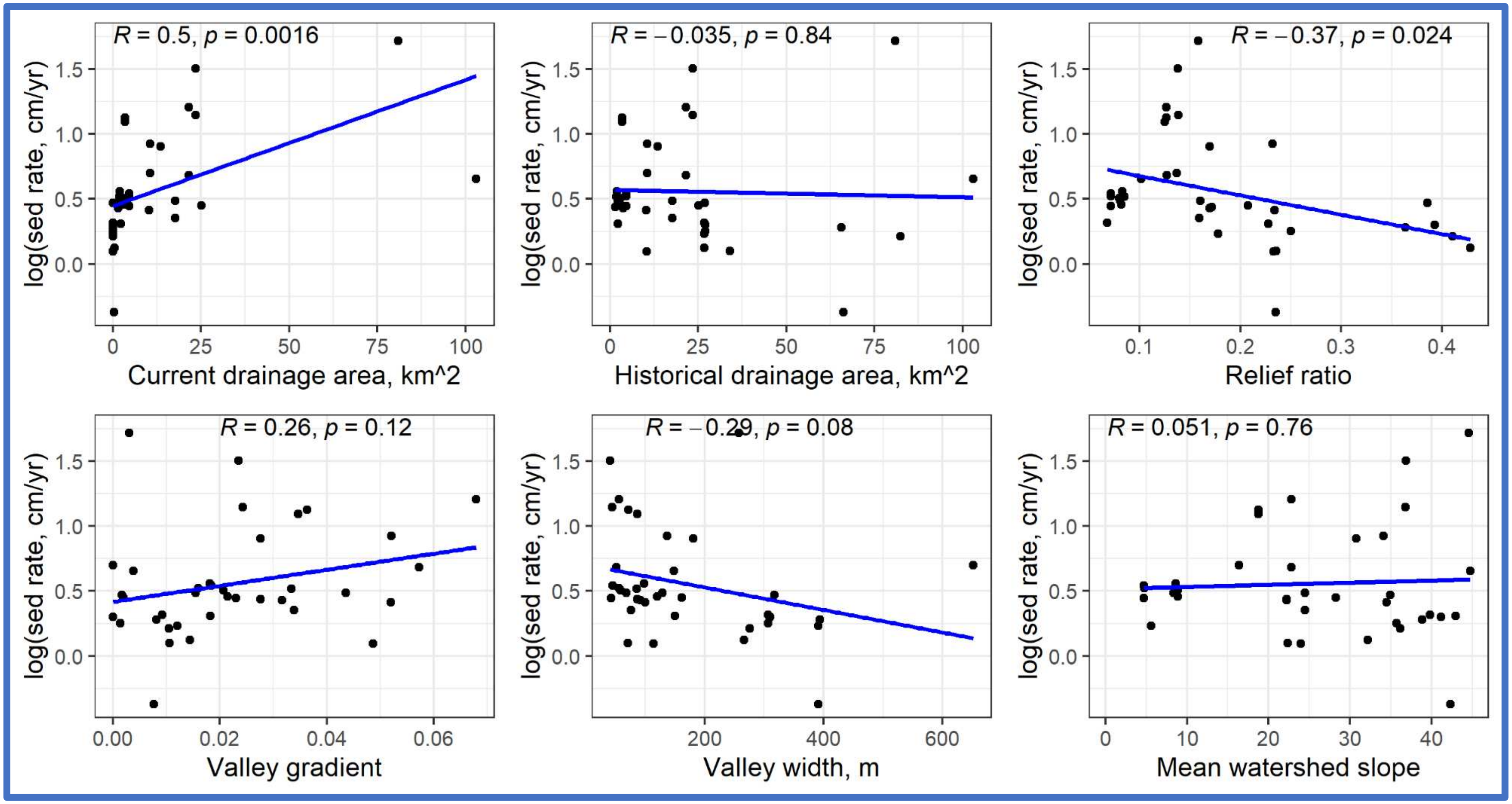

Figure 37: Results of pairwise analyses of explanatory variables and lifetime sedimentation rate. The linear relationship between continuous explanatory variables and log-10 transformed lifetime sedimentation rate (cm/yr) is indicated by the blue line. The R value describes the direction and goodness of fit of the model, and the p-value is used to evaluate model significance. Burn characteristic comparisons are boxed in red, pond in gold, vegetation in green, and geomorphology in blue.

Post-fire Sedimentation Rates

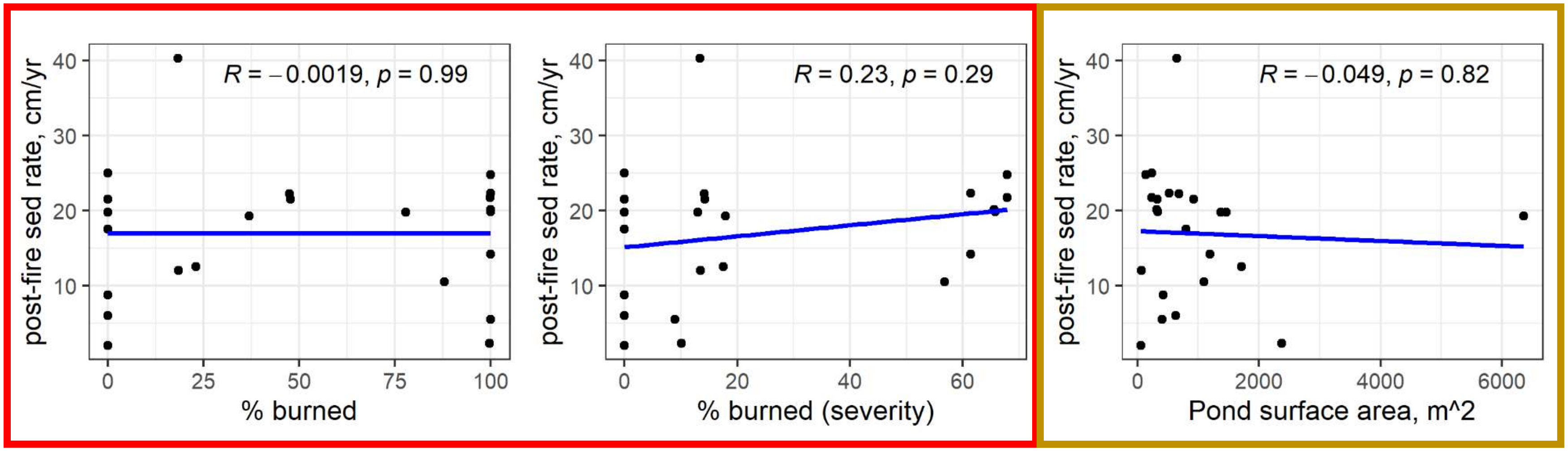

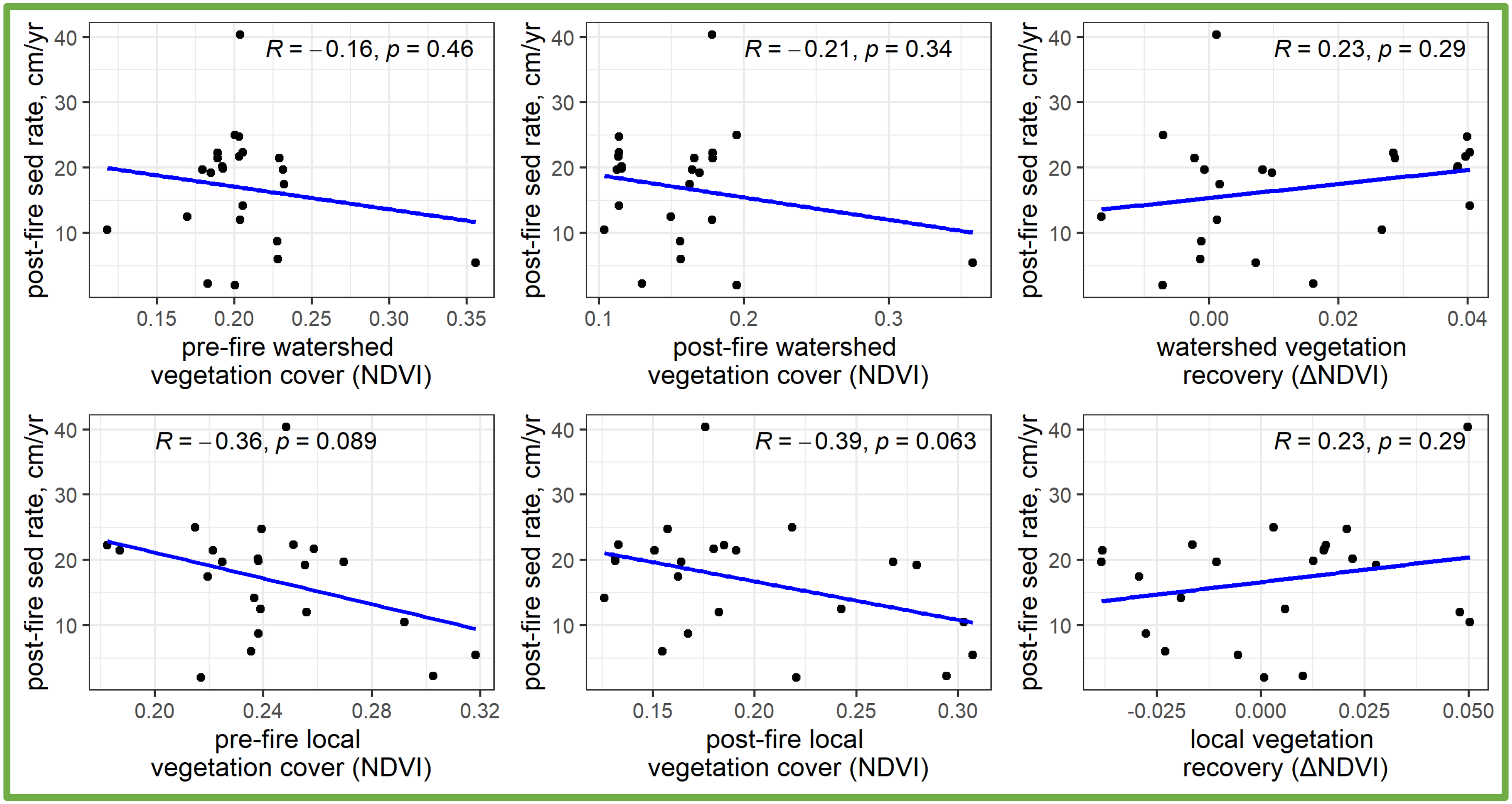
R = −0.16, p = 0.46
post-fire sed rate, cm/yr
pre-fire watershed vegetation cover (NDVI)
R = −0.21, p = 0.34
post-fire watershed vegetation cover (NDVI)
R = 0.23, p = 0.29
watershed vegetation recovery (ΔNDVI)
R = −0.36, p = 0.089
pre-fire local vegetation cover (NDVI)
R = −0.39, p = 0.063
post-fire local vegetation cover (NDVI)
R = 0.23, p = 0.29
local vegetation recovery (ΔNDVI)

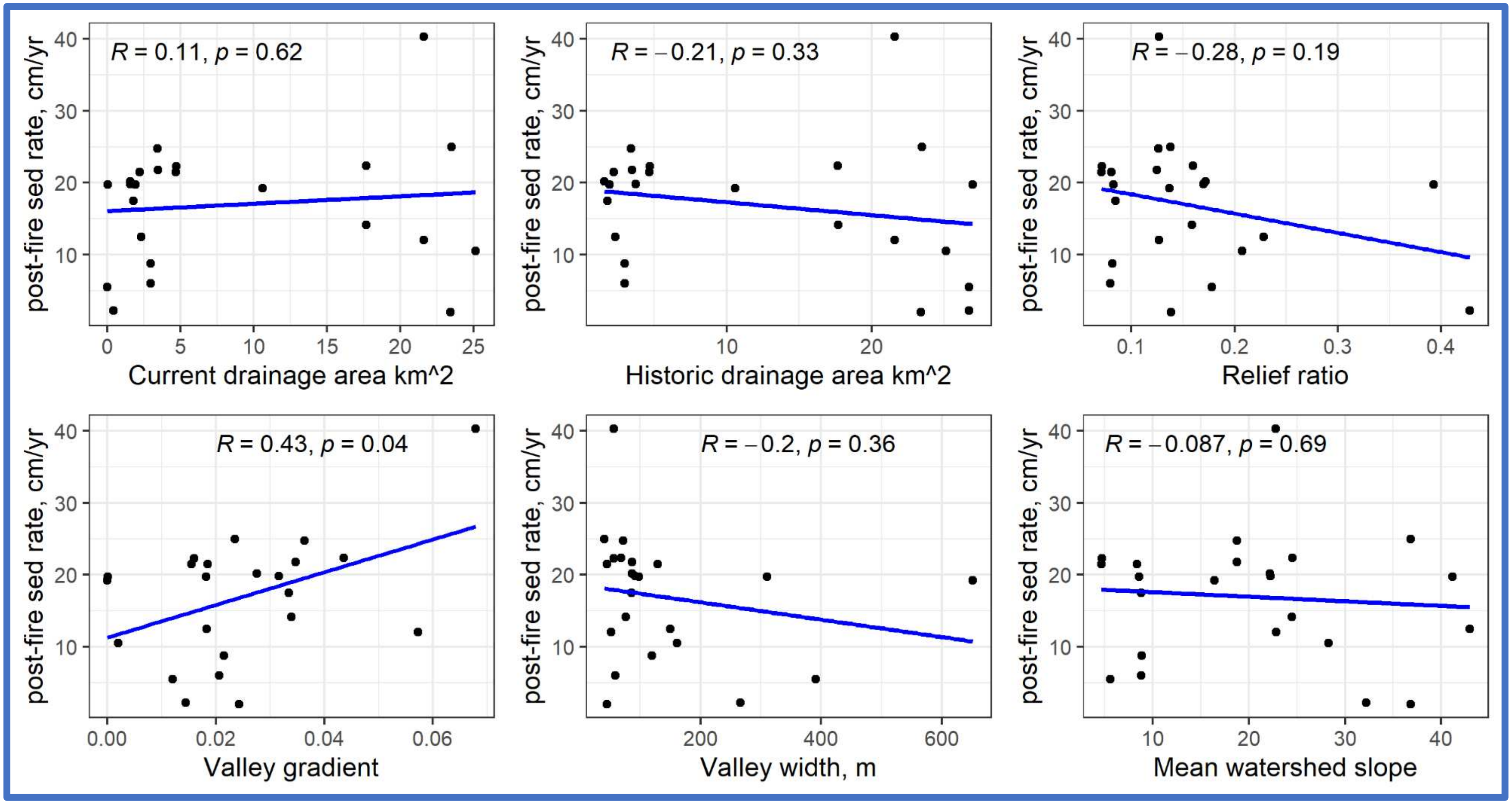

Figure 38: Results of pairwise analyses of explanatory variables and post-fire sedimentation rates (cm/yr). The linear relationship between continuous explanatory variables and post-fire sedimentation rate sedimentation rate is indicated by the blue line. The R value describes the direction and goodness of fit of the model, and the p-value is used to evaluate model significance. Burn characteristic comparisons are boxed in red, pond in gold, vegetation in green, and geomorphology in blue.

TOC

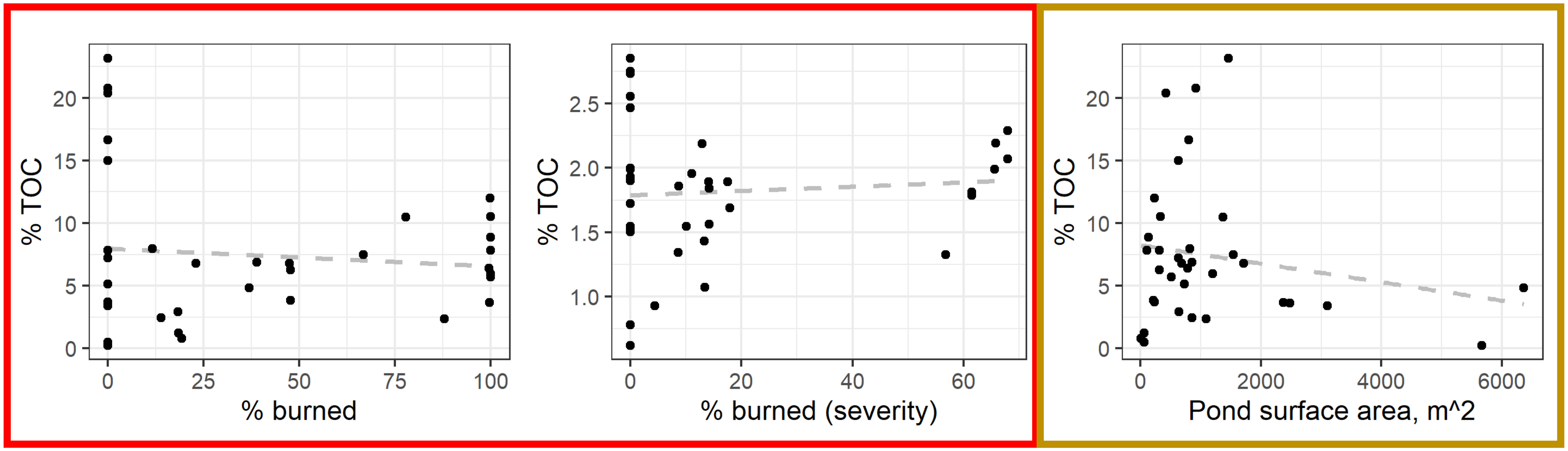

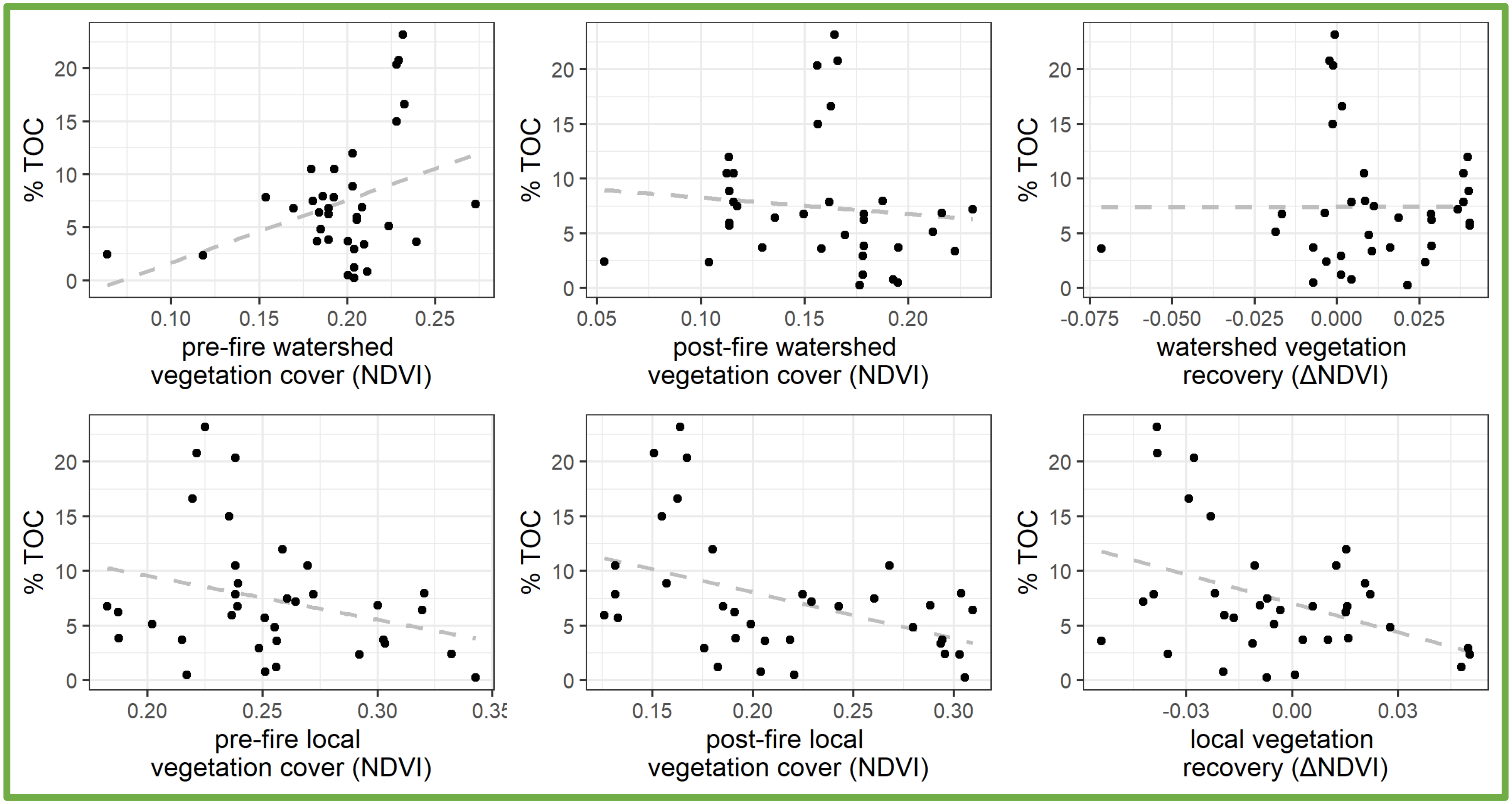
% TOC
pre-fire watershed
vegetation cover (NDVI)
post-fire watershed
vegetation cover (NDVI)
watershed vegetation
recovery (ΔNDVI)
pre-fire local
vegetation cover (NDVI)
post-fire local
vegetation cover (NDVI)
local vegetation
recovery (ΔNDVI)

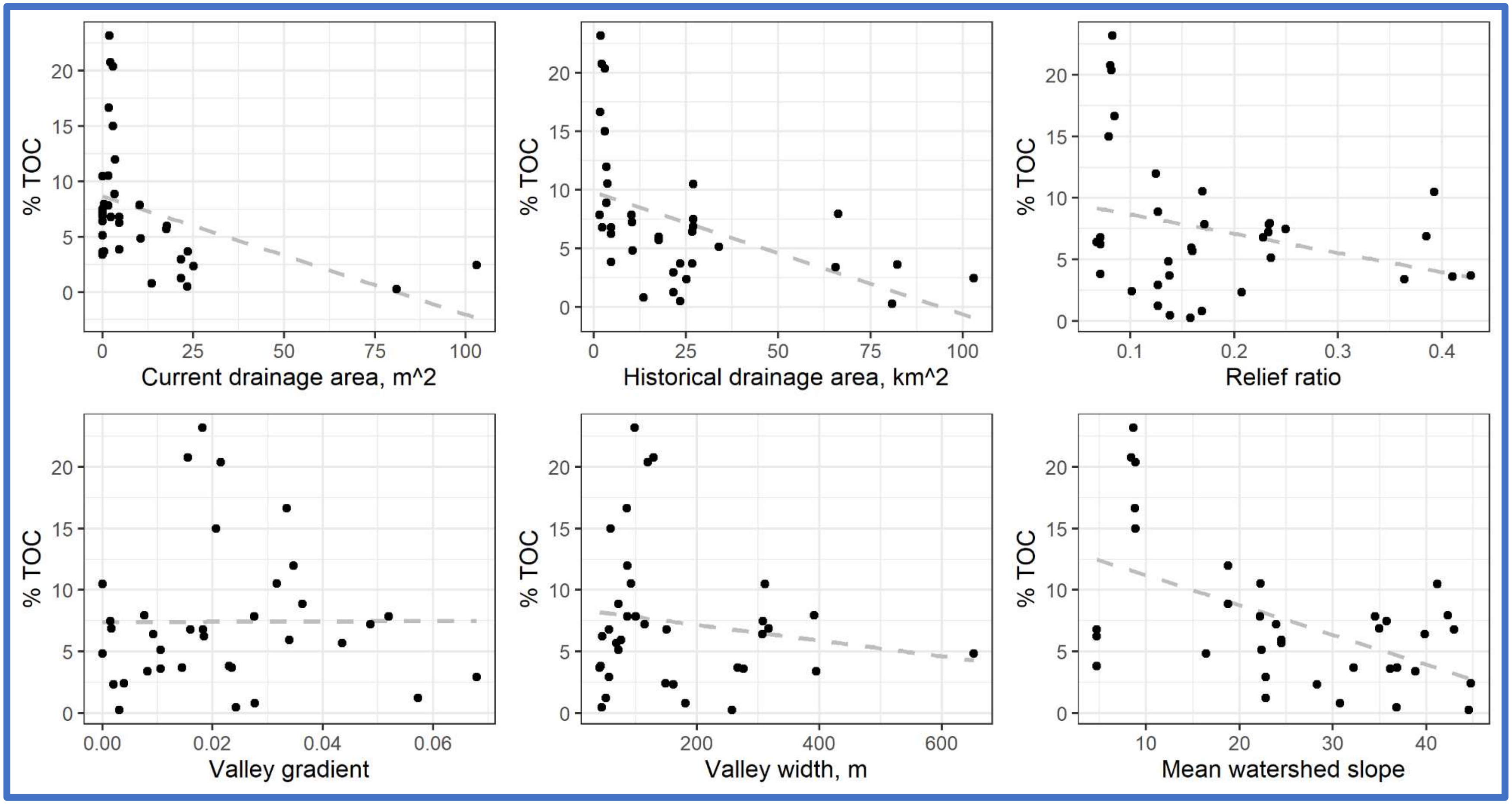

Figure 39: Results of pairwise analyses of explanatory variables and percent total organic carbon (% TOC). The linear relationship between continuous explanatory variables and TOC is indicated by the dotted grey line. Because beta regression rather than linear regression was used for assessing these relationships, the linear correlation and equation are not shown. Burn characteristic comparisons are boxed in red, pond in gold, vegetation in green, and geomorphology in blue.

Grain Size

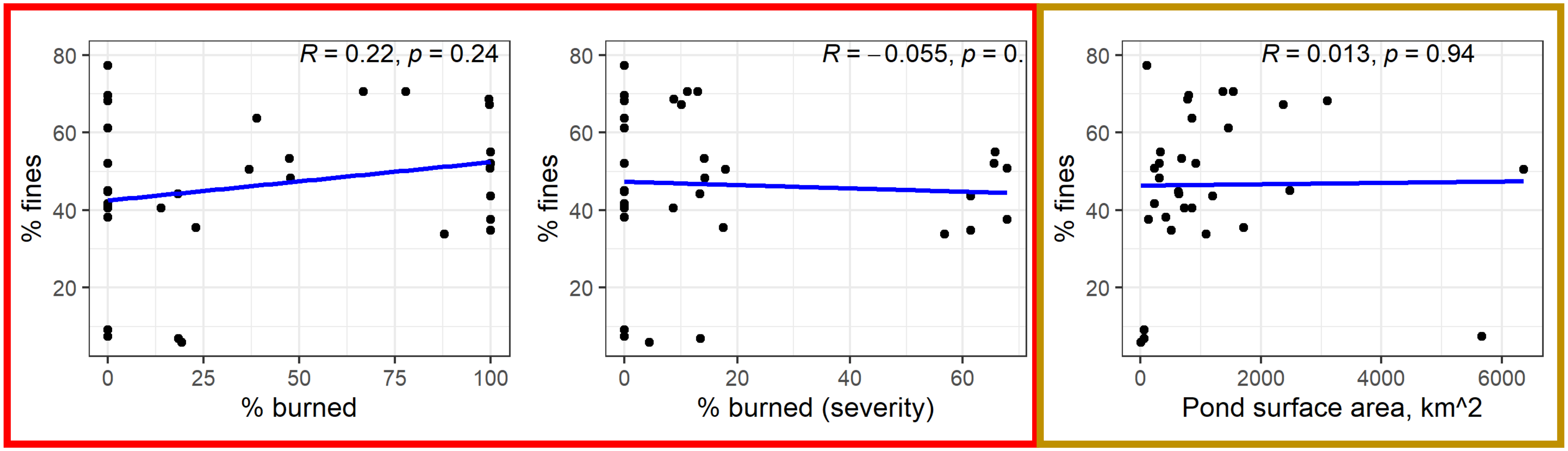

R = 0.22, p = 0.24
% fines
% burned
R = −0.055, p = 0.
% fines
% burned (severity)
R = 0.013, p = 0.94
% fines
Pond surface area, km^2

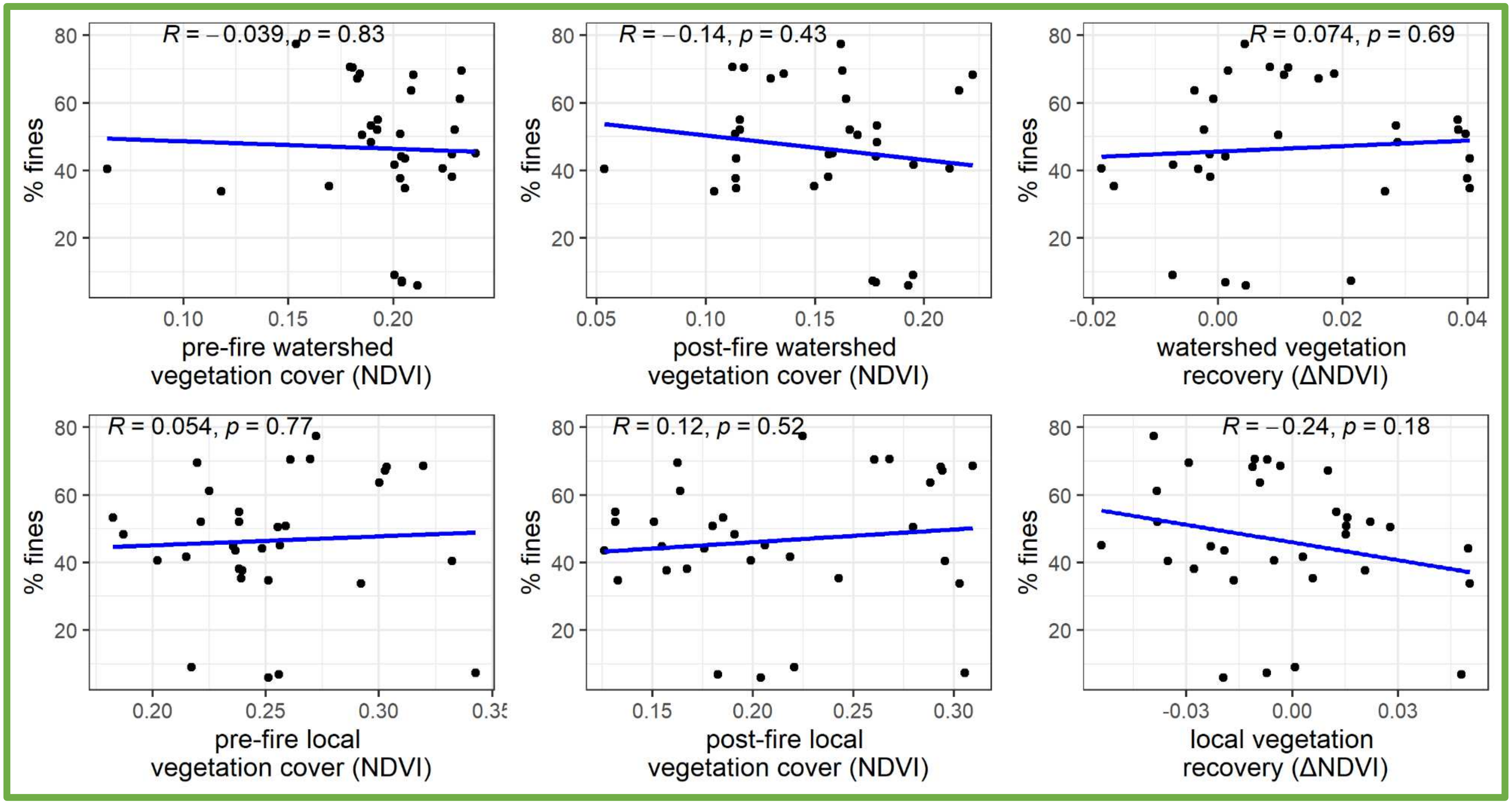

R = −0.039, p = 0.83
% fines
pre-fire watershed vegetation cover (NDVI)
R = −0.14, p = 0.43
% fines
post-fire watershed vegetation cover (NDVI)
R = 0.074, p = 0.69
% fines
watershed vegetation recovery (ΔNDVI)
R = 0.054, p = 0.77
% fines
pre-fire local vegetation cover (NDVI)
R = 0.12, p = 0.52
% fines
post-fire local vegetation cover (NDVI)
R = −0.24, p = 0.18
% fines
local vegetation recovery (ΔNDVI)

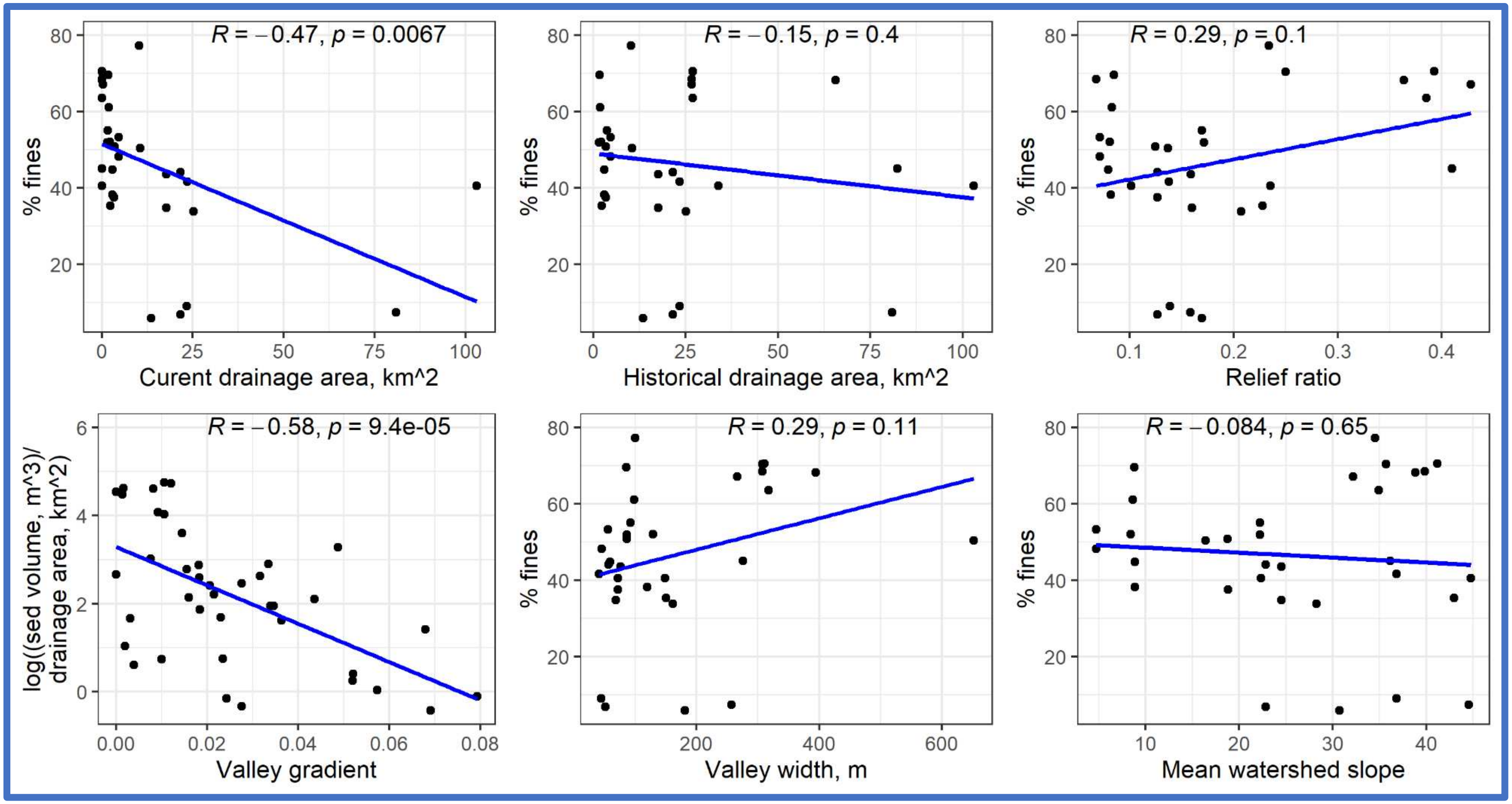

Figure 40: Results of pairwise analyses of explanatory variables and grain size. The linear relationship between continuous explanatory variables and percent fines (silt and clay) is indicated by the blue line. The R value describes the direction and goodness of fit of the model, and the p-value is used to evaluate model significance. Burn characteristic comparisons are boxed in red, pond in gold, vegetation in green, and geomorphology in blue

APPENDIX V

Reach Sediment Storage

Sediment volumes from individual ponds were summed to calculate reach sediment storage for 17 unique reaches. The median reach sediment storage is 913 m^3 with a range from 6 m^3 to 5434 m^3 (Appendix I). A cube root transformation of reach sediment storage corrected the strong right-skewed distribution and was used for pairwise comparison with explanatory variables. Reach sediment storage showed no significant relationship with burn, vegetation, or geomorphic characteristics. Multiple linear regression analysis was not conducted due to the small sample size.

The percent of the watershed burned (adjusted R^2 = -0.03, p = 0.45) and the percent burned at moderate to high severities (adjusted R^2 = -0.04, p = 0.52) both related positively to sediment volume, such that reaches in watersheds that burned more stored more sediment. Watershed pre- (adjusted R^2 = -0.03, p = 0.51) and post-fire vegetation cover (adjusted R^2 = -0.05, p = 0.63) and post-fire vegetation recovery (adjusted R^2 = 0.00, p = 0.33) also exhibited positive relationships with reach sediment volume. The mean local pre- (adjusted R^2 = -0.03, p = 0.48) and post-fire (adjusted R^2 = -0.06, p = 0.76) vegetation cover also exhibited positive relationships, though the mean local post-fire vegetation recovery (adjusted R^2 = -0.07, p = 0.91) showed no relationship. The mean valley width also positively related to reach sediment volume (adjusted R^2 = 0.18, p = 0.05). In contrast, the mean watershed slope (adjusted R^2 = -0.01, p = 0.39) and mean valley gradient (adjusted R^2 = 0.04, p = 0.22) negatively related to sediment volume such that steeper drainages stored less sediment. The current drainage area (adjusted R^2 = -0.07, p = 0.97) and relief ratio (adjusted R^2 = -0.06, p = 0.70) showed no relationship with reach sediment volumes. Generally, reaches with more measured ponds stored greater volumes of sediment but the difference is not significant, likely due to the small group sizes (p = 0.55) (Table 17).

Table 17: Sediment storage and normalized storage by number of ponds measured on each reach.

number of ponds measured on a reach	**number of reaches**	**median sediment volume, m^3**	**median normalized sediment volume, m^3/km^2**
1	8	666	219
2	4	517	78
3	1	1210	257
4	1	4918	278
5	2	2842	925
7	1	4625	173

3.1.2 Normalized reach sediment storage

The reach total storage divided by the drainage area gave normalized sediment storage. Three reaches (WLD, LLR-lower, GLC) were statistical outliers and excluded from analysis. At WLD and GLC, only one pond was measured on each reach, with a small current drainage area, but several other ponds were present with much larger drainage areas meaning that logically the pond was not representative of reach conditions either. LRR-lower was disconnected from the channel with a small current drainage area but large historical area. The median normalized storage for the 14 reaches was 87 m^3/km^2 with a range from 0.5 m^3/km^2 to 1825 m^3/km^2 (Appendix I). Pairwise comparison of normalized reach sediment volumes with explanatory variables showed no significant relationship with any burn, vegetation, or geomorphic characteristics. Multiple linear regression analysis was not conducted due to the small sample size.

Burn characteristics including the percent of watershed burned (adjusted $R^2 = -0.05$, $p = 0.54$) and the percent burned at moderate and high severities (adjusted $R^2 = -0.05$, $p = 0.55$) corresponded negatively with normalized storage. Watershed pre- (adjusted $R^2 = 0.07$, $p = 0.19$) and post-fire (adjusted $R^2 = -0.08$, $p = 0.80$) vegetation cover both exhibited positive relationships with normalized storage.

However, watershed (adjusted R^2 = -0.04, p = 0.53) and local (adjusted R^2 = 0.00, p = 0.35) post-fire vegetation recovery and local pre- (adjusted R^2 = -0.03, p = 0.25) and post-fire (adjusted R^2 = 0.05, p = 0.22) vegetation cover negatively related to normalized storage. The mean valley bottom width (adjusted R^2 = -0.08, p = 0.90) positively related to normalized storage. In contrast, the relief ratio (adjusted R^2 = 0.07, p = 0.19), mean valley gradient (adjusted R^2 = -0.07, p = 0.74), and watershed slope (adjusted R^2 = 0.20, p = 0.06) negatively related. There is no significant relationship between normalized sediment storage and the number of ponds measured on a reach, likely due to small group sizes (p = 0.77) (Table 17).